UNCERTAIN GROWTH OPTIONS AND ASSET PRICING

by

Brian Hogle

A Dissertation

Submitted to the Faculty of Purdue University

In Partial Fulfillment of the Requirements for the degree of

Doctor of Philosophy

Department of Mathematics

West Lafayette, Indiana

August 2021

THE PURDUE UNIVERSITY GRADUATE SCHOOL
STATEMENT OF COMMITTEE APPROVAL

Dr. Kiseop Lee, Chair

College of Science

Dr. Samy Tindel

College of Science

Dr. Aaron Yip

College of Science

Dr. Jing Wang

College of Science

Approved by:

Dr. Plamen Stefanov

This dissertation is dedicated to my family, especially my grandparents.

ACKNOWLEDGMENTS

I would like to greatly thank my advisor Professor Kiseop Lee for all the help and patience I've received over the past few years. Dr. Lee's style of advising was very suitable to me, and I was able to learn and make progress while enjoying my time here. Dr Lee is a great person, and he always kept my best interests in mind. It's been a pleasure working with him.

I would also like to thank Professor Hwagyun Kim of the Texas A&M Mays Business School. Dr. Kim acted as an advisor to me and spent a significant amount of time with me discussing my project. I'm very grateful for this. Dr. Kim and Dr. Lee came up with the idea for this project, and I've really learned a lot from this process.

I'd like to thank my dissertation committee for their time spent reading this thesis, their time spent doing my advanced topics exam, and for being willing to discuss and answer questions that I had while working on this project. I have already mentioned Dr. Lee and Dr. Kim, and I would also like to very much thank Professors Samy Tindel, Aaron Yip, and Jing Wang.

I'd like to thank my family, especially my mom and Ray Enzweiler. Finally, I'd like to thank all of my friends, especially David Katz, Dillon Prash, John Rached, Miguel Ramirez, Daniel Shankman, and Dongming She.

TABLE OF CONTENTS

LIST OF TABLES

LIST OF FIGURES

LIST OF SYMBOLS

r	the interest rate process
a	the rate of mean reversion of r
b_2	the long run mean of r
σ_r	the volatility of r
M	the stochastic discount factor process (SDF)
λ	the price of market risk
I	the initial investment process
μ_I	the percentage drift when I follows a GBM
σ_I	the percentage volatility when I follows a GBM,
$C_j(t)$	cash flow at time t from a project beginning at date $j < t$
μ	percentage drift of the cash flow process
σ	percentage volatility of the cash flow process
$\overline{C}$	parameter affecting the mean of the cash flow
W^{C_j}	SBM driving the cash flow process
W^M	SBM driving the SDF
W^r	SBM driving r
W^I	SBM driving I
W^{V_j}	SBM driving V_j
ρ^{M,C_j}	correlation between SBMs driving the SDF and C_j
$\rho^{M,r}$	correlation between SBMs driving the SDF and r
ρ^{r,C_j}	correlation between W^r and W^{C_j}
$\upsilon_{\min}$	lower bound of the Jacobi process
$\upsilon_{\max}$	upper bound of the Jacobi process
V_j	Jacobi process for the j-th project
κ	rate of mean reversion of the Jacobi process
θ	long run mean of the Jacobi process
σ_V	volatility of the Jacobi process
$\{\chi_j(t)\}_{t\geq j}$	sequence of indicator random variables determining if

$\{\chi_j(t)\}_{t\geq j}$	(Cont.) the j-th project is still alive at time t
$Y_j(t+1)$	Bernoulli random variables determining the value of $\{\chi_j(t)\}_{t\geq j}$
π	parameter of Bernoulli random variable $Y_j(t+1)$, $P(Y_j(t+1)=1)=\pi$
$\mathcal{N}(\mu,\sigma^2)$	normal distribution with mean μ and variance σ^2
$\mathbb{N}$	the natural numbers including 0.
$\subset$	subset, not necessarily proper subset.
$\mathbb{R}$	the real numbers.
$\mathcal{B}(\mathbb{R})$	the Borel sigma algebra on $\mathbb{R}$.
$\mathbb{Z}^+$	the positive integers.
$\mathbb{R}^+$	the nonnegative real numbers.
ρ^{M,C_s}	SDF and cash flow correlation
Ψ	conditional expectation used in calculation of growth options.
Φ	conditional expectaiton used in calculation of growth options next period.
$\mathbb{E}$	expectation
$\mathbb{V}$	variance

ABBREVIATIONS

BGN	Berk, Green, Naik
SDF	stochastic discount factor
NPV	net present value
iff	if and only if
ME	market equity
BE	book equity
CAPM	Capital Asset Pricing Model
SBM	Standard Brownian Motion

NOMENCLATURE

Market value	number of shares outstanding times price per share
book value	firm value determined by the accountant
book-to-market	the ratio of the book value to the market value

ABSTRACT

We develop a growth option and asset pricing model that incorporates uncertain cash flow volatility by way of a bounded quadratic diffusion. Using different measures of risk uncertainty, we study the combined effects of risk and its associated uncertainty on project values, firm investment, and the resulting returns. Uncertain cash flow volatility is modeled by a Jacobi process, and our main interest is the effect of the max uncertainty arising from the diffusion term. For comparison, we also model the volatility by a CIR process. In regards to the Jacobi process, we consider upper and lower bounds on cash flow volatility as measures of uncertainty. For the max uncertainty and upper bound, we find that higher uncertainty leads to less investment, higher returns, and lower project values. In the case of the lower bound, we find that higher uncertainty leads to more investment, lower returns, and higher project values. Comparatively, using a CIR process in place of the Jacobi process yields differences in returns and growth option values, showing the importance of the diffusion term in the volatility process. Finally, we have reduced the computational complexity of the simulation. This allows the user to generate long time series and run cross sectional regressions with many firms.

1. INTRODUCTION

When a firm considers the prospect of taking on a new project, it is useful to estimate the project value. As discussed in Schulmerich [1], the most basic way of finding the value of a project is by discounted cash flow valuation, in which it is known that cash flows from a project will arrive at dates $t_1, t_2, \cdots, t_n$ (with $0 \leq t_1 \leq \cdots \leq t_n$) and the discount factor is r. Then, the net present value (NPV) of the project at time $t = 0$ is given by

$$\mathrm{NPV} = \sum_{j=1}^{n} \frac{C_{t_j}}{(1+r)^{t_j}},$$

where the cash flows C_{t_j} may be positive or negative. This model is known to be very inaccurate, as noted in Schulmerich [1] and Dixit and Pindyck [2]. One drawback of this model is that it assumes deterministic cash flows. Our first aim is to develop a model that takes into account random cash flows with random volatility. Second, we desire a model that provides different measures of risk uncertainty. For example, an upper bound and a lower bound on the random risk would be two different measures of uncertainty. To this end, we will model cash flow volatility by two different mean reverting stochastic processes, and the difference in these processes is in the diffusion terms.

Our main contribution is demonstrating the importance of correctly modeling the time varying risk uncertainty. In other words, as the risk changes over time, the uncertainty about the risk changes too. How the risk changes as the uncertainty changes must be properly taken into account through the model. By cash flow risk, we mean cash flow volatility. In our two different cash flow volatility models, the risk uncertainty changes in different ways. In our first model, we assume a bounded mean-reverting quadratic diffusion process to model the cash flow volatility. Let $Q(v)$ denote the quadratic polynomial in the diffusion term of the volatility process. In this case, risk uncertainty is the highest at the local max of Q, which occurs at the midpoint of the volatility bounds. As the volatility approaches either bound, uncertainty decreases as the drift term of the volatility process gets larger in magnitude and the diffusion term gets smaller in magnitude. Our second model uses Feller process. This means that we replace the quadratic function inside the square root of the diffusion term in the previous process by the current state of the volatility. Thus, as the volatility increases, the magnitude of the diffusion term increases. As the volatility drifts down below the long run mean, the uncertainty decreases while the magnitude of the drift term increases. On the other hand, as volatility drifts above the long run mean, the uncertainty increases as the magnitude of the drift increases. Aside from accurately capturing the time varying uncertainty, the quadratic diffusion model allows project managers to put bounds on both the risk and the uncertainty coefficient. This is critical because they are most likely unable to calculate accurate volatility parameter estimates for their model.

Volatility modeling and estimation in the context of option pricing is nontrivial, and detailed discussions can be found in Musiela and Rutkowski [3]. Volatility is not observable. It must be estimated, and the estimates used matter. To circumvent this issue, uncertain volatility models have been develop in Avellaneda, Levy, and ParÁs [4] and Fouque and Ning [5]. A benefit of the uncertainty modeling is that we can establish worst case scenario bounds, as seen in Buff [6], and this is quite useful when it is not realistically possible to accurately estimate model parameters. This is certainly the case in the context of real options. In the case of real options, Brandão [7] studied volatility estimation when project values are uncertain. Our model is different, since we focus on the cash flows, not the project value directly. We believe that parameter estimates for the process modeling firm specific cash flows should be easier to accurately obtain than estimates for the corresponding volatility process, since we do not observe the volatility. Again, an uncertain volatility model allows the firm to make investment decisions when its not possible to have good estimates for the volatility parameters. Now, we will briefly discuss the models used for the cash flow volatility.

A good candidate model for our purposes is a bounded quadratic diffusion process in which uncertainty is highest at the midpoint between the bounds and decreases when approaching the bounds. The Jacobi process satisfies this property. Also known as the Wright-Fisher diffusion, the Jacobi process has been used in mathematical biology to model changes in allele frequency in a population over time, as can be seen in Durrett [8], Fleming and Viot [9], Jenkins and Spano [10], and the references therein. In mathematical finance, Delbaen and Shirakawa [11] use a Jacobi process to model the interest rate, and Ackerer, Filipovic, and Pulido [12] develop a stochastic volatility model in which a Jacobi process represents the square of the volatility. The Jacobi process is mean-reverting, and the state-dependent diffusion term of the Jacobi process allows for time varying changes in risk uncertainty. Methods for simulation and parameter estimation of the Jacobi process along with associated difficulties are described in Gourieroux and Jasiak [13], Gourieroux and Valery [14], and Jenkins and Spano [10]. One notable difficulty is the lack of closed form expression for the transition probability density function. Along these lines, we were not able to derive closed form expressions for the desired quantities in our model. Due to this, the model is very computationally expensive. This trouble is not due specifically to the Jacobi process but rather to adding stochastic volatility to the model. We believe the study of risk and time varying risk uncertainty justifies the difficulties associated with the addition of stochastic cash flow volatility. We now provide more motivation for our work from the real options literature.

A useful way to analyze the investment decision of a firm is through the framework of options, as opposed to the discounted cash flow valuation method previously mentioned. Berk, Green, and Naik [15] develop a model to study the relationship between risk, expected returns, and firm properties. In their model, firms choose whether or not to take on a new project each month, and the prospective project is called a growth option. Berk, Green, and Naik [15] use $I(j)$ to denote the one time cost of investment in a project available in month j, and $C_j(t)$ denotes the cash flow at month t from the j-th project. Then, $\frac{C_j(t)}{I(j)}$ is log-normally distributed in their model. Unlike Berk, Green, and Naik [15], in our model, $\frac{C_j(t)}{I(j)}$ is not log-normally distributed. The parameter σ_j in their paper controls the variance of the cash flows. It is determined at time j and fixed for the lifetime of the project. We develop a model that includes stochastic cash flow volatility. We use a geometric Brownian motion to model the cash flows and a Jacobi process to model cash flow volatility. The bounds on the Jacobi process $v_{\min}$ and $v_{\max}$ may in some sense be considered analogous to σ_j in Berk, Green, and Naik [15] as the bounds determine a minimum and maximum allowable volatility for the cash flows of a certain project. We consider these bounds to be measures of volatility uncertainty. Another source of uncertainty arises from the diffusion term of the Jacobi process. We study the effect of the uncertainty due to the bounds and the quadratic diffusion on returns, project values, and the rate of project investment. We now motivate the need for an uncertain volatility model.

McDonald and Siegel [16] study irreversible investment using a model in which project values, which represent expected discounted cash flows, and the cost of investment both follow geometric Brownian motions. Although our model is distinct from theirs in many ways, including the fact that we derive project values after describing the dynamics of cash flows, they remark that an increase in the variance of the value divided by the cost of investment yields higher project values. They remark that this is due to the constants in the diffusion terms of the geometric Brownian motions, and as noted in Brock, Rothschild, and Stiglitz [17], the effect of the variance on the option value is not so straightforward. Grullon, Lyandres, and Zhdanov [18] provide an explanation for the positive relationship between firm level volatility and returns and mention that in the study of real options, an increase in volatility yields an increase in value of the option. On the other hand, Nishimura and Ozaki [19] study Knightian uncertainty in the context of irreversible investment. They find that an increase in uncertainty decreases the value of an investment, but an increase in risk increases the value. Knightian uncertainty refers to not knowing the correct probability measure. In our model, we assume the correct probability measure is known and capture uncertainty through the diffusion term of the Jacobi process. We intend to see if uncertainty decreases growth option values under our new perspective of uncertainty. Moreover, few, if any, real options papers consider stochastic volatility. So, this alone is a valuable addition to the literature. In addition to Berk, Green, and Naik [15], several papers study the cross-sectional and time series relationships between expected stock returns and firm properties, including Gomes, Kogan, and Zhang [20] and Kogan and Papanikolaou [21]. Although we do not investigate these properties in this thesis, we have designed a framework in which it is possible. This is important because the correct set up is necessary to prevent the simulation from being computationally infeasible. More motivation comes from Zhang [22], who studies the value premium through basic firm properties and concludes that "assets in place much are riskier than growth options". Is this still true if the growth option risk is not known? Ai and Kiku [23] develop a growth option model in which the volatility of both consumption and cash flows is a two-state Markov process. One of their conclusions is that an increase in idiosyncratic volatility yields larger growth option values. What happens when the volatility is uncertain? In this paper, we study this question when two different diffusion processes are used to model cash flow volatility.

The remainder of the thesis is organised as follows: In the second chapter, we describe the model set up and how it differs from that of Berk, Green, and Naik [15]. Then, we write expressions required for firm valuation as a function whose value is known at time t multiplied by a time t conditional expectation defined in Equation (2.13). This greatly reduces the computational complexity of the problem. The expressions required for firm valuation include formulas for the expected future cash flows of projects currently alive and the value of future growth options. We show that under certain parameter restrictions (which make sense in practice) that the firm value does not explode. We show that our model reproduces the desirable quality that ceteris paribus firms are more likely to invest in lower interest rate environments and less likely to invest in higher interest rate environments. In the third chapter, we discuss parameter estimation. Then, we present simulation results. Our focus is on how different parameter combinations of the volatility processes affect realized returns. Interestingly, we find the rate of mean reversion to be a dominant parameter in the case of the Feller process, while the long run mean is a dominant parameter in the case of the Jacobi process. Our main result is a description of the effects of different measures of uncertainty on growth option values, realized returns, and the rate of project investment.

2. THEORY

This chapter contains the theoretical development of the model. Using continuous time stochastic processes and sampling in discrete time, we extend the model of Berk, Green, and Naik [15], henceforth referred to as BGN, to include stochastic volatility. Our main innovation is the use of a Jacobi process as the stochastic volatility of the cash flow process, and our foremost objective is demonstrating the importance of the functional form of the diffusion term in the volatility process. The Jacobi process affords us several measures of uncertainty. First, we consider the local maximum of the quadratic function in the diffusion term of the Jacobi process. This is the location of "max uncertainty." Also, we consider the upper and lower bounds of the Jacobi process as measures of uncertainty. We will explain why the lower bound acts as a measure of "good" uncertainty, while the upper bound and "max uncertainty" act as measures of "bad" uncertainty. In addition, the difference in the bounds of the paths of the Jacobi process are a measure of uncertainty, and the individual parameters of the Jacobi process will be shown to have an effect too. In our model, uncertainty represents lack of knowledge about the cash flow volatility for a specific firm. For the model to make sense, certain properties need to be satisfied. Our model reproduces the effect that firms are more likely to invest during periods of lower interest rates rather than periods of higher interest rates. Our model also reproduces the effect that a firm is more likely to accept projects with lower systematic risk, which in this case refers to the covariance between the SDF and the cash flow process. We show that the relevant series converge, which is required to prevent the explosion of firm values. Most importantly, we reduce the computational complexity of the model.

2.1 Background material

In this section, we recall the definitions necessary for the development of our model. Most importantly, we recall the definition of standard Brownian motion, which can be found in Protter [24], Privault [25], or Schilling and Partzsch [26]. We begin with the definition of a complete probability space.

Definition 2.1.1. *A probability space* $(\Omega, \mathcal{F}, \mathbb{P})$ *is complete if for every subset* A *of* B*, with* $B \in \mathcal{F}$ *and* $\mathbb{P}(B) = 0$*, it follows that* $A \in \mathcal{F}$*.*

In finance, it is useful to condition on the latest information. To this end, we recall the definition of a filtration on a complete probability space.

Definition 2.1.2. *Given a complete probability space* $(\Omega, \mathcal{F}, \mathbb{P})$*, a filtration is an increasing sequence of sigma algebras* $\mathbb{F} = (\mathcal{F}_t)_{t \in [0,\infty]}$ *contained in* $\mathcal{F}$*, i.e.,* $\forall s \leq t \; \mathcal{F}_s \subset \mathcal{F}_t \subset \mathcal{F}$*.*

It is standard to assume that a complete filtered probability space $(\Omega, \mathcal{F}, \mathcal{F}_t, \mathbb{P})$ satisfies the "usual conditions," as defined below.

Definition 2.1.3. *The usual conditions for* $(\Omega, \mathcal{F}, \mathcal{F}_t, \mathbb{P})$*, as defined in Protter [24], are as follows:*

1. *If* $A \in \mathcal{F}$ *and* $\mathbb{P}(A) = 0$*, then* $A \in \mathcal{F}_0$*.*

2. *For every* $t \in [0, \infty)$*, we have* $\mathcal{F}_t = \bigcap_{u>t} \mathcal{F}_u$*.*

We are now in a position to define standard Brownian motion, which will be driving the stochastic processes used in our model.

Definition 2.1.4. *A standard Brownian motion is a collection of random variables* $B = (B_t)_{t \in [0,\infty)}$ *satisfying the following properties:*

1. B *is a real-valued function on* $[0, \infty) \times \Omega$*, namely* $B : [0, \infty) \times \Omega \to \mathbb{R}$*, and for every* $t \in [0, \infty)$ *the function* $B_t : \Omega \to \mathbb{R}$ *is* $\mathcal{F}/\mathcal{B}(\mathbb{R})$ *measurable.*

2. $\mathbb{P}(\omega \in \Omega : B_0(w) = 0) = 1$*.*

3. $\mathbb{P}(\omega \in \Omega : t \mapsto B_t(\omega) \text{ is continuous}) = 1$*.*

4. $B(s) - B(t) \sim \mathcal{N}(0, s - t)$*, i.e.* $B(s) - B(t)$ *is normally distributed with mean* 0 *and variance* $s - t$*.*

5. *For every* $n \in \mathbb{N}$ *and for every subset* $\{t_i\}_{i=1}^{i=n} \subset [0, \infty)$ *with* $0 = t_0 < t_1 < \cdots < t_n < \infty$*, it follows that* $B_{t_1} - B_{t_0}, \cdots, B_{t_n} - B_{t_{n-1}}$ *are mutually independent.*

In everything that follows, we will assume every Brownian motion is a standard Brownian motion. Next, we explain what it means for a Brownian motion to be adapted to a filtration, define its natural filtration, and define an admissible filtration.

Definition 2.1.5. *A Brownian motion $B = (B_t)_{t\in[0,\infty)}$ is adapted to the filtration $\mathbb{F} = (\mathcal{F}_t)_{t\in[0,\infty)}$ if for every $t \in [0, \infty)$ it follows that B_t is an $\mathcal{F}_t$ measurable random variable.*

Definition 2.1.6. *The natural filtration of a Brownian motion $B = (B_t)_{t\in[0,\infty)}$ is the collection of sigma algebras $\mathbb{F}^B = (\mathcal{F}_t^B)_{t\in[0,\infty)}$ defined by $\mathcal{F}_t^B = \sigma(B_s : s \leq t)$. This is the smallest filtration making B adapted.*

Definition 2.1.7 (Schilling and Partzsch [26])**.** *An admissible filtration $\mathbb{F} = (\mathcal{F}_t)_{t\in[0,\infty)}$ for the Brownian motion $B = (B_t)_{t\in[0,\infty)}$ satisfies*

1. *For every $t \in [0, \infty)$ it follows that $\mathcal{F}_t^B \subset \mathcal{F}_t$.*

2. *For every $s \in [0, t)$ it follows that $B_t - B_s \perp\!\!\!\perp \mathcal{F}_s$.*

2.2 Stochastic processes

In this section, we present the stochastic processes that will be used in the model. Let $(\Omega, \mathcal{F}, \mathcal{F}_t', \mathbb{P})$ be a complete filtered probability space satisfying the usual conditions. For every $j \in \mathbb{Z}^+$, let $W^I, W^r, W^{C_j}, W^{V_j},$ and W^M be $\mathbb{P}$-standard Brownian motions adapted to the filtration $\mathcal{F}_t'$. Here, j is the index of the j-th project arriving for a particular firm at month j. Each firm has its own collection of W^{C_j} and W^{V_j} for all j. Though we have suppressed the index identifying the individual firm, we include here the collection of all W^{C_j} and W^{V_j} across all firms in existence. Since for all j, W^{C_j} are correlated with W^M and W^r, W^{C_j} and W^{C_i} can't be independent for any value of i, including j. It's possible to find bounds on the correlation between W^{C_j} and W^{C_i}, but knowledge of the value of this correlation is not required in our model. Also, for $s \leq t$, we assume that $W^{C_j}(s)$ and $W^{V_j}(s)$ are $\mathcal{F}_t'$ measurable, but we assume that the individual firm does not see the information regarding a project until it arrives. From now on, we now focus our attention on the individual firm. Everything is easily generalized to the case of many firms. In that case, all firms experience the same interest rate and SDF processes. Thus, the information available to the firm at time t is given by the join of the sigma algebras generated by $\sigma(W^I(s) : 0 \leq s \leq t)$, $\sigma(W^r(s) : 0 \leq s \leq t)$, $\sigma(W^M(s) : 0 \leq s \leq t)$, $\sigma(W^{V_j}(s) : j \leq s \leq t)$, and $\sigma(W^{C_j}(s) : j \leq s \leq t)$ for all integers $j \leq t$, and we denote this sigma algebra by $\mathcal{F}_t$. Again, W^{V_j} and $V_j(j)$ are not observed until time j when the j-th project becomes available. We now go into details of the processes used in our model.

Let $I(j)$ be the cost of the project that arrives at month j. This is the initial investment cost that is paid once, only if a project that arrives at month j is going to be executed. Thus, from the standpoint of an option, this is a strike price that is known at month j, but future strike prices are unknown. Let this initial investment of the project follow the dynamics

$$\frac{\mathrm{d}I(t)}{I(t)} = \mu_I dt + \sigma_I \, \mathrm{d}W^I(t). \tag{2.1}$$

This of course has the solution for $s > t$:

$$I(s) = I(t)\mathrm{e}^{(\mu_I - \frac{\sigma_I^2}{2})(s-t) + \sigma_I W^I(s-t)}. \tag{2.2}$$

The computation is done by applying Ito's formula to $\log(I(t))$, and the derivation can be found in Klebaner [27]. We assume I is independent of all the other processes in this model. Note that $I(t)$ could also be represented as a mean reverting process to account for the flows of the business cycle. Unfortunately, this significantly complicates an already computationally expensive problem. One factor affecting the decision to invest is the interest rate process and its value at the time of the potential investment.

We model the interest rate with the Vasicek model. The interest rate follows the dynamics

$$\mathrm{d}r(t) = a(b_2 - r(t)) \, \mathrm{d}t + \sigma_r \, \mathrm{d}W^r(t). \tag{2.3}$$

We desire to find a way to relate the interest rate $r(s)$ at time s to the interest rate $r(t)$ at time t, for $s > t$. We do this in the following derivation, which is standard. We begin by differentiating $\mathrm{e}^{at}r(t)$.

$$\begin{aligned}
\mathrm{d}(\mathrm{e}^{at}r(t)) &= a\mathrm{e}^{at}r(t)\,\mathrm{d}t + \mathrm{e}^{at}\,\mathrm{d}r(t) \\
&= a\mathrm{e}^{at}r(t)\,\mathrm{d}t + \mathrm{e}^{at}(a(b_2 - r(t))\,\mathrm{d}t + \sigma_r\,\mathrm{d}W^r(t)) \\
&= ab_2\mathrm{e}^{at}\,\mathrm{d}t + \sigma_r\mathrm{e}^{at}\,\mathrm{d}W^r(t).
\end{aligned}$$

Integrating yields

$$\mathrm{e}^{as}r(s) = \mathrm{e}^{at}r(t) + ab_2\int_t^s \mathrm{e}^{au}\,\mathrm{d}u + \sigma_r\int_t^s \mathrm{e}^{au}\,\mathrm{d}W^r(u).$$

Multiplying each side by e^{-as} leads to an expression for $r(s)$ given $r(t)$:

$$r(s) = r(t)\mathrm{e}^{-a(s-t)} + b_2(1 - \mathrm{e}^{-a(s-t)}) + \sigma_r\mathrm{e}^{-as}\int_t^s \mathrm{e}^{au}\,\mathrm{d}W^r(u). \tag{2.4}$$

We are now in a position to give formulas for the conditional expectation and variance of the interest rate at time s, given the value of the interest rate at time t.

Lemma 2.2.1. *The conditional distribution of $r(s)$ given $r(t) = r$ is normal with conditional mean*

$$\mathbb{E}\left[r(s)|r(t) = r\right] = r(t)\mathrm{e}^{-a(s-t)} + b_2(1 - \mathrm{e}^{-a(s-t)})$$

and conditional variance

$$\mathbb{V}\left[r(s)|r(t) = r\right] = \frac{\sigma_r^2}{2a}(1 - \mathrm{e}^{-2a(s-t)}).$$

Proof. Since $\int_t^s \mathrm{e}^{au}\,\mathrm{d}W^r(u)$ is normally distributed, normality of the conditional distribution is obvious. We proceed to calculate the desired conditional expectation.

$$\begin{aligned}
\mathbb{E}\left[r(s)|r(t) = r\right] = \mathbb{E}\left[r(t)\mathrm{e}^{-a(s-t)}|r(t) = r\right] + \mathbb{E}\left[b_2(1 - \mathrm{e}^{-a(s-t)})|r(t) = r\right] \\
+ \mathbb{E}\left[\sigma_r\mathrm{e}^{-as}\int_t^s \mathrm{e}^{au}\,\mathrm{d}W^r(u)|r(t) = r\right]
\end{aligned}$$

$$= r(t)\mathrm{e}^{-a(s-t)} + b_2(1 - \mathrm{e}^{-a(s-t)}).$$

Next, the conditional variance is given as follows. The third equality will use Ito's isometry and independence.

$$\begin{aligned}
\mathbb{V}\,[r(s)|r(t) = r] &= \mathbb{V}\,[r(t)\mathrm{e}^{-a(s-t)} + b_2(1 - \mathrm{e}^{-a(s-t)}) + \sigma_r \mathrm{e}^{-as} \int_t^s \mathrm{e}^{au}\,\mathrm{d}W^r(u)|r(t) = r] \\
&= \mathbb{V}\,[\sigma_r \mathrm{e}^{-as} \int_t^s \mathrm{e}^{au}\,\mathrm{d}W^r(u)|r(t) = r] \\
&= \mathbb{E}\,[\sigma_r \mathrm{e}^{-as} \int_t^s \mathrm{e}^{au}\,\mathrm{d}W^r(u)]^2 \\
&= \sigma_r^2 \mathrm{e}^{-2as}\,\mathbb{E}\,[\int_t^s \mathrm{e}^{2au}\,\mathrm{d}u] = \frac{\sigma_r^2}{2a}(1 - \mathrm{e}^{-2a(s-t)}).
\end{aligned}$$

This completes our proof. □

Lemma 2.2.2. *For all $s > t$, the conditional distribution of the random variable $-\int_t^s r(u)\,\mathrm{d}u$ given $r(t) = r$ is normal with conditional mean*

$$\mathbb{E}\,[-\int_t^s r(u)\,\mathrm{d}u|r(t) = r] = (\frac{b_2 - r(t)}{a})[1 - \mathrm{e}^{-a(s-t)}] - b_2(s-t)$$

and conditional variance

$$\mathbb{V}\,[-\int_t^s r(u)\,\mathrm{d}u|r(t) = r] = \frac{\sigma_r^2}{a^2}(s - t + \frac{1}{2a} - \frac{1}{2a}[\mathrm{e}^{a(t-s)} - 2]^2).$$

Proof. First, note the following equality.

$$-\int_t^s r(u)\,\mathrm{d}u = (b_2 - r(t))\int_t^s \mathrm{e}^{-a(u-t)}\,\mathrm{d}u - \int_t^s b_2\,\mathrm{d}u - \sigma_r \int_t^s \mathrm{e}^{-au}\left(\int_t^u \mathrm{e}^{ap}\,\mathrm{d}W^r(p)\right)\mathrm{d}u.$$

Let us consider the integral $\int_t^u \mathrm{e}^{ap}\,\mathrm{d}W_p^r$, which is normally distributed. The mean of this random variable is clearly zero. Using the Ito isometry, we now calculate the variance.

$$\begin{aligned}
\mathbb{V}(\int_t^u \mathrm{e}^{ap}\,\mathrm{d}W_p^r|\mathcal{F}_t) &= \mathbb{E}\,[(\int_t^u \mathrm{e}^{ap}\,\mathrm{d}W_p^r)^2|\mathcal{F}_t] \\
&= \mathbb{E}\,[\int_t^u \mathrm{e}^{2ap}\,\mathrm{d}p|\mathcal{F}_t]
\end{aligned}$$

$$
\begin{aligned}
&= \int_t^u \mathrm{e}^{2ap}\,\mathrm{d}p \\
&= \frac{\mathrm{e}^{2au}-\mathrm{e}^{2at}}{2a}.
\end{aligned}
$$

Thus, $\int_t^u \mathrm{e}^{ap}\,\mathrm{d}W_p^r \sim \mathcal{N}(0, \frac{\mathrm{e}^{2au}-\mathrm{e}^{2at}}{2a})$, and it follows that

$$
\sigma_r \mathrm{e}^{-au}\int_t^u \mathrm{e}^{ap}\,\mathrm{d}W_p^r \sim \mathcal{N}(0, \frac{\sigma_r^2}{2a}(1-\mathrm{e}^{2a(t-u)})).
$$

Now, let $I(t,s) := \int_t^s \int_t^u \mathrm{e}^{-a(u-p)}\,\mathrm{d}W_p^r\,\mathrm{d}u$. By Fubini's theorem,

$$
\begin{aligned}
I(t,s) &= \int_t^s \int_p^s \mathrm{e}^{-a(u-p)}\,\mathrm{d}u\,\mathrm{d}W_p^r \\
&= \int_t^s \mathrm{e}^{ap} \int_p^s \mathrm{e}^{-au}\,\mathrm{d}u\,\mathrm{d}W_p^r \\
&= \int_t^s \mathrm{e}^{ap} \left[-\frac{1}{a}\mathrm{e}^{-au}\right]_{u=p}^{u=s} \mathrm{d}W_p^r \\
&= \frac{1}{a}\int_t^s (1-\mathrm{e}^{a(p-s)})\,\mathrm{d}W_p^r.
\end{aligned}
$$

Clearly, $I(t,s)$ is normally distributed, with conditional mean and conditional variance as follows:

$$
\mathbb{E}\left[I(t,s)|\mathcal{F}_t\right] = \frac{1}{a}\,\mathbb{E}\left[\int_t^s (1-\mathrm{e}^{a(p-s)})\,\mathrm{d}W_p^r|\mathcal{F}_t\right] = 0,
$$

$$
\mathbb{V}(I(t,s)|\mathcal{F}_t) = \frac{1}{a^2}\,\mathbb{E}\left[\left(\int_t^s (1-\mathrm{e}^{a(p-s)})\,\mathrm{d}W_p^r\right)^2|\mathcal{F}_t\right] = \frac{1}{a^2}\int_t^s (1-\mathrm{e}^{a(p-s)})^2\,\mathrm{d}p.
$$

We calculate the following integral appearing in the variance:

$$
\begin{aligned}
K(t,s) :&= \int_t^s [1-\mathrm{e}^{a(p-s)}]^2\,\mathrm{d}p \\
&= \int_t^s \mathrm{d}p - 2\mathrm{e}^{-as}\int_t^s \mathrm{e}^{ap}\,\mathrm{d}p + \mathrm{e}^{-2as}\int_t^s \mathrm{e}^{2ap}\,\mathrm{d}p \\
&= s-t-\frac{2\mathrm{e}^{-as}}{a}(\mathrm{e}^{as}-\mathrm{e}^{at}) + \frac{\mathrm{e}^{-2as}}{2a}[\mathrm{e}^{2as}-\mathrm{e}^{2at}] \\
&= s-t-\frac{1}{2a}[3-4\mathrm{e}^{a(t-s)}+(\mathrm{e}^{a(t-s)})^2] \\
&= s-t+\frac{1}{2a}-\frac{1}{2a}[\mathrm{e}^{a(t-s)}-2]^2.
\end{aligned}
$$

Thus, we have $\sigma_r I(t,s) \sim \mathcal{N}(0, \frac{\sigma_r^2}{a^2}K(t,s))$. Returning to the integral in question,

$$-\int_t^s r(u)\,\mathrm{d}u = (\frac{b_2 - r(t)}{a})[1-\mathrm{e}^{-a(s-t)}] - b_2(s-t) - \frac{\sigma_r}{a}\int_t^s (1-\mathrm{e}^{-a(s-p)})\,\mathrm{d}W^r(p).$$

From here, we can easily calculate the conditional expectation and variance of $-\int_t^s r(u)\,\mathrm{d}u$ given the interest rate at time t.

$$\mathbb{E}\left[-\int_t^s r(u)\,\mathrm{d}u | r(t) = r\right] = \left(\frac{b_2 - r(t)}{a}\right)(1-\mathrm{e}^{-a(s-t)}) - b_2(s-t),$$

and

$$\begin{aligned}\mathbb{V}\,[-\int_t^s r(u)\,\mathrm{d}u | r(t) = r] &= \mathbb{E}\,[-\frac{\sigma_r}{a}\int_t^s (1-\mathrm{e}^{-a(s-p)})\,\mathrm{d}W^r(p)]^2 \\ &= \frac{\sigma_r^2}{a^2}\int_t^s (1-\mathrm{e}^{-a(s-p)})^2\,\mathrm{d}p \\ &= \frac{\sigma_r^2}{a^2}(s-t+\frac{1}{2a} - \frac{1}{2a}[\mathrm{e}^{a(t-s)}-2]^2),\end{aligned}$$

where the first equality follows by independence and the Ito isometry. □

Cash flow volatility is modeled by a Jacobi process, as its properties are conducive to properly modeling risk uncertainty. The following definition of the Jacobi process and the notation employed here are from Ackerer, Filipovic, and Pulido [12]. Similar definitions, though possibly for the case when $v_{\min} = 0$ or $v_{\max} = 1$ can be found in Delbaen and Shirakawa [11], Gourieroux and Jasiak [13], and Gourieroux and Valery [14]. Let $v_{\min}, v_{\max} \in \mathbb{R}^+$, with $0 < v_{\min} < v_{\max}$. Let $\theta \in (v_{\min}, v_{\max})$, $\kappa \in \mathbb{R}^+$ (the positive real numbers), and $\sigma_V \in \mathbb{R}^+$. As stated in Delbaen and Shirakawa [11], under these conditions, the Jacobi process will have a stationary Beta distribution. Let W^V be a $\mathbb{P}$-standard Brownian motion adapted to the filtration $\mathcal{F}_t$. Let the function $Q : [v_{\min}, v_{\max}] \to \mathbb{R}$ be defined by

$$Q(v) = \frac{(v - v_{\min})(v_{\max} - v)}{(\sqrt{v_{\max}} - \sqrt{v_{\min}})^2}. \tag{2.5}$$

The diffusion process V satisfying the dynamics

$$\mathrm{d}V(t) = \kappa(\theta - V(t))\,\mathrm{d}t + \sigma_V\sqrt{Q(V(t))}\,\mathrm{d}W^V(t) \tag{2.6}$$

is called a Jacobi process. As noted in Ackerer, Filipovic, and Pulido [12], if $V(t) \in (v_{\min}, v_{\max})$, then $V(t) - v_{\min} > 0$ and $v_{\max} - V(t) > 0$ implies $Q(V(t)) > 0$. So, it is clear that if V stays within the bounds $v_{\min}$ and $v_{\max}$, then V is real-valued. It is also noted, without proof, in Ackerer, Filipovic, and Pulido [12] that $V(t) \geq Q(V(t))$, where equality holds if and only if $v = \sqrt{v_{\min}v_{\max}}$. We will prove this.

Proof. We want to first prove that $V(t) \geq Q(V(t))$. To this aim, we first expand the square in the relation $(V(t) - \sqrt{v_{\min}v_{\max}})^2 \geq 0$. In the second step below, we rearrange terms and add $V(t)v_{\max} + V(t)v_{\min}$ to each side of the inequality. In the third step, we factor out $V(t)$ on the left hand side.

$$\begin{aligned}
V^2(t) - 2V(t)\sqrt{v_{\min}v_{\max}} + v_{\min}v_{\max} &\geq 0\\
V(t)v_{\max} - 2V(t)\sqrt{v_{\min}v_{\max}} + V(t)v_{\min} &\geq V(t)v_{\max} - V^2(t) - v_{\min}v_{\max} + v_{\min}V(t)\\
V(t)(v_{\max} - 2\sqrt{v_{\min}v_{\max}} + v_{\min}) &\geq V(t)v_{\max} - V^2(t) - v_{\min}v_{\max} + v_{\min}V(t).
\end{aligned}$$

Rearranging and factoring yields

$$\begin{aligned}
V(t)(\sqrt{v_{\max}} - \sqrt{v_{\min}})^2 &\geq V(t)(v_{\max} - V(t)) - v_{\min}(v_{\max} - V(t))\\
&= (v_{\max} - V(t))(V(t) - v_{\min}).
\end{aligned}$$

This gives the conclusion that $V(t) \geq Q(V(t))$, where Q is defined in Equation (2.5).

Let us now show that $V(t) = Q(V(t))$ if and only if $V(t) = \sqrt{v_{\min}v_{\max}}$. First, suppose that $V(t) = \sqrt{v_{\min}v_{\max}}$. Then, recalling the definition of Q given in Equation (2.5), we use algebra to see that $Q(V(t)) = \sqrt{v_{\min}v_{\max}}$. This is done below.

$$Q(V(t)) = \frac{(v_{\max} - \sqrt{v_{\min}v_{\max}})(\sqrt{v_{\min}v_{\max}} - v_{\min})}{(\sqrt{v_{\max}} - \sqrt{v_{\min}})^2}$$

$$
\begin{aligned}
&= \frac{v_{\min}^{1/2} v_{\max}^{3/2} - 2 v_{\min} v_{\max} + v_{\min}^{3/2} v_{\max}^{1/2}}{(\sqrt{v_{\max}} - \sqrt{v_{\min}})^2} \\
&= \frac{\sqrt{v_{\min} v_{\max}}(v_{\max} - 2\sqrt{v_{\min} v_{\max}} + v_{\min})}{(\sqrt{v_{\max}} - \sqrt{v_{\min}})^2} \\
&= \frac{\sqrt{v_{\min} v_{\max}}(\sqrt{v_{\max}} - \sqrt{v_{\min}})^2}{(\sqrt{v_{\max}} - \sqrt{v_{\min}})^2} \\
&= \sqrt{v_{\min} v_{\max}}.
\end{aligned}
$$

Finally, suppose that $V(t) = Q(V(t))$. Then,

$$
V(t)(v_{\max} - 2\sqrt{v_{\min} v_{\max}} + v_{\min}) = v_{\max} V(t) - v_{\min} v_{\max} - V^2(t) + V(t) v_{\min}.
$$

By cancelling terms in the above expression we arrive at the following equation.

$$
-2V(t)\sqrt{v_{\min} v_{\max}} = -v_{\min} v_{\max} - V^2(t).
$$

We now rearrange and factor.

$$
\begin{aligned}
0 &= V^2(t) - 2V(t)\sqrt{v_{\min} v_{\max}} + v_{\min} v_{\max} \\
&= (V(t) - \sqrt{v_{\min} v_{\max}})^2.
\end{aligned}
$$

Thus, we arrive at the desired conclusion $V(t) = \sqrt{v_{\min} v_{\max}}$.

□

We now record a special case of a theorem justifying the existence and uniqueness of the Jacobi process. A proof can be found on page 2 of Delbaen and Shirakawa [11].

Theorem 2.2.3 (Theorem 2.1 of Ackerer, Filipovic, and Pulido [12])**.** *Given a deterministic initial state $V_0 \in [v_{\min}, v_{\max}]$, there exists a unique solution $V(t)$ of 2.6 taking values in $[v_{\min}, v_{\max}]$ such that $\int_0^\infty 1_{V(t)=v}\, \mathrm{d}t = 0$ for every $v \in [v_{\min}, v_{\max})$. Also, the process $V(t)$ takes values in $(v_{\min}, v_{\max})$ iff $V(0) \in (v_{\min}, v_{\max})$ and*

$$
\frac{\sigma_V^2 (v_{\max} - v_{\min})}{(\sqrt{v_{\max}} - \sqrt{v_{\min}})^2} \leq 2\kappa \min\{v_{\max} - \theta, \theta - v_{\min}\}. \tag{2.7}
$$

The condition (2.7) is critical as it ensures the Jacobi process stays within the bounds.

We now turn our attention to the derivation of conditional expectations.

Lemma 2.2.4. *If $u < t$, then the conditional expectation $\mathbb{E}\left[V(t)|V(u) = v\right]$ is given by*

$$\mathbb{E}\left[V(t)|V(u) = v\right] = \theta + (v - \theta)\mathrm{e}^{-\kappa(t-u)}. \tag{2.8}$$

Proof. Recall the definition of Q: $Q(V(t)) = \frac{(v_{\max}-V(t))(V(t)-v_{\min})}{(\sqrt{v_{\max}}-\sqrt{v_{\min}})^2}$. First, we differentiate the product $\mathrm{e}^{\kappa t}V(t)$.

$$\begin{aligned}
\mathrm{d}(\mathrm{e}^{\kappa t}V(t)) &= \mathrm{e}^{\kappa t}\,\mathrm{d}V(t) + \kappa\mathrm{e}^{\kappa t}V(t)\,\mathrm{d}t \\
&= \kappa\mathrm{e}^{\kappa t}V(t)\,\mathrm{d}t + \mathrm{e}^{\kappa t}(\kappa\theta - \kappa V(t))\,\mathrm{d}t + \sigma_V\mathrm{e}^{\kappa t}\sqrt{Q(V(t))}\,\mathrm{d}W^V(t) \\
&= \kappa\theta\mathrm{e}^{\kappa t}\,\mathrm{d}t + \sigma_V\mathrm{e}^{\kappa t}\sqrt{Q(V(t))}\,\mathrm{d}W^V(t).
\end{aligned}$$

Integrating from u to t yields the following.

$$\mathrm{e}^{\kappa t}V(t) = \mathrm{e}^{\kappa u}V(u) + \kappa\theta\int_u^t \mathrm{e}^{\kappa s}\,\mathrm{d}s + \sigma_V\int_u^t \mathrm{e}^{\kappa s}\sqrt{Q(V(s))}\,\mathrm{d}W^V(s).$$

Now, we multiply each side by $\mathrm{e}^{-\kappa t}$.

$$\begin{aligned}
V(t) &= V(u)\mathrm{e}^{-\kappa(t-u)} + \kappa\theta\mathrm{e}^{-\kappa t}\int_u^t \mathrm{e}^{\kappa s}\,\mathrm{d}s + \sigma_V\mathrm{e}^{-\kappa t}\int_u^t \mathrm{e}^{\kappa s}\sqrt{Q(V(s))}\,\mathrm{d}W^V(s) \\
&= V(u)\mathrm{e}^{-\kappa(t-u)} + \theta(1 - \mathrm{e}^{-\kappa(t-u)}) + \sigma_V\mathrm{e}^{-\kappa t}\int_u^t \mathrm{e}^{\kappa s}\sqrt{Q(V(s))}\,\mathrm{d}W^V(s).
\end{aligned}$$

We now arrive at our conclusion.

$$\begin{aligned}
\mathbb{E}\left[V(t)|V(u) = v\right] &= V(u)\mathrm{e}^{-\kappa(t-u)} + \theta(1 - \mathrm{e}^{-\kappa(t-u)}) \\
&= v\mathrm{e}^{-\kappa(t-u)} + \theta(1 - \mathrm{e}^{-\kappa(t-u)}).
\end{aligned}$$

□

We will use a stochastic discount factor (SDF) process which follows the dynamics

$$\frac{\mathrm{d}M(t)}{M(t)} = -r(t)\,\mathrm{d}t - \lambda(t)\,\mathrm{d}W^M(t),$$

where λ is the market price of risk, which we will assume to be a constant. The SDE for the SDF has the following solution for $s > t$:

$$M(t) = M(0)\mathrm{e}^{-\int_0^t \lambda(s)\,\mathrm{d}W^M(s) - \frac{1}{2}\int_0^t \lambda^2(s)\,\mathrm{d}s - \int_0^t r(s)\,\mathrm{d}s}. \tag{2.9}$$

We are now in a position to describe the model.

2.3 The model

Our model is an extension of the one in Berk, Green, and Naik [15]. When possible, the notation has been kept the same or similar. Their model is designed to explain standard results in the empirical finance literature from the perspective of individual firm investment decisions. In our model, as in theirs, a project becomes available at every month to each firm, and this investment opportunity is called a **growth option**.

Let $\boldsymbol{\pi} \in (0, 1)$ be a parameter affecting project lifetimes. The random variables $\{Y_j(t+1)\}$ with $t \geq j$ are a collection of Bernoulli random variables for every $j \in \mathbb{Z}^+$ with probability mass function $\mathbb{P}(Y_j(t+1) = 1) = \boldsymbol{\pi}$ and $\mathbb{P}(Y_j(t+1) = 0) = 1 - \boldsymbol{\pi}$. We assume the random variables Y_j are independent of all other random variables in the model. Also, we assume that $Y_j(t)$ is adapted to the filtration $\mathcal{F}_t$ for all real t and for all positive integers j. In practice, we will only be concerned with $Y_j(t)$ for positive integer values of t, since cash flows come in on a monthly basis. We now make remarks on the parameter $\boldsymbol{\pi}$, which can be made to be firm specific or even random. Our model for cash flow volatility is mean-reverting. If $\boldsymbol{\pi}$ is large for a particular project, the project will tend to have a long lifetime. The information available at a particular month, especially the value of the Jacobi process at that month, may not have a significant effect on the value of the cash flows if the project has a long lifetime. What matters is what happens "on average" in our model set up. We now describe how the project lifetime is determined.

Let $j \in \mathbb{Z}^+$ be the month that a project has arrived. The indicator random variables $\{\chi_j(t)\}_{t \geq j}$ determine the lifetime of the j-th project. For every j, for every $t \geq j$, $\chi_j(t)$ is defined by $\chi_j(t+1) = \chi_j(t)Y_j(t+1)$. This has the following meaning:

$$\chi_j(t) = \begin{cases} 0 & \text{if the project has been terminated on or before time } t. \\ 1 & \text{if the project has not yet been terminated at time } t. \end{cases}$$

The value of $\chi_j(j)$ is determined at time j, when the option to take on the project is available.

$$\chi_j(j) = \begin{cases} 0 & \text{if the project is not taken on.} \\ 1 & \text{if the project is taken on.} \end{cases}$$

The j-th project is taken on if its net present value, henceforth NPV, is positive. The NPV is the current expected value of all future cash flows from the project minus the initial cost of investment. We now describe project cash flows for a specific firm, and we begin with cash flow volatility.

The volatility of the cash flows of projects are modeled by a Jacobi process. For comparison, we also use a Cox-Ingersoll-Ross (CIR) process to model cash flow volatility. The difference arises in the diffusion term of the volatility process, which is bounded for the Jacobi process but not bounded for the CIR process. Furthermore, in the case of the Jacobi process, volatility uncertainty decreases as it moves from the location of max volatility uncertainty to the bounds. In the case of the CIR process, volatility uncertainty increases monotonically as volatility increases. We begin with the Jacobi process.

We consider a time-varying and stochastic volatility that is likely to capture cash flow uncertainty for the specific firm in question. Assume that for every j, $V_j(t)$ is a Jacobi process. The subscript j on the Jacobi process indicates that V_j is specific to the j-th project. We assume that the parameters of the Jacobi process are firm specific, so $\kappa, \sigma_V, v_{\min}, v_{\max}$, and θ are all firm specific. Thus, $v_{\min} \leq V_j(t) \leq v_{\max}$, and we consider the difference in the bounds, $v_{\max} - v_{\min}$, as a measure of the scope of cash flow uncertainty. Additionally, we consider the local max of Q, the lower bound $v_{\min}$, and the upper bound $v_{\max}$ to be other measures of uncertainty. Let $\theta \in (v_{\min}, v_{\max})$ and $\kappa > 0$. The Jacobi process for the j-th project follows the dynamics

$$\mathrm{d}V_j(t) = \kappa(\theta - V_j(t))\,\mathrm{d}t + \sigma_V \sqrt{Q(V_j(t))}\,\mathrm{d}W^{V_j}(t). \tag{2.10}$$

In the current set up, all growth options for a certain firm are ex ante identical. For every j, let $\mathcal{F}^j_{t,s} = \sigma(V_j(u) : t \leq u \leq s)$. Conditioning on $\mathcal{F}^j_{t,s}$ allows for a reduction in computational complexity, which will be seen later. This reduction is extremely useful because the problem ultimately requires the computation of a large number of monte carlo simulations. For comparison, we will consider a different form of the diffusion term. We also study the case in which the cash flow volatility follows a CIR process, which is given below.

$$\mathrm{d}V_j(t) = \kappa(\theta - V_j(t))\,\mathrm{d}t + \sigma_V \sqrt{V_j(t)}\,\mathrm{d}W^{V_j}(t). \tag{2.11}$$

For the CIR process, we require that κ, θ, and σ_V satisfy the Feller condition $2\kappa\theta > \sigma_V^2$, so that $V_j(t) > 0$ for all $t \geq j$. We now turn our attention to the cash flows.

The cash flows of a project beginning at date j follow the dynamics

$$\frac{\mathrm{d}C_j(t)}{C_j(t)} = \mu\,\mathrm{d}t + \sigma V_j(t)\,\mathrm{d}W^{C_j}(t),$$

which has the solution for $t \geq j$:

$$C_j(t) = C_j(j)\mathrm{e}^{\mu(t-j)+R(j,j,t)}, \tag{2.12}$$

where $R(j,t,s) = \sigma \int_t^s V_j(u)\,\mathrm{d}W^{C_j}(u) - \frac{\sigma^2}{2}\int_t^s V_j^2(u)\,\mathrm{d}u$ for every $j, t, s \in \mathbb{R}^+$ with $s \geq t$. The firm does not receive the cash flow $C_j(j)$ at time j. The first possible cash inflow is at time $j+1$ for the j-th project. Define $\overline{C}(j) = \ln \frac{C_j(j)}{I(j)}$, but we will write $\overline{C}$ instead of $\overline{C}(j)$, as this parameter will be the same across all projects for a specific firm.

Now, we define the following constant and functions. Let the constant C_1 be defined by $C_1 = \frac{\lambda\sigma_r\rho^{Mr}}{a} - b_2 + \frac{\sigma_r^2}{2a^2}$. Let $C_2 : [0,\infty) \to \mathbb{R}$ and $C_3 : [0,\infty) \to \mathbb{R}$ be functions of the interest rate defined as follows: $C_2(t) = \frac{b_2 - r(t)}{a} - \frac{\lambda\sigma_r\rho^{Mr}}{a^2} - \frac{3\sigma_r^2}{4a^3}$ and $C_3(t) = \frac{\sigma_r^2}{4a^3} - C_2(t)$. After defining

$C_{41} : (\mathbb{R}^+)^3 \to \mathbb{R},\ C_{42} : (\mathbb{R}^+)^2 \to \mathbb{R},$ and $C_{43} : (\mathbb{R}^+)^2 \to \mathbb{R}$, we will define $C_4 : (\mathbb{R}^+)^3 \to \mathbb{R}$ as a combination of these functions.

$$\begin{aligned}
C_{41}(j,t,s) &= \overline{C} + \mu(s-j) + (s-t-1)C_1 - \frac{\sigma_r^2}{4a^3}\mathrm{e}^{-2a(s-t-1)},\\
C_{42}(t,s) &= \frac{\sigma_r^2}{4a^3} + \frac{\sigma_r^2}{4a^3}(1-\mathrm{e}^{-a(s-t-1)})^2(1-\mathrm{e}^{-2a}) + (\frac{b_2}{a} - \frac{\lambda\sigma_r\rho^{Mr}}{a^2} - \frac{\sigma_r^2}{a^3})(1-\mathrm{e}^{-a(s-t-1)}),\\
C_{43}(t,s) &= (\frac{r(t)\mathrm{e}^{-a} + b_2(1-\mathrm{e}^{-a})}{a})(\mathrm{e}^{-a(s-t-1)} - 1),\\
C_4(j,t,s) &= \mathrm{e}^{C_{41}(j,t,s)+C_{42}(t,s)+C_{43}(t,s)}.
\end{aligned}$$

Our model incorporates multiple sources of risk in addition to the risk and uncertainty associated with the Jacobi process. These other sources include the correlations between the standard Brownian motions driving the interest rate, the SDF, and the cash flow processes for each of the projects. Let ρ^{r,C_j} represent the correlation between the standard Brownian motions driving the interest rate process and the cash flow process of the j-th project. Let $\rho^{M,r}$ represent the correlation between the standard Brownian motions driving the interest rate process and the SDF process. Let ρ^{M,C_j} represent the correlation between the standard Brownian motions driving the SDF process and the cash flow process of the j-th project. We list restrictions on the following parameters: $\rho^{r,C_j} > 0$, $a > 0$, $\sigma > 0$, and $\sigma_r > 0$. Let ρ^{M,C_j} be a random variable. Let $\rho_l^{M,C_j}, \rho_u^{M,C_j} \in [-1,1]$ be lower and upper bounds on ρ^{M,C_j}, respectively. Let $\mathcal{P}_j$ denote the set $[\rho_l^{M,C_j}, \rho_u^{M,C_j}]$. Define the constant $C_6 = \frac{\sigma\sigma_r\rho^{r,C_j}}{a}$. Let the function $C_7 : \mathbb{Z}^+ \to \mathbb{R}$ be defined by $C_7(j) = -\frac{\sigma\sigma_r\rho^{r,C_j}}{a} - \lambda\sigma\rho^{M,C_j}$. Let $f : [0,\infty)^2 \times \mathbb{Z}^+ \to \mathbb{R}$ be defined by $f(s,p,j) = C_6\mathrm{e}^{-a(s-p)} + C_7(j)$. By our parameter assumptions, $C_6 > 0$ and $C_7(j) \le f(s,p,j)$.

Writing cash flows and growth options in terms of the following function g will allow for a reduction in the computational complexity of the monte carlo simulations. For all $T \ge t$, define the function $g : [v_{\min}, v_{\max}] \times [0,\infty) \times [0,\infty) \times \mathbb{Z}^+ \to \mathbb{R}$ by

$$g(v,t,T,j) = \mathbb{E}\,[\mathrm{e}^{\int_t^T V_j(p)f(T,p,j)\,\mathrm{d}p} | V_j(t) = v]. \tag{2.13}$$

Remark 2.3.1. *The function g is really a function of the parameters $\theta, v_{\min}, v_{\max}, \kappa,\ \sigma_V$, and the parameters involved in f, in addition to v, t, T, and j. We suppress the former parameters when writing g because we assume they are firm specific. The dependence on so many parameters makes the problem very computationally expensive. Without reducing our expressions to nice functions multiplied by the conditional expectation which we call g, running the simulation would have been even more difficult compared to what is already a challenging problem computationally. The definitions and derivations in the remainder of this chapter are for one specific firm, and differences in the firm specific parameters will be taken into account during the simulation. Its possible to derive an infinite series representation for g, which is very similar to the result of Delbaen and Shirakawa [11]. Unfortunately, our simulations require the generation of long time series, and the expansion of the series becomes too cumbersome to be useful as an approximation for g.*

2.4 A series expansion for the conditional expectation

Following Delbaen and Shirakawa [11], we derive a series representation for the conditional expectation g. Our definitions and lemma are very similar to theirs. The main difference is the addition of the function f, and the difference becomes apparent in the second order expansion. We have tried using this approximation for g up to second order in our model, but it is not accurate over our long time horizons. Theoretically, the approximation can be made to be very good, but as will be seen below, expanding past the second order term in the series is very cumbersome. The representation given in this section will show the effect of changing the bounds of the Jacobi process on the function g. Specifically, if $v_{\min} = 0$, then g will be an increasing function of $v_{\max}$. Let $\mathcal{L}^n = \{(l_1, \cdots, l_n) \in \mathbb{N}^n :\ |l_j - l_{j-1}| \le 1,\ 1 \le j \le n,\ l_0 = 0\}$. In the definition of q below, let $l = \max(l_{j-1}, l_j)$. Now, let

$$q(l_{j-1}, l_j) = \begin{cases} \frac{(2l(a+b+l-1)+a(a+b-2))\Gamma^2(a) l! \Gamma(b+l)}{(a+b+2l)(a+b+2l-1)(a+b+2l-2)\Gamma(a+l)\Gamma(a+b+l-1)}, & \text{if } l_j = l_{j-1}, \\ -\frac{l! \Gamma^2(a)\Gamma(b+l)}{(a+b+2l-1)(a+b+2l-2)(a+b+2l-3)\Gamma(a+l-1)\Gamma(a+b+l-2)}, & \text{if } |l_j - l_{j-1}| = 1. \end{cases}$$

For every $n \in \mathbb{Z}^+$ and for every n-tuple $(\lambda_{l_1}, \cdots, \lambda_{l_n}) \in \mathcal{L}^n$, let $s_{n+1} = t$, and define for every $j \in \mathbb{Z}^+$ the following function:

$$I^{n,j}_{t,T}(\lambda_{l_1}, \cdots, \lambda_{l_n}) = \int_t^T \int_{s_n}^T \cdots \int_{s_2}^T \{\prod_{i=1}^n f(T, s_i, j)\} \mathrm{e}^{-\sum_{i=1}^n \lambda_{l_i}(s_i - s_{i+1})} \, \mathrm{d}s_1 \cdots \mathrm{d}s_n. \tag{2.14}$$

Define $\gamma = \frac{\theta - v_{\min}}{v_{\max} - v_{\min}}$, $\beta = \frac{\sigma_V}{\sqrt{v_{\max}} - \sqrt{v_{\min}}}$, $(a_1)_k = \frac{\Gamma(a_1+k)}{\Gamma(a_1)}$, $a = \frac{2\kappa\gamma}{\beta^2}$, $b = \frac{2\kappa(1-\gamma)}{\beta^2}$, and $w(x) = x^{a-1}(1-x)^{b-1}$. Note that $a > 0$ and $b > 0$. For every n, let $\lambda_n = \kappa n + \frac{\beta^2}{2} n(n-1)$, $k_n = \frac{(a+b+2n-1)\Gamma(a+n)\Gamma(a+b+n-1)}{n!\Gamma(a)^2\Gamma(b+n)}$, and $\psi_n(x) = \sum_{k=0}^n (-1)^k \binom{n}{k} \frac{(a+b+n-1)_k}{(a)_k} x^k$.

Lemma 2.4.1. *Let $T > t$. Then,*

$$\begin{aligned} g(v, t, T, j) = {} & \mathrm{e}^{v_{\min}\left(C_7(j)(T-t) - \frac{C_6\left(\mathrm{e}^{-a(T-t)} - 1\right)}{a}\right)} \\ & \times (1 + \sum_{n=1}^{\infty} (v_{\max} - v_{\min})^n \{ \sum_{(l_1, \cdots, l_n) \in \mathcal{L}^n} \psi_{l_n}(z) \left(\prod_{i=1}^n k_{l_i} q(l_{i-1}, l_i) \right) \\ & \times \int_t^T \int_{s_n}^T \cdots \int_{s_2}^T \{\prod_{i=1}^n f(T, s_i, j)\} \mathrm{e}^{-\sum_{i=1}^n \lambda_{l_i}(s_i - s_{i+1})} \, \mathrm{d}s_1 \, \mathrm{d}s_2 \cdots \mathrm{d}s_{n-1} \, \mathrm{d}s_n \}). \end{aligned} \tag{2.15}$$

Proof. The argument is nearly identical to what is in Delbaen and Shirakawa [11]. We use similar notation, and the only difference in our proof is the extra function f inside the integration. For the Jacobi process, we suppress the subscript j and simply write V instead of V_j. Let $Z(t) = \frac{V(t) - v_{\min}}{v_{\max} - v_{\min}}$. Note that $V(t) = Z(t)(v_{\max} - v_{\min}) + v_{\min}$. Under this transformation, by Equation (2.6),

$$\mathrm{d}Z(t) = \kappa(\gamma - Z(t)) \, \mathrm{d}t + \beta \sqrt{Z(t)(1 - Z(t))} \, \mathrm{d}W^V(t).$$

Let $z(v) = \frac{v - v_{\min}}{v_{\max} - v_{\min}}$ so that in the conditional expectation below, we can switch from conditioning on $V(t) = v$ to $Z(t) = z$.

$$\begin{aligned} \mathbb{E}\, [\mathrm{e}^{\int_t^T V(p) f(T,p,j) \, \mathrm{d}p} | V(t) = v] &= \mathbb{E}\, [\mathrm{e}^{\int_t^T (z(p)(v_{\max} - v_{\min}) + v_{\min}) f(T,p,j) \, \mathrm{d}p} | Z(t) = z] \\ &= \mathrm{e}^{v_{\min} \int_t^T f(T,p,j) \, \mathrm{d}p} \\ &\times \mathbb{E}\, [\mathrm{e}^{(v_{\max} - v_{\min}) \int_t^T z(p) f(T,p,j) \, \mathrm{d}p} | Z(t) = z] \end{aligned}$$

$$= \mathrm{e}^{v_{\min}\int_t^T f(T,p,j)\,\mathrm{d}p}\,\mathbb{E}\,[1+\sum_{n=1}^{\infty}\frac{(v_{\max}-v_{\min})^n}{n!}$$
$$\times (\int_t^T z(p)f(T,p,j)\,\mathrm{d}p)^n|Z(t)=z]$$
$$= \mathrm{e}^{v_{\min}\int_t^T f(T,p,j)\,\mathrm{d}p}\left(1+\sum_{n=1}^{\infty}\frac{(v_{\max}-v_{\min})^n}{n!}\right.$$
$$\left.\times\,\mathbb{E}\,[(\int_t^T z(p)f(T,p,j)\,\mathrm{d}p)^n|Z(t)=z]\right),$$

where the last line follows by Fubini's theorem. Let $\mathrm{d}\mathbf{s}=\mathrm{d}s_1\,\mathrm{d}s_2\cdots\mathrm{d}s_{n-1}\,\mathrm{d}s_n$. Now,

$$\begin{aligned}\mathbb{E}\,[(\int_t^T z(p)f(T,p,j)\,\mathrm{d}p)^n|Z(t)=z] &= n!\int_t^T\int_{s_n}^T\cdots\int_{s_2}^T\mathbb{E}\,[\prod_{i=1}^n\{z_{s_i}\\ &\quad\times f(T,s_i,j)\}|Z(t)=z]\,\mathrm{d}\mathbf{s}\\ &= n!\int_t^T\int_{s_n}^T\cdots\int_{s_2}^T\{\prod_{i=1}^n f(T,s_i,j)\}\\ &\quad\times\mathbb{E}\,[\{\prod_{i=1}^n z_{s_i}\}|Z(t)=z]\,\mathrm{d}\mathbf{s}.\end{aligned}$$

From Equation (3.10) of Delbaen and Shirakawa [11],

$$\mathbb{E}\,[\{\prod_{i=1}^n z_{s_i}\}|Z(t)=z]=\sum_{(l_1,\cdots,l_n)\in\mathcal{L}^n}\psi_{l_n}(z)(\prod_{i=1}^n k_{l_i}q(l_{i-1},l_i))\mathrm{e}^{-\sum_{i=1}^n\lambda_{l_i}(s_i-s_{i+1})}.$$

Thus, combining the equations above yields

$$\begin{aligned}\mathbb{E}\,[\mathrm{e}^{\int_t^T V(p)f(T,p,j)\,\mathrm{d}p}|V(t)=v] &= \mathrm{e}^{v_{\min}\int_t^T f(T,p,j)\,\mathrm{d}p}(1+\sum_{n=1}^{\infty}(v_{\max}-v_{\min})^n\\ &\quad\times\int_t^T\int_{s_n}^T\cdots\int_{s_2}^T\{\prod_{i=1}^n f(T,s_i,j)\}\\ &\quad\times\{\sum_{(l_1,\cdots,l_n)\in\mathcal{L}^n}\psi_{l_n}(z)(\prod_{i=1}^n k_{l_i}q(l_{i-1},l_i))\mathrm{e}^{-\sum_{i=1}^n\lambda_{l_i}(s_i-s_{i+1})}\}\,\mathrm{d}\mathbf{s})\\ &= \mathrm{e}^{v_{\min}((T-t)C_7(j)-\frac{C_6(\mathrm{e}^{a(t-T)}-1)}{a})}(1+\sum_{n=1}^{\infty}(v_{\max}-v_{\min})^n\\ &\quad\times\{\sum_{(l_1,\cdots,l_n)\in\mathcal{L}^n}\psi_{l_n}(z)(\prod_{i=1}^n k_{l_i}q(l_{i-1},l_i))\\ &\quad\times\int_t^T\int_{s_n}^T\cdots\int_{s_2}^T\{\prod_{i=1}^n f(T,s_i,j)\}\mathrm{e}^{-\sum_{i=1}^n\lambda_{l_i}(s_i-s_{i+1})}\,\mathrm{d}\mathbf{s}\}),\end{aligned}$$

where the last equality follows since $\sum_{(l_1,\cdots,l_n)\in\mathcal{L}^n}\psi_{l_n}(z)(\prod_{i=1}^n k_{l_i}q(l_{i-1},l_i))$ does not depend on s_i for any i. The proof is complete. □

Remark 2.4.2. *Suppose that $v_{\min}=0$. The representation given in Lemma 2.4.1 makes clear that $g(v,t,T,j)$ is an increasing function of $v_{\max}$.*

In the next section, we will expand the series up to second order.

2.5 Second order approximation for the conditional expectation

The goal of this section is to calculate a second order approximation for the conditional expectation from Lemma 2.4.1. As this section is not necessary, the reader is welcome to proceed to Section 2.7. First, we calculate the necessary constants and functions. We begin by listing the constants λ_n, which correspond to the eigenvalues arising in Delbaen and Shirakawa [11].

1. $\lambda_0=0$.
2. $\lambda_1=\kappa$.
3. $\lambda_2=2\kappa+\beta^2$.
4. $\lambda_3=3\kappa+3\beta^2$.
5. $\lambda_4=4\kappa+6\beta^2$.
6. $\lambda_5=5\kappa+10\beta^2$.
7. $\lambda_6=6\kappa+15\beta^2$.

We now calculate the constants k_n. Below, Γ denotes the Gamma function. Recall that $z\Gamma(z)=\Gamma(z+1)$ and $\Gamma(1)=1$. Also, note that $(x)_0=\frac{\Gamma(x)}{\Gamma(x)}=1$, $(x)_1=\frac{\Gamma(x+1)}{\Gamma(x)}=x$, and $(x)_2=\frac{\Gamma(x+2)}{\Gamma(x)}=\frac{\Gamma(x+2)}{\Gamma(x+1)}\frac{\Gamma(x+1)}{\Gamma(x)}=\frac{x+1}{x}$.

1. $k_0=\frac{(a+b-1)\Gamma(a)\Gamma(a+b-1)}{\Gamma(a)^2\Gamma(b)}=\frac{\Gamma(a+b)}{\Gamma(a)\Gamma(b)}$.
2. $k_1=\frac{(a+b+1)\Gamma(a+1)\Gamma(a+b)}{\Gamma(a)^2\Gamma(b+1)}=\frac{(a+b+1)a\Gamma(a+b)}{\Gamma(a)\Gamma(b+1)}$.

3. $k_2 = \frac{(a+b+3)\Gamma(a+2)\Gamma(a+b+1)}{2\Gamma(a)^2\Gamma(b+2)}$.

4. $k_3 = \frac{(a+b+5)\Gamma(a+3)\Gamma(a+b+2)}{6\Gamma(a)^2\Gamma(b+3)}$.

We record useful computations below.

1. $a+b = \frac{2\kappa}{\beta^2} > 0$.

2. $\frac{a}{a+b} = \gamma$.

3. $\frac{a+b+1}{a} = \frac{2\kappa+\beta^2}{2\kappa\gamma}$.

4. $a+b+2 = \frac{2(\kappa+\beta^2)}{\beta^2}$.

5. $\frac{a+b+2}{a+1} = \frac{2(\kappa+\beta^2)}{2\kappa\gamma+\beta^2}$.

6. $a+1 = \frac{2\kappa\gamma+\beta^2}{\beta^2}$.

7. $\frac{a+1}{a} = \frac{2\kappa\gamma+\beta^2}{2\kappa\gamma}$.

8. $\frac{(a+b+2)a}{(a+1)(a+b+1)} = \frac{4(\kappa+\beta^2)\kappa\gamma}{(2\kappa\gamma+\beta^2)(2\kappa+\beta^2)}$.

9. $1-\gamma = 1 - \frac{\theta - v_{\min}}{v_{\max}-v_{\min}} = \frac{v_{\max}-v_{\min}-\theta+v_{\min}}{v_{\max}-v_{\min}} = \frac{v_{\max}-\theta}{v_{\max}-v_{\min}}$.

10. $a^2+ab+2b = \frac{4\kappa^2\gamma}{\beta^4} + \frac{4\kappa(1-\gamma)}{\beta^2} = \frac{4(\kappa^2\gamma+\kappa\beta^2-\kappa\gamma\beta^2)}{\beta^4}$.

Now, we record the first few functions $\psi_n(x)$.

1. $\psi_0(x) = 1$.

2. $\psi_1(x) = 1 - \frac{1}{\gamma}x$.

3. $\psi_2(x) = \sum_{k=0}^{2}(-1)^k \binom{2}{k} \frac{(a+b+1)_k}{(a)_k} x^k = 1 - \frac{2(a+b+1)}{a}x + \frac{(a+b+1)_2}{(a)_2}x^2 = 1 - \frac{2(a+b+1)}{a}x$
$+ \frac{(a+b+2)a}{(a+b+1)(a+1)}x^2 = 1 - \frac{(2\kappa+\beta^2)}{\kappa\gamma}x + \frac{4(\kappa+\beta^2)\kappa\gamma}{(2\kappa\gamma+\beta^2)(2\kappa+\beta^2)}x^2$.

Note that $\mathcal{L}^1 = \{(0),(1)\}$ and $\mathcal{L}^2 = \{(0,0),(0,1),(1,0),(1,1),(1,2)\}$. So, we will need to use the following in our evaluation:

1. $\psi_0(\frac{v-v_{\min}}{v_{\max}-v_{\min}}) = 1$.

2. $\psi_1(\frac{v-v_{\min}}{v_{\max}-v_{\min}}) = 1 - \frac{1}{\gamma}(\frac{v-v_{\min}}{v_{\max}-v_{\min}})$.

3. $\psi_2(\frac{v-v_{\min}}{v_{\max}-v_{\min}}) = 1 - \frac{(2\kappa+\beta^2)}{\kappa\gamma}(\frac{v-v_{\min}}{v_{\max}-v_{\min}}) + \frac{4(\kappa+\beta^2)\kappa\gamma}{(2\kappa\gamma+\beta^2)(2\kappa+\beta^2)}(\frac{v-v_{\min}}{v_{\max}-v_{\min}})^2$.

We record the possible products $A = k_{l_1} q(l_0, l_1)$ from $\mathcal{L}^1$.

1. For the case $l_1 = 0$, $A = k_0 q(0,0) = \gamma$.

2. For the case $l_1 = 1$, $A = k_1 q(0,1) = -\gamma$.

Here, we record the possible products $A = \prod_{j=1}^{2} k_{l_j} q(l_{j-1}, l_j)$ from $\mathcal{L}^2$.

1. For the case $(l_1 = 0, l_2 = 0)$, $A = k_0^2 q(0,0)^2 = (\frac{\Gamma(a+b)}{\Gamma(a)\Gamma(b)})^2 q(0,0)^2 = \gamma^2$.

2. For the case $(l_1 = 0, l_2 = 1)$, $A = k_0 k_1 q(0,0) q(0,1) = -\gamma^2$.

3. For the case $(l_1 = 1, l_2 = 0)$, $A = k_1 k_0 q(0,1) q(1,0) = \frac{\gamma(1-\gamma)\beta^2}{2\kappa+\beta^2}$.

4. For the case $(l_1 = 1, l_2 = 1)$, $A = k_1^2 q(0,1) q(1,1) = -\frac{\gamma(\kappa\gamma+\beta^2-\gamma\beta^2)}{\kappa+\beta^2}$.

5. For the case $(l_1 = 1, l_2 = 2)$, $A = k_1 k_2 q(0,1) q(1,2) = \frac{a(a+1)}{(a+b+2)(a+b+1)} = \frac{(2\kappa\gamma+\beta^2)\kappa\gamma}{(\kappa+\beta^2)(2\kappa+\beta^2)}$.

Finally, we calculate the required integrals using Definition 2.14. If $n = 0$, there are no integrals to calculate. Consider the case when $n = 1$. So, we are summing over $\mathcal{L}^1$. This requires us to calculate the integrals $I_{t,T}^{1,j}(\lambda_{l_1})$ for $l_1 = 0$ and $l_1 = 1$. Recalling that $\lambda_0 = 0$ and $\lambda_1 = \kappa$, we calculate the integrals $I_{t,T}^{1,j}(0)$ and $I_{t,T}^{1,j}(\kappa)$. Note that $I_{t,T}^{1,j}(\lambda_{l_1}) = \int_t^T f(T, s_1, j) \mathrm{e}^{-\lambda_{l_1}(s_1 - s_2)} \, \mathrm{d}s_1$.

1. For the case $\lambda_0 = 0$,
   $I_{t,T}^{1,j}(0) = \int_t^T (C_6 \mathrm{e}^{-a(T-s_1)} + C_7(j)) \, \mathrm{d}s_1 = \frac{C_6(1-\mathrm{e}^{-a(T-t)})}{a} + C_7(j)(T-t)$.

2. For the case $\lambda_1 = \kappa$,

$$\begin{aligned} I_{t,T}^{1,j}(\kappa) &= \int_t^T (C_6 \mathrm{e}^{-a(T-s_1)} + C_7(j)) \mathrm{e}^{-\kappa(s_1-t)} \, \mathrm{d}s_1 \\ &= C_6 \mathrm{e}^{\kappa t - aT} \int_t^T \mathrm{e}^{(a-\kappa)s_1} \, \mathrm{d}s_1 + C_7(j) \int_t^T \mathrm{e}^{-\kappa(s_1-t)} \, \mathrm{d}s_1, \end{aligned}$$

   so

$$I^{1,j}_{t,T}(\kappa) = \begin{cases} C_6 \mathrm{e}^{\kappa t - aT}(T-t) + C_7(j)(\frac{1-\mathrm{e}^{-\kappa(T-t)}}{\kappa}) \ \text{ if } a = \kappa, \\ C_6 \mathrm{e}^{\kappa t - aT} \frac{\mathrm{e}^{(a-\kappa)T} - \mathrm{e}^{(a-\kappa)t}}{a-\kappa} + C_7(j)(\frac{1-\mathrm{e}^{-\kappa(T-t)}}{\kappa}) = \\ C_6 \frac{\mathrm{e}^{-\kappa(T-t)} - \mathrm{e}^{-a(T-t)}}{a-\kappa} + C_7(j)(\frac{1-\mathrm{e}^{-\kappa(T-t)}}{\kappa}) \ \text{ if } a \neq \kappa. \end{cases}$$

In the calculation of the integral $I^{1,j}_{t,T}(\kappa)$ above, it is important to note that we will select parameters so that $a \neq \kappa$. Thus, we do not need to consider the case when $a = \kappa$. From now on, we assume $a \neq \kappa$ and $2a \neq \kappa$. Now, consider the case when $n = 2$. In this case, we are summing over $\mathcal{L}^2$. This requires us to calculate the integrals $I^{2,j}_{t,T}(\lambda_{l_1}, \lambda_{l_2}) = \int_t^T \int_{s_2}^T f(T, s_1, j) f(T, s_2, j) \mathrm{e}^{-\lambda_{l_1}(s_1 - s_2) - \lambda_{l_2}(s_2 - t)} \, \mathrm{d}s_1 \, \mathrm{d}s_2$ for all $(\lambda_{l_1}, \lambda_{l_2}) \in \mathcal{L}^2$.

1. For the case $l_1 = 0, l_2 = 0$,

$$\begin{aligned} I^{2,j}_{t,T}(0,0) &= \int_t^T \int_{s_2}^T (C_6 \mathrm{e}^{-a(T-s_1)} + C_7(j))(C_6 \mathrm{e}^{-a(T-s_2)} + C_7(j)) \, \mathrm{d}s_1 \, \mathrm{d}s_2 \\ &= \frac{\mathrm{e}^{-2aT}[C_6 \mathrm{e}^{at} - \mathrm{e}^{aT}(C_6 + aC_7(j)(T-t))]^2}{2a^2}. \end{aligned}$$

2. For the case $l_1 = 0, l_2 = 1$,

$$\begin{aligned} I^{2,j}_{t,T}(0,\kappa) &= \int_t^T \int_{s_2}^T f(T, s_1, j) f(T, s_2, j) \mathrm{e}^{-\lambda_{l_1}(s_1 - s_2) - \lambda_{l_2}(s_2 - t)} \, \mathrm{d}s_1 \, \mathrm{d}s_2 \\ &= \int_t^T \int_{s_2}^T (C_6 \mathrm{e}^{-a(T-s_1)} + C_7(j))(C_6 \mathrm{e}^{-a(T-s_2)} + C_7(j)) \mathrm{e}^{-\kappa(s_2 - t)} \, \mathrm{d}s_1 \, \mathrm{d}s_2 \\ &= \frac{\mathrm{e}^{2C_7(j)} C_6^2 (a \mathrm{e}^{\kappa(t-T)} + \mathrm{e}^{a(t-T)}((a-\kappa)\mathrm{e}^{a(t-T)} - 2a + \kappa))}{a(a-\kappa)(2a-\kappa)}. \end{aligned}$$

   We remark that when doing this integration, it would be necessary to consider the three cases $a = \kappa, a = 2\kappa$, and $a \neq \kappa$ separately, but we can adjust parameters to avoid the cases $a = \kappa$ and $a = 2\kappa$.

3. For the case $l_1 = 1, l_2 = 0$,

$$\begin{aligned} I^{2,j}_{t,T}(\kappa, 0) &= \int_t^T \int_{s_2}^T (C_6 \mathrm{e}^{-a(T-s_1)} + C_7(j))(C_6 \mathrm{e}^{-a(T-s_2)} + C_7(j)) \mathrm{e}^{-\kappa(s_1 - s_2)} \, \mathrm{d}s_1 \, \mathrm{d}s_2 \\ &= \frac{\mathrm{e}^{2C_7(j)} C_6^2 (a(-2\mathrm{e}^{(a+\kappa)(t-T)} + \mathrm{e}^{2a(t-T)} + 1) + \kappa(\mathrm{e}^{2a(t-T)} - 1))}{2a(a-\kappa)(a+\kappa)}. \end{aligned}$$

Note that it's required that $a \neq 0, a \neq \kappa,$ and $a \neq -\kappa$.

4. For the case $l_1 = 1, l_2 = 1$,

$$\begin{aligned} I_{t,T}^{2,j}(\kappa,\kappa) &= \int_t^T \int_{s_2}^T (C_6 \mathrm{e}^{-a(T-s_1)} + C_7(j))(C_6 \mathrm{e}^{-a(T-s_2)} + C_7(j)) \mathrm{e}^{-\kappa(s_1-s_2)-\kappa(s_2-t)} \, \mathrm{d}s_1 \, \mathrm{d}s_2 \\ &= \frac{C_6^2 \mathrm{e}^{2C_7(j)-T(a+\kappa)}(a(-2\mathrm{e}^{t(a+\kappa)} + \mathrm{e}^{aT+\kappa t} + \mathrm{e}^{2at-aT+\kappa T}) + \kappa \mathrm{e}^{\kappa t}(\mathrm{e}^{at} - \mathrm{e}^{aT}))}{a(a-\kappa)(2a-\kappa)}. \end{aligned}$$

Again, its required that $a \neq 0, a \neq \kappa$, and $2a \neq \kappa$.

5. For the case $l_1 = 1, l_2 = 2$,

$$\begin{aligned} I_{t,T}^{2,j}(\kappa, 2\kappa+\beta^2) = \int_t^T \int_{s_2}^T & (C_6 \mathrm{e}^{-a(T-s_1)} + C_7(j))(C_6 \mathrm{e}^{-a(T-s_2)} \\ & + C_7(j)) \mathrm{e}^{-\kappa(s_1-s_2)-(2\kappa+\beta^2)(s_2-t)} \, \mathrm{d}s_1 \, \mathrm{d}s_2 \\ & = \mathrm{e}^{2C_7(j)} C_6^2 \Big(\frac{\mathrm{e}^{2a(t-T)} - \mathrm{e}^{(\beta^2+2\kappa)(t-T)}}{(a-\kappa)(2a-\beta^2-2\kappa)} + \frac{\mathrm{e}^{(\beta^2+2\kappa)(t-T)} - \mathrm{e}^{(a+\kappa)(t-T)}}{(\kappa-a)(-a+\beta^2+\kappa)} \Big). \end{aligned}$$

In addition to $a \neq \kappa$, we now have the additional requirements that $-a + \beta^2 + \kappa \neq 0$ and $2a - \beta^2 - 2\kappa \neq 0$. We can avoid these requirements by calculating the integral case by case.

Proposition 2.5.1. *Let $g^{(n)}(v,t,T,j)$ denote the approximation for $g(v,t,T,j)$ by truncating the summation representation for g at the n-th term (note $g^{(n)}$ does not represent the n-th derivative). Below, we list approximations in which the sum in Lemma 2.4.1 is truncated at order $n = 2$.*

1. *For the case $n = 0$, $g^{(0)}(v,t,T,j) = \mathrm{e}^{v_{\min}\left(C_7(j)(T-t) - \frac{C_6(\mathrm{e}^{-a(T-t)}-1)}{a}\right)}$.*

2. *For the case $n = 1$,*

$$\begin{aligned} g^{(1)}(v,t,T,j) = \mathrm{e}^{v_{\min}\left(C_7(j)(T-t) - \frac{C_6(\mathrm{e}^{-a(T-t)}-1)}{a}\right)} & (1 + (\theta - v_{\min})(\frac{C_6(1-\mathrm{e}^{-a(T-t)})}{a} \\ & + C_7(j)(T-t)) + (v-\theta)(C_6 \frac{\mathrm{e}^{-\kappa(T-t)} - \mathrm{e}^{-a(T-t)}}{a-\kappa} \\ & + C_7(j)(\frac{1-\mathrm{e}^{-\kappa(T-t)}}{\kappa}))). \end{aligned}$$

3. For the case $n=2$,

$$
\begin{aligned}
g^{(2)}(v,t,T,j) = {} & \mathrm{e}^{\left((T-t)C_7(j)-\frac{(-1+\mathrm{e}^{-a(T-t)})C_6}{a}\right)v_{\min}}((-\frac{A_0^*}{a(a-\kappa)(2a-\kappa)} \\
& -\frac{A_1^*}{a(a-\kappa)(2a-\kappa)(v_{\max}-v_{\min})(\sigma_v^2+\kappa)} \\
& +\frac{A_2^*}{2a(a-\kappa)(a+\kappa)(v_{\max}-v_{\min})(\sigma_v^2+2\kappa)} \\
& +\frac{A_3^*}{(v_{\max}-v_{\min})(\sigma_v^2+\kappa)(\sigma_v^2+2\kappa)} \\
& +\frac{\mathrm{e}^{-2aT}(\mathrm{e}^{at}C_6-\mathrm{e}^{aT}(C_6+a(T-t)C_7(j)))^2(\theta-v_{\min})^2}{2a^2}) \\
& +(v-\theta)(\frac{(-\mathrm{e}^{-a(T-t)}+\mathrm{e}^{-(T-t)\kappa})C_6}{a-\kappa}+\frac{(1-\mathrm{e}^{-(T-t)\kappa})C_7(j)}{\kappa}) \\
& +(\frac{(1-\mathrm{e}^{-a(T-t)})C_6}{a}+(T-t)C_7(j))(\theta-v_{\min})+1),
\end{aligned}
$$

where

$$
\begin{aligned}
A_0^* = {} & \mathrm{e}^{2C_7(j)}(\mathrm{e}^{(t-T)\kappa}a+\mathrm{e}^{a(t-T)}(-2a+\mathrm{e}^{a(t-T)}(a-\kappa)+\kappa)) \\
& \times(\frac{(\theta-v_{\min})^2}{(v_{\max}-v_{\min})^2}-\frac{(v-v_{\min})(\theta-v_{\min})}{(v_{\max}-v_{\min})^2})C_6^2, \\
A_1^* = {} & C_6^2\mathrm{e}^{2C_7(j)-T(a+\kappa)}(a(-2\mathrm{e}^{t(a+\kappa)}+\mathrm{e}^{aT+t\kappa}+\mathrm{e}^{2at-aT+T\kappa})+\mathrm{e}^{t\kappa}(\mathrm{e}^{at}-\mathrm{e}^{aT})\kappa) \\
& \times(\theta-v)(-\frac{(\theta-v_{\min})\sigma_v^2}{v_{\max}-v_{\min}}+\sigma_v^2+\frac{\kappa(\theta-v_{\min})}{v_{\max}-v_{\min}}), \\
A_2^* = {} & \mathrm{e}^{2C_7(j)}(a(1+\mathrm{e}^{2a(t-T)}-2\mathrm{e}^{(t-T)(a+\kappa)}) \\
& +(-1+\mathrm{e}^{2a(t-T)})\kappa)(1-\frac{\theta-v_{\min}}{v_{\max}-v_{\min}})(\theta-v_{\min})\sigma_v^2C_6^2, \\
A_3^* = {} & \mathrm{e}^{2C_7(j)}\kappa C_6^2(\theta-v_{\min})(\sigma_v^2+\frac{2\kappa(\theta-v_{\min})}{v_{\max}-v_{\min}}) \\
& \times(\frac{\mathrm{e}^{2a(t-T)}-\mathrm{e}^{(t-T)(\sigma_v^2+2\kappa)}}{(a-\kappa)(-\sigma_v^2+2a-2\kappa)}+\frac{-\mathrm{e}^{(t-T)(a+\kappa)}+\mathrm{e}^{(t-T)(\sigma_v^2+2\kappa)}}{(\kappa-a)(\sigma_v^2-a+\kappa)}) \\
& \times(\frac{4\kappa(\theta-v_{\min})(\sigma_v^2+\kappa)(v-v_{\min})^2}{(v_{\max}-v_{\min})^3(\sigma_v^2+2\kappa)(\sigma_v^2+\frac{2\kappa(\theta-v_{\min})}{v_{\max}-v_{\min}})}-\frac{(\sigma_v^2+2\kappa)(v-v_{\min})}{\kappa(\theta-v_{\min})}+1).
\end{aligned}
$$

Proof. The approximation for $g^{(0)}$ is obvious. Consider $n = 1$.

$$g^{(1)}(v,t,T,j) = \mathrm{e}^{v_{\min}\left(C_7(j)(T-t)-\frac{C_6(\mathrm{e}^{-a(T-t)}-1)}{a}\right)}$$
$$\times (1 + (v_{\max} - v_{\min})\{\sum_{(l_1)\in\mathcal{L}^1} \psi_{l_1}(z)k_{l_1}q(l_0,l_1)I^{1,j}_{t,T}(\lambda_{l_1})\}).$$

Let $\Xi_1 = (v_{\max} - v_{\min})\sum_{(l_1)\in\mathcal{L}^1} \psi_{l_1}(z)k_{l_1}q(l_0,l_1)I^{1,j}_{t,T}(\lambda_{l_1})$. We expand Ξ_1 to obtain an explicit formula.

$$\begin{aligned}
\Xi_1 &= (v_{\max} - v_{\min})(\psi_0(z)k_0q(0,0)I^{1,j}_{t,T}(\lambda_0) + \psi_1(z)k_1q(0,1)I^{1,j}_{t,T}(\lambda_1)) \\
&= (v_{\max} - v_{\min})(\gamma I^{1,j}_{t,T}(\lambda_0) - (1 - \frac{1}{\gamma}(\frac{v - v_{\min}}{v_{\max} - v_{\min}}))\gamma I^{1,j}_{t,T}(\lambda_1)) \\
&= (v_{\max} - v_{\min})(\gamma I^{1,j}_{t,T}(\lambda_0) - (\gamma - (\frac{v - v_{\min}}{v_{\max} - v_{\min}}))I^{1,j}_{t,T}(\lambda_1)) \\
&= (\theta - v_{\min})(\frac{C_6(1-\mathrm{e}^{-a(T-t)})}{a} + C_7(j)(T-t) \\
&- (C_6\frac{\mathrm{e}^{-\kappa(T-t)} - \mathrm{e}^{-a(T-t)}}{a-\kappa} + C_7(j)(\frac{1-\mathrm{e}^{-\kappa(T-t)}}{\kappa}))) \\
&+ (v - v_{\min})(C_6\frac{\mathrm{e}^{-\kappa(T-t)} - \mathrm{e}^{-a(T-t)}}{a-\kappa} + C_7(j)(\frac{1-\mathrm{e}^{-\kappa(T-t)}}{\kappa})) \\
&= (\theta - v_{\min})(\frac{C_6(1-\mathrm{e}^{-a(T-t)})}{a} + C_7(j)(T-t)) \\
&+ (v - \theta)(C_6\frac{\mathrm{e}^{-\kappa(T-t)} - \mathrm{e}^{-a(T-t)}}{a-\kappa} + C_7(j)(\frac{1-\mathrm{e}^{-\kappa(T-t)}}{\kappa})).
\end{aligned}$$

Substitution yields the result. Consider $n = 2$. Let

$$\Xi_2 = (v_{\max} - v_{\min})^2\{\sum_{(l_1,l_2)\in\mathcal{L}^2} \psi_{l_2}(z)k_{l_1}k_{l_2}q(l_0,l_1)q(l_1,l_2)I^{2,j}_{t,T}(\lambda_{l_1},\lambda_{l_2})\}.$$

Expansion yields the following:

$$\begin{aligned}
\Xi_2 &= (v_{\max} - v_{\min})^2\{\psi_0(z)k_0^2q(0,0)^2I^{2,j}_{t,T}(\lambda_0,\lambda_0) + \psi_1(z)k_0k_1q(0,0)q(0,1)I^{2,j}_{t,T}(\lambda_0,\lambda_1) \\
&+ \psi_0(z)k_1k_0q(0,1)q(1,0)I^{2,j}_{t,T}(\lambda_1,\lambda_0) + \psi_1(z)k_1^2q(0,1)q(1,1)I^{2,j}_{t,T}(\lambda_1,\lambda_1) \\
&+ \psi_2(z)k_1k_2q(0,1)q(1,2)I^{2,j}_{t,T}(\lambda_1,\lambda_2)\} \\
&= (v_{\max} - v_{\min})^2\{\gamma^2(\frac{\mathrm{e}^{-2aT}[C_6\mathrm{e}^{at} - \mathrm{e}^{aT}(C_6 + aC_7(j)(T-t))]^2}{2a^2})
\end{aligned}$$

$$
\begin{aligned}
&-(1-\frac{1}{\gamma}(\frac{v-v_{\min}}{v_{\max}-v_{\min}}))\gamma^2(\frac{\mathrm{e}^{2C_7(j)}C_6^2(a\mathrm{e}^{\kappa(t-T)}+\mathrm{e}^{a(t-T)}((a-\kappa)\mathrm{e}^{a(t-T)}-2a+\kappa))}{a(a-\kappa)(2a-\kappa)})\\
&+(\frac{\gamma(1-\gamma)\beta^2}{2\kappa+\beta^2})(\frac{\mathrm{e}^{2C_7(j)}C_6^2(a(-2\mathrm{e}^{(a+\kappa)(t-T)}+\mathrm{e}^{2a(t-T)}+1)+\kappa(\mathrm{e}^{2a(t-T)}-1))}{2a(a-\kappa)(a+\kappa)})\\
&-(1-\frac{1}{\gamma}(\frac{v-v_{\min}}{v_{\max}-v_{\min}}))(\frac{\gamma(\kappa\gamma+\beta^2-\gamma\beta^2)}{\kappa+\beta^2})\\
&\times(\frac{C_6^2\mathrm{e}^{2C_7(j)-T(a+\kappa)}(a(-2\mathrm{e}^{t(a+\kappa)}+\mathrm{e}^{aT+\kappa t}+\mathrm{e}^{2at-aT+\kappa T})+\kappa\mathrm{e}^{\kappa t}(\mathrm{e}^{at}-\mathrm{e}^{aT}))}{a(a-\kappa)(2a-\kappa)})\\
&+(1-\frac{(2\kappa+\beta^2)}{\kappa\gamma}(\frac{v-v_{\min}}{v_{\max}-v_{\min}})+\frac{4(\kappa+\beta^2)\kappa\gamma}{(2\kappa\gamma+\beta^2)(2\kappa+\beta^2)}(\frac{v-v_{\min}}{v_{\max}-v_{\min}})^2)\\
&\times(\frac{(2\kappa\gamma+\beta^2)\kappa\gamma}{(\kappa+\beta^2)(2\kappa+\beta^2)})(\mathrm{e}^{2C_7(j)}C_6^2(\frac{\mathrm{e}^{2a(t-T)}-\mathrm{e}^{(\beta^2+2\kappa)(t-T)}}{(a-\kappa)(2a-\beta^2-2\kappa)}+\frac{\mathrm{e}^{(\beta^2+2\kappa)(t-T)}-\mathrm{e}^{(a+\kappa)(t-T)}}{(\kappa-a)(-a+\beta^2+\kappa)}))\}.
\end{aligned}
$$

Substituting this into the formula below yields the result.

$$
\begin{aligned}
g^{(2)}(v,t,T,j)=\mathrm{e}^{v_{\min}(C_7(j)(T-t)-\frac{C_6(\mathrm{e}^{-a(T-t)}-1)}{a})}&(1+(v_{\max}-v_{\min})\\
&\times\{\sum_{(l_1)\in\mathcal{L}^1}\psi_{l_1}(z)k_{l_1}q(l_0,l_1)I^{1,j}_{t,T}(\lambda_{l_1})\}\\
&+(v_{\max}-v_{\min})^2\{\sum_{(l_1,l_2)\in\mathcal{L}^2}\psi_{l_2}(z)k_{l_1}k_{l_2}q(l_0,l_1)q(l_1,l_2)I^{2,j}_{t,T}(\lambda_{l_1},\lambda_{l_2})\}).
\end{aligned}
$$

□

2.6 Bounds on the conditional expectation

We derive useful bounds on the conditional expectation given by g from Equation (2.13). These bounds allow us to prove that the firm value does not explode and that the function $\frac{L_j(j)}{I(j)}$ is a monotonic function of the interest rate. This is particularly useful if an approximation for the growth option values is desired. It is possible to calculate the growth option values on a grid of interest rate values and interpolate to reduce computation time. The bounds may also be useful in finding error estimates. Let $v_{\min}>0$. We now define functions for clarity when writing complicated expressions. Define the random variable $K(t,T,j)=\int_t^T f(T,p,j)V_j(p)\,\mathrm{d}p$ for all positive integers t,T,j. Let the functions $K_l:[0,\infty)^2\times\mathbb{Z}^+\to\mathbb{R}$ and $K_u:[0,\infty)^2\times\mathbb{Z}^+\to\mathbb{R}$ be defined by

$$K_l(t,T,j)=C_7(j)v_{\max}(T-t),$$
$$K_u(t,T,j)=\lambda\sigma\rho^{M,C_j}v_{\min}(T-t).$$

These are lower and upper bounds on $K(t,T,j)$, respectively. Define the set D by the Cartesian product $D=(0,\infty)^2\times\mathbb{Z}^+$. Let the functions $A_{11}:D\to\mathbb{R}$, $A_{12}:[v_{\min},v_{\max}]\times D\to\mathbb{R}$, and $A_1:[v_{\min},v_{\max}]\times D\to\mathbb{R}$ be defined by

$$\begin{aligned}
A_{11}(t,T,j)&=C_6\theta(\frac{1-\mathrm{e}^{-a(T-t)}}{a})+\theta(T-t)C_7(j),\\
A_{12}(v,t,T,j)&=C_6(v-\theta)(\frac{\mathrm{e}^{-\kappa(T-t)}-\mathrm{e}^{-a(T-t)}}{a-\kappa})+(v-\theta)(\frac{1-\mathrm{e}^{-\kappa(T-t)}}{\kappa})C_7(j),\\
A_1(v,t,T,j)&=A_{11}(t,T,j)+A_{12}(v,t,T,j).
\end{aligned}$$

Now, we define the functions $l_b:[v_{\min},v_{\max}]\times D\to\mathbb{R}$ and $u_b:[v_{\min},v_{\max}]\times D\to\mathbb{R}$.

$$\begin{aligned}
l_b(v,t,T,j)&=\mathrm{e}^{A_1(v,t,T,j)},\\
u_b(v,t,T,j)&=\frac{K_u(t,T,j)\mathrm{e}^{K_l(t,T,j)}-K_l(t,T,j)\mathrm{e}^{K_u(t,T,j)}+(\mathrm{e}^{K_u(t,T,j)}-\mathrm{e}^{K_l(t,T,j)})A_1(v,t,T,j)}{K_u(t,T,j)-K_l(t,T,j)}.
\end{aligned}$$

Note that given $\kappa>0$, $a>0$, $\theta>0$, $\rho^{M,C_j}>0$, and $\rho^{r,C_j}>0$, it follows that $\lim_{T\to\infty}l_b(v,t,T,j)=0$. We now state our result on the bounds of g.

Theorem 2.6.1. *The function $g(v,t,T,j)$ has the following bounds:*

$$\max(\mathrm{e}^{K_l(t,T,j)},l_b(v,t,T,j))\le g(v,t,T,j)\le\min(\mathrm{e}^{-K_u(t,T,j)},u_b(v,t,T,j)).$$

Proof. The proof is similar to Theorem 4.2 of Delbaen and Shirakawa [11]. Throughout the proof, we assume that we are considering the Jacobi process for the j-th project of a specific firm, and thus the Jacobi process parameters are fixed. We begin with some useful calculations. By Equation (2.8),

$$\mathbb{E}\left[V_j(p)|V_j(t)=v\right]=\theta+(v-\theta)\mathrm{e}^{-\kappa(p-t)}.$$

Integration from t to T yields

$$\begin{aligned}
\int_t^T \mathbb{E}\left[V_j(p)|V_j(t)=v\right]f(T,p,j)\,\mathrm{d}p &= \int_t^T(\theta+(v-\theta)\mathrm{e}^{-\kappa(p-t)})(C_6\mathrm{e}^{-a(T-p)}+C_7(j))\,\mathrm{d}p\\
&= C_6\theta\int_t^T \mathrm{e}^{-a(T-p)}\,\mathrm{d}p + C_7(j)\theta\int_t^T \mathrm{d}p\\
&+ C_6(v-\theta)\int_t^T \mathrm{e}^{-a(T-p)}\mathrm{e}^{-\kappa(p-t)}\,\mathrm{d}p\\
&+ C_7(j)(v-\theta)\int_t^T \mathrm{e}^{-\kappa(p-t)}\,\mathrm{d}p\\
&= A_1(v,t,T,j).
\end{aligned}$$

Below, the second equality follows by Fubini's theorem, and the inequality follows by Jensen's inequality (since e^x is convex).

$$\begin{aligned}
\mathrm{e}^{A_1(v,t,T,j)} &= \mathrm{e}^{\int_t^T \mathbb{E}\left[V_j(p)|V_j(t)=v\right]f(T,p,j)\,\mathrm{d}p}\\
&= \mathrm{e}^{\mathbb{E}\left[\int_t^T V_j(p)f(T,p,j)\,\mathrm{d}p|V_j(t)=v\right]}\\
&\le \mathbb{E}\left[\mathrm{e}^{\int_t^T V_j(p)f(T,p,j)\,\mathrm{d}p}|V_j(t)=v\right].
\end{aligned}$$

We now establish an upper bound. Recall that for every t, $V_j(t)\in[v_{\min},v_{\max}]\subset[0,\infty)$. So,

$$v_{\min}(T-t)=v_{\min}\int_t^T \mathrm{d}p \le \int_t^T V_j(p)\,\mathrm{d}p \le v_{\max}\int_t^T \mathrm{d}p = v_{\max}(T-t). \tag{2.16}$$

Recall that $f(s,p,j)=C_6\mathrm{e}^{-a(s-p)}+C_7(j)$ with $C_6>0$ and $C_7(j)<0$. By assumption $s\ge p$ and $a>0$. Below, we establish an upper bound on f. The last line uses the fact $0<\mathrm{e}^{-a(s-p)}\le 1$.

$$f(s,p,j)=\frac{\sigma\sigma_r\rho^{r,C_j}}{a}(\mathrm{e}^{-a(s-p)}-1)-\lambda\sigma\rho^{M,C_j}$$

$$
\begin{aligned}
&= \frac{\sigma\sigma_r\rho^{r,C_j}}{a}\mathrm{e}^{-a(s-p)} - \frac{\sigma\sigma_r\rho^{r,C_j}}{a} - \lambda\sigma\rho^{M,C_j} \\
&\leq -\lambda\sigma\rho^{M,C_j}.
\end{aligned}
$$

A lower bound is given by $f(s,p,j) \geq -\frac{\sigma\sigma_r\rho^{r,C_j}}{a} - \lambda\sigma\rho^{M,C_j} = C_7(j)$. Thus,

$$C_7(j) \leq f(s,p,j) \leq -\lambda\sigma\rho^{M,C_j}. \tag{2.17}$$

Since for every p, $V_j(p) \in [v_{\min}, v_{\max}] \subset [0,\infty)$, it follows that

$$C_7(j)V_j(p) \leq f(s,p,j)V_j(p) \leq -\lambda\sigma\rho^{M,C_j}V_j(p).$$

This implies the following inequalities:

$$C_7(j)\int_t^T V_j(p)\,\mathrm{d}p \leq \int_t^T f(s,p,j)V_j(p)\,\mathrm{d}p \leq -\lambda\sigma\rho^{M,C_j}\int_t^T V_j(p)\,\mathrm{d}p < 0. \tag{2.18}$$

Note that

$$C_7(j)v_{\max}(T-t) \leq C_7(j)v_{\min}(T-t)$$

and

$$-\lambda\sigma\rho^{M,C_j}v_{\max}(T-t) \leq -\lambda\sigma\rho^{M,C_j}v_{\min}(T-t).$$

By Equations (2.16) and (2.18),

$$C_7(j)v_{\max}(T-t) \leq \int_t^T f(s,p,j)V_j(p)\,\mathrm{d}p \leq -\lambda\sigma\rho^{M,C_j}v_{\min}(T-t) \leq 0. \tag{2.19}$$

By monotonicity of the exponential function, we have the bounds

$$0 \leq \mathrm{e}^{C_7(j)v_{\max}(T-t)} \leq \mathrm{e}^{\int_t^T f(s,p,j)V_j(p)\,\mathrm{d}p} \leq \mathrm{e}^{-\lambda\sigma\rho^{M,C_j}v_{\min}(T-t)} \leq \mathrm{e}^0 = 1. \tag{2.20}$$

We now find another set of bounds. Let $\mathcal{J}(t) = \frac{K_u(t,T,j)-K(t,T,j)}{K_u(t,T,j)-K_l(t,T,j)}$. It now follows that $1-\mathcal{J}(t) = \frac{K(t,T,j)-K_l(t,T,j)}{K_u(t,T,j)-K_l(t,T,j)}$. Note that $\mathcal{J}(t) > 0$. As seen below, it is clear that $|\mathcal{J}(t)| \leq 1$.

$$|\mathcal{J}(t)| = |\frac{K_u(t,T,j)-K(t,T,j)}{K_u(t,T,j)-K_l(t,T,j)}| \leq |\frac{K_u(t,T,j)-K_l(t,T,j)}{K_u(t,T,j)-K_l(t,T,j)}| = 1.$$

So, $\mathcal{J}(t) \in [0,1]$ and $1-\mathcal{J}(t) \in [0,1]$. We are now able to write K as a combination of K_l and K_u, namely $K(t,T,j) = \mathcal{J}(t)K_l(t,T,j) + (1-\mathcal{J}(t))K_u(t,T,j)$. By the definition of convexity,

$$\begin{aligned}
\mathrm{e}^{K(t,T,j)} &\leq \mathcal{J}(t)\mathrm{e}^{K_l(t,T,j)} + (1-\mathcal{J}(t))\mathrm{e}^{K_u(t,T,j)} \\
&= \frac{K_u(t,T,j)-K(t,T,j)}{K_u(t,T,j)-K_l(t,T,j)}\mathrm{e}^{K_l(t,T,j)} + \frac{K(t,T,j)-K_l(t,T,j)}{K_u(t,T,j)-K_l(t,T,j)}\mathrm{e}^{K_u(t,T,j)}.
\end{aligned}$$

Taking conditional expectations yields

$$\begin{aligned}
\mathbb{E}\left[\mathrm{e}^{K(t,T,j)}|V_j(t)=v\right] &\leq \frac{K_u(t,T,j)-\mathbb{E}\left[K(t,T,j)|V_j(t)=v\right]}{K_u(t,T,j)-K_l(t,T,j)}\mathrm{e}^{K_l(t,T,j)} \\
&+ \frac{\mathbb{E}\left[K(t,T,j)|V_j(t)=v\right]-K_l(t,T,j)}{K_u(t,T,j)-K_l(t,T,j)}\mathrm{e}^{K_u(t,T,j)} \\
&= \frac{K_u(t,T,j)\mathrm{e}^{K_l(t,T,j)}-K_l(t,T,j)\mathrm{e}^{K_u(t,T,j)}}{K_u(t,T,j)-K_l(t,T,j)} \\
&+ \frac{(\mathrm{e}^{K_u(t,T,j)}-\mathrm{e}^{K_l(t,T,j)})\,\mathbb{E}\left[K(t,T,j)|V_j(t)=v\right]}{K_u(t,T,j)-K_l(t,T,j)} \\
&= \frac{K_u(t,T,j)\mathrm{e}^{K_l(t,T,j)}-K_l(t,T,j)\mathrm{e}^{K_u(t,T,j)}}{K_u(t,T,j)-K_l(t,T,j)} \\
&+ \frac{(\mathrm{e}^{K_u(t,T,j)}-\mathrm{e}^{K_l(t,T,j)})A_1(v,t,T,j)}{K_u(t,T,j)-K_l(t,T,j)},
\end{aligned}$$

where the last equality follows by the definition of A_1.

$\square$

Corollary 2.6.2. *If $\rho^{r,C_j} > 0$, $v_{\min} > 0$, and $\rho^{M,C_j} > 0$, then*

$$\lim_{T\to\infty} g(v,t,T,j) = 0.$$

Proof. By Theorem 2.6.1,

$$0 = \lim_{T\to\infty} \mathrm{e}^{C_7(j)v_{\max}(T-t)} \leq \lim_{T\to\infty} g(v,t,T,j) \leq \lim_{T\to\infty} \mathrm{e}^{-\lambda\sigma\rho^{M,C_j}v_{\min}(T-t)} = 0.$$

□

2.7 Main theoretical results: firm valuation and returns

We begin this section by presenting a roadmap for our path to the main results. Berk, Green, and Naik [15] state that their simulation is only feasible due to the closed form solutions developed within their framework. Incorporating stochastic cash flow volatility renders computational difficulties. These difficulties arise due to the large number of conditional expectations that must be computed, each of which requires the generation of many long time series and depends upon many different possible combinations of the monthly interest rate, the correlation between the SDF and the cash flow process (ρ^{M,C_j}), and the Jacobi process parameters. Through conditioning, the computational complexity of the problem is significantly reduced. The goal of this section is to derive expressions for the value of each firm at every point in time for the duration of the simulation. We outline our solution here.

First, the goal is to compute the value of a firm at time $t \in \mathbb{Z}^+$, where t represents month t. The firm value is calculated by adding the time t expected value of all the future cash flows of all the projects alive at time t to the time t value of all growth opportunities. We reduce the computational complexity of the problem by writing the expression for the cash flows and growth options in terms of the conditional expectation from Equation (2.13).

Let $P(t)$ be the firm value at time t. Later, a formula will be derived to express $P(t)$ in terms of the value of growth options and future cash flows from alive projects. The realized rate of return for holding a claim on the firm for exactly one month starting at time t is given by $R_{t+1} = \frac{P(t+1)}{P(t)} - 1$. Similarly, the expected rate of return is $\mathbb{E}\left[R_{t+1}|\mathcal{F}_t\right] = \frac{\mathbb{E}\left[P(t+1)|\mathcal{F}_t\right]}{P(t)} - 1$.

We show that our model reproduces the desirable property that, ceteris paribus, a firm is more likely to take on projects during periods of low interest rates and less likely to take on projects during periods of high interest rates.

In the next section, we begin our quest to find expressions for the firm value at each month in time by deriving formulas for the value of future cash flows from alive projects. Before we begin, we comment on notation in this section. Since the Jacobi process models firm specific cash flows, each firm has its own Jacobi process parameters. Thus, we will derive all of our formulas for the j-th project of a specific firm, and the formulas regarding other projects of the same firm will be identical.

2.7.1 Value of ongoing projects this period

In this section, we calculate the value of ongoing projects at each month in time by calculating the expected value of cash flows from projects that are still alive for the firm in question at that time. In the next section, we calculate the expected value of these cash flows next period given the current information. Here, we state a lemma that gives the expected value of cash flows for a particular month, say month s, in the future given that the project is known to be alive at month t prior to s. First, we define some functions to make the exposition clear. Let the functions $h : (\mathbb{Z}^+)^3 \to \mathbb{R}$, $h_l : (\mathbb{Z}^+)^2 \to \mathbb{R}$, and $h_u : (\mathbb{Z}^+)^2 \to \mathbb{R}$ be defined by

$$\begin{aligned}
h(j,t,s) &= \overline{C} + C_1(s-t) + C_2(t) + \mu(s-j) + R(j,j,t) - \frac{\sigma_r^2}{4a^3}\mathrm{e}^{-2a(s-t)} + C_3(t)\mathrm{e}^{-a(s-t)},\\
h_l(j,t) &= \overline{C} + C_2(t) + R(j,j,t) + \mu(t-j),\\
h_u(t,s) &= C_1(s-t) + \mu(s-t) - \frac{\sigma_r^2}{4a^3}\mathrm{e}^{-2a(s-t)} + C_3(t)\mathrm{e}^{-a(s-t)}.
\end{aligned}$$

Note that $h(j,t,s) = h_l(j,t) + h_u(t,s)$. For every $s,t,j \in \mathbb{R}^+$, we define the random variables $X_1(t,s), F_1(t,s), \mathcal{Z}(t,s), \mathcal{X}(j,t,s)$, and the function F_2 as follows:

$$\begin{aligned}
X_1(t,s) &= W^M(s) - W^M(t),\\
F_1(t,s) &= -\lambda X_1(t,s) - \frac{\sigma_r}{a}\int_t^s (1-\mathrm{e}^{-a(s-p)})\,\mathrm{d}W^r(p),\\
F_2(t,s) &= \frac{\lambda^2}{2}(s-t) + \frac{\sigma_r^2}{2a^2}\int_t^s (1-\mathrm{e}^{-a(s-p)})^2\,\mathrm{d}p + \frac{\lambda\sigma_r\rho^{Mr}}{a}(s-t+\frac{\mathrm{e}^{-a(s-t)}-1}{a}),\\
\mathcal{Z}(t,s) &= -\frac{\sigma_r}{a}\int_t^s (1-\mathrm{e}^{-a(s-p)})\,\mathrm{d}W^r(p),
\end{aligned}$$

$$\mathcal{X}(j,t,s) = -\frac{\sigma\sigma_r\rho^{r,C_j}}{a}\int_t^s V_j(p)(1-\mathrm{e}^{-a(s-p)})\,\mathrm{d}p.$$

The Lemma regarding the cash flows at one month in the future for a project still alive is given below.

Lemma 2.7.1. *Suppose that the j-th project for a specific firm is known to be alive at time t. Then, the time t value of the future cash flow at time s ($s \geq t$) from the jth project ($j \leq t$) is given by*

$$\mathbb{E}\,[\frac{M(s)}{M(t)}C_j(s)\chi_j(s)|\mathcal{F}_t] = I(j)\mathrm{e}^{h(j,t,s)}g(v,t,s,j)\boldsymbol{\pi}^{s-t}. \tag{2.21}$$

Proof. We begin by establishing notation. For every $s,t,j \in \mathbb{R}^+$, we define the random variable

$$h_1(j,t,s) = I(j)\mathrm{e}^{\overline{C}-(\frac{\lambda^2}{2}+b_2)(s-t)+(\frac{b_2-r(t)}{a})[1-\mathrm{e}^{-a(s-t)}]+\mu(s-j)+R(j,j,t)}.$$

Note that by Equation (2.9), $\frac{M(s)}{M(t)} = \mathrm{e}^{-\frac{\lambda^2}{2}(s-t)-\lambda X_1(t,s)-\int_t^s r_u\,\mathrm{d}u}$. The main idea in what follows will be to use the tower property to condition on the paths of the Jacobi process from time t up to time s. This standard technique can be found in Privault [25]. Because of independence, it is enough to calculate $\mathbb{E}\,[\frac{M(s)}{M(t)}C_j(s)|\mathcal{F}_t]$.

$$\begin{aligned}\mathbb{E}\,[\frac{M(s)}{M(t)}C_j(s)|\mathcal{F}_t] &= I(j)\,\mathbb{E}\,[\mathrm{e}^{\overline{C}-\frac{\lambda^2}{2}(s-t)-\lambda X_1(t,s)-\int_t^s r_u\,\mathrm{d}u+\mu(s-j)+R(j,j,s)}|\mathcal{F}_t] \\ &= h_1(j,t,s)\,\mathbb{E}\,[\mathrm{e}^{F_1(t,s)+R(j,t,s)}|\mathcal{F}_t] \\ &= h_1(j,t,s)\,\mathbb{E}\,[\mathrm{e}^{-\frac{\sigma^2}{2}\int_t^s V_j^2(u)\,\mathrm{d}u}\,\mathbb{E}\,[\mathrm{e}^{F_1(t,s)+\sigma\int_t^s V_j(u)\,\mathrm{d}W^{C_j}(u)}|\mathcal{F}_t\vee\mathcal{F}_{t,s}^j]|\mathcal{F}_t].\end{aligned} \tag{2.22}$$

To proceed, we need three conditional covariances. The calculations proceed the results.

1. $\mathrm{cov}_{\mathcal{F}_t\vee\mathcal{F}_{t,s}^j}(-\lambda X_1(t,s),\mathcal{Z}(t,s)) = \frac{\lambda\sigma_r\rho^{Mr}}{a}(s-t+\frac{\mathrm{e}^{-a(s-t)}-1}{a})$,

2. $\mathrm{cov}_{\mathcal{F}_t\vee\mathcal{F}_{t,s}^j}(-\lambda X_1(t,s),\sigma\int_t^s V_j(u)\,\mathrm{d}W^{C_j}(u)) = -\lambda\sigma\rho^{M,C_j}\int_t^s V_j(u)\,\mathrm{d}u$,

3. $\mathrm{cov}_{\mathcal{F}_t\vee\mathcal{F}_{t,s}^j}(\sigma\int_t^s V_j(p)\,\mathrm{d}W^{C_j}(p),\mathcal{Z}(t,s)) = \mathcal{X}(j,t,s)$.

First, let $\Lambda_1 = \mathrm{cov}_{\mathcal{F}_t\vee\mathcal{F}_{t,s}^j}(-\lambda X_1(t,s),\mathcal{Z}(t,s))$. Then,

$$\Lambda_1 = \frac{\lambda\sigma_r}{a}\,\mathrm{cov}_{\mathcal{F}_t\vee\mathcal{F}_{t,s}^j}(X_1(t,s),\int_t^s(1-\mathrm{e}^{-a(s-p)})\,\mathrm{d}W^r(p))$$

$$
\begin{aligned}
&= \frac{\lambda\sigma_r}{a}\operatorname{cov}_{\mathcal{F}_t\vee\mathcal{F}^j_{t,s}}\Big(\int_t^s \mathrm{d}W^M(p), \int_t^s (1-\mathrm{e}^{-a(s-p)})\,\mathrm{d}W^r(p)\Big)\\
&= \frac{\lambda\sigma_r}{a}\,\mathbb{E}\Big(\int_t^s \mathrm{d}W^M(p)\int_t^s (1-\mathrm{e}^{-a(s-p)})\,\mathrm{d}W^r(p)|\mathcal{F}_t\vee\mathcal{F}^j_{t,s}\Big)\\
&= \frac{\lambda\sigma_r}{a}\,\mathbb{E}\Big(\int_t^s (1-\mathrm{e}^{-a(s-p)})\,\mathrm{d}[W^M,W^r](p)|\mathcal{F}_t\vee\mathcal{F}^j_{t,s}\Big)\\
&= \frac{\lambda\sigma_r\rho^{Mr}}{a}\int_t^s \mathbb{E}(1-\mathrm{e}^{-a(s-p)}|\mathcal{F}_t\vee\mathcal{F}^j_{t,s})\,\mathrm{d}p\\
&= \frac{\lambda\sigma_r\rho^{Mr}}{a}\int_t^s (1-\mathrm{e}^{-a(s-p)})\,\mathrm{d}p\\
&= \frac{\lambda\sigma_r\rho^{Mr}}{a}\Big(s-t+\frac{\mathrm{e}^{-a(s-t)}-1}{a}\Big).
\end{aligned}
$$

Second, let $\Lambda_2 = \operatorname{cov}_{\mathcal{F}_t\vee\mathcal{F}^j_{t,s}}(-\lambda X_1(t,s), \sigma\int_t^s V_j(u)\,\mathrm{d}W^{C_j}(u))$. The calculation is shown below.

$$
\begin{aligned}
\Lambda_2 &= -\lambda\sigma\operatorname{cov}_{\mathcal{F}_t\vee\mathcal{F}^j_{t,s}}\Big(\int_t^s \mathrm{d}W^M(u), \int_t^s V_j(u)\,\mathrm{d}W^{C_j}(u)\Big)\\
&= -\lambda\sigma\,\mathbb{E}\Big[\int_t^s V_j(u)\,\mathrm{d}[W^M,W^{C_j}](u)|\mathcal{F}^1_t\vee\mathcal{F}^2_s\Big]\\
&= -\lambda\sigma\rho^{M,C_j}\int_t^s V_j(u)\,\mathrm{d}u.
\end{aligned}
$$

Let $\Lambda_3 = \operatorname{cov}_{\mathcal{F}_t\vee\mathcal{F}^j_{t,s}}(\sigma\int_t^s V_j(p)\,\mathrm{d}W^{C_j}(p), \mathcal{Z}(t,s))$. Then,

$$
\begin{aligned}
\Lambda_3 &= -\frac{\sigma\sigma_r}{a}\operatorname{cov}_{\mathcal{F}_t\vee\mathcal{F}^j_{t,s}}\Big(\int_t^s V_j(p)\,\mathrm{d}W^{C_j}(p), \int_t^s (1-\mathrm{e}^{-a(s-p)})\,\mathrm{d}W^r(p)\Big)\\
&= -\frac{\sigma\sigma_r}{a}E\Big[\int_t^s V_j(p)(1-\mathrm{e}^{-a(s-p)})\rho^{r,C_j}\,\mathrm{d}p|\mathcal{F}^1_t\vee\mathcal{F}^2_s\Big]\\
&= -\frac{\sigma\sigma_r\rho^{r,C_j}}{a}\int_t^s \mathbb{E}\left[V_j(p)(1-\mathrm{e}^{-a(s-p)})|\mathcal{F}^1_t\vee\mathcal{F}^2_s\right]\mathrm{d}p\\
&= -\frac{\sigma\sigma_r\rho^{r,C_j}}{a}\int_t^s V_j(p)(1-\mathrm{e}^{-a(s-p)})\,\mathrm{d}p.
\end{aligned}
$$

Now, note that $a > 0$, $s > t$, and $\mathrm{e}^{-x} < 1\ \forall x > 0$. Using a well known property of normal random variables and letting

$$
\Lambda_4 = \mathbb{E}\left[\mathrm{e}^{-\lambda X_1(t,s)+\mathcal{Z}(t,s)+\sigma\int_t^s V_j(u)\,\mathrm{d}W^{C_j}(u)}|\mathcal{F}_t\vee\mathcal{F}^j_{t,s}\right],
$$

it follows that

$$
\begin{aligned}
\Lambda_4 &= \mathrm{e}^{F_2(t,s)+\frac{\sigma^2}{2}\int_t^s V_j^2(u)\,\mathrm{d}u-\lambda\sigma\rho^{M,C_j}\int_t^s V_j(u)\,\mathrm{d}u-\frac{\sigma\sigma_r\rho^{r,C_j}}{a}\int_t^s V_j(p)(1-\mathrm{e}^{-a(s-p)})\,\mathrm{d}p} \\
&= \mathrm{e}^{F_2(t,s)+\int_t^s V_j(p)f(s,p,j)\,\mathrm{d}p+\frac{\sigma^2}{2}\int_t^s V_j^2(u)\,\mathrm{d}u}. \qquad (2.23)
\end{aligned}
$$

Substitution of Equation (2.23) into Equation (2.22) yields

$$
\begin{aligned}
\mathbb{E}\,[\frac{M(s)}{M(t)}C_j(s)|\mathcal{F}_t] &= h_1(j,t,s)\,\mathbb{E}\,[\mathrm{e}^{-\frac{\sigma^2}{2}\int_t^s V_j^2(u)\,\mathrm{d}u}\,\mathbb{E}\,[\mathrm{e}^{F_1(t,s)+\sigma\int_t^s V_j(u)\,\mathrm{d}W^{C_j}(u)}|\mathcal{F}_t\vee\mathcal{F}_{t,s}^j]|\mathcal{F}_t] \\
&= h_1(j,t,s)\mathrm{e}^{F_2(t,s)}\,\mathbb{E}\,[\mathrm{e}^{\int_t^s V_j(p)f(s,p,j)\,\mathrm{d}p}|\mathcal{F}_t] \\
&= h_1(j,t,s)\mathrm{e}^{F_2(t,s)}g(v,t,s,j).
\end{aligned}
$$

Expanding $h_1(j,t,s)\mathrm{e}^{F_2(t,s)}$ and rearranging terms yields

$$
\begin{aligned}
h_1(j,t,s)\mathrm{e}^{F_2(t,s)} &= I(j)\mathrm{e}^{\overline{C}+(\frac{\lambda\sigma_r\rho^{Mr}}{a}-b_2)(s-t)+(\frac{b_2-r(t)}{a})[1-\mathrm{e}^{-a(s-t)}]+\mu(s-j)+R(j,j,t)} \\
&\quad\times\mathrm{e}^{\frac{\sigma_r^2}{2a^2}\int_t^s(1-\mathrm{e}^{-a(s-p)})^2\,\mathrm{d}p+\frac{\lambda\sigma_r\rho^{Mr}}{a}(\frac{\mathrm{e}^{-a(s-t)}-1}{a})} \\
&= I(j)\mathrm{e}^{\overline{C}+C_1(s-t)+(\frac{b_2-r(t)}{a})[1-\mathrm{e}^{-a(s-t)}]+\mu(s-j)+R(j,j,t)-\frac{\sigma_r^2}{4a^3}\mathrm{e}^{-2a(s-t)}-\frac{3\sigma_r^2}{4a^3}} \\
&\quad\times\mathrm{e}^{(\frac{\sigma_r^2}{a^3}+\frac{\lambda\sigma_r\rho^{Mr}}{a^2})\mathrm{e}^{-a(s-t)}-\frac{\lambda\sigma_r\rho^{Mr}}{a^2}} \\
&= I(j)\mathrm{e}^{\overline{C}+C_1(s-t)+C_2(t)+\mu(s-j)+R(j,j,t)-\frac{\sigma_r^2}{4a^3}\mathrm{e}^{-2a(s-t)}+C_3(t)\mathrm{e}^{-a(s-t)}}.
\end{aligned}
$$

Using the definition of h, we now have the desired formula for $\mathbb{E}\,[\frac{M(s)}{M(t)}C_j(s)|\mathcal{F}_t]$. Now, note that by independence,

$$
\mathbb{E}\,[\frac{M(s)}{M(t)}C_j(s)\chi_j(s)|\mathcal{F}_t] = \mathbb{E}\,[\frac{M(s)}{M(t)}C_j(s)|\mathcal{F}_t]\,\mathbb{E}\,[\chi_j(s)|\mathcal{F}_t] = \boldsymbol{\pi}^{s-t}\,\mathbb{E}\,[\frac{M(s)}{M(t)}C_j(s)|\mathcal{F}_t].
$$

Combining these results yields the Lemma. □

As noted earlier, in order to find the value of a firm at month t, we will need to calculate the time t expected value of the cash flows from the projects which are still ongoing for the firm. This is accomplished by summing over terms of the form $\mathbb{E}\,[\frac{M(s)}{M(t)}C_j(s)\chi_j(s)|\mathcal{F}_t]$. The value at time t of the cash flows of a project beginning at time $j \leq t$ and still alive at time

t is $L_j(t) = \mathbb{E}\,[\sum_{s=t+1}^{\infty} \frac{M(s)}{M(t)} C_j(s)\chi_j(s)|\mathcal{F}_t] = \sum_{s=t+1}^{\infty} \mathbb{E}\,[\frac{M(s)}{M(t)} C_j(s)\chi_j(s)|\mathcal{F}_t]$, which follows by Fubini's theorem. Under suitable parameter selection, this infinite series will converge, and this is shown below in Lemma 2.7.3. An application of Lemma 2.7.1 yields the following Theorem.

Theorem 2.7.2. *The value at time t of the cash flows of a project that arrived at time $j \le t$ and is still alive at time t is*

$$L_j(t) = I(j)\mathrm{e}^{h_l(j,t)} \sum_{s=t+1}^{\infty} \boldsymbol{\pi}^{s-t} \mathrm{e}^{h_u(t,s)} g(v,t,s,j). \tag{2.24}$$

In particular,

$$L_j(j) = I(j)\mathrm{e}^{\overline{C}+C_2(j)} \sum_{s=j+1}^{\infty} \boldsymbol{\pi}^{s-j} \mathrm{e}^{h_u(j,s)} g(v,j,s,j). \tag{2.25}$$

Proof. First note that the project still being alive at time t implies $\chi_j(t) = 1$. Below, the first equality is by definition, the second equality is by Fubini's Theorem, the third equality is by Lemma 2.7.1, and the last equality is by the definitions of h_l and h_u.

$$\begin{aligned} L_j(t) &= \mathbb{E}\,[\sum_{s=t+1}^{\infty} \frac{M(s)}{M(t)} C_j(s)\chi_j(s)|\mathcal{F}_t] \\ &= \sum_{s=t+1}^{\infty} \mathbb{E}\,[\frac{M(s)}{M(t)} C_j(s)\chi_j(s)|\mathcal{F}_t] \\ &= I(j) \sum_{s=t+1}^{\infty} \boldsymbol{\pi}^{s-t} \mathrm{e}^{h(j,t,s)} g(v,t,s,j) \\ &= I(j)\mathrm{e}^{h_l(j,t)} \sum_{s=t+1}^{\infty} \boldsymbol{\pi}^{s-t} \mathrm{e}^{h_u(t,s)} g(v,t,s,j). \end{aligned} \tag{2.26}$$

In particular,

$$L_j(j) = I(j)\mathrm{e}^{h_l(j,j)} \sum_{s=j+1}^{\infty} \boldsymbol{\pi}^{s-j} \mathrm{e}^{h_u(j,s)} g(v,j,s,j). \tag{2.27}$$

□

We now state a Lemma concerning the convergence of the series in $L_j(t)$.

Lemma 2.7.3. *Let $a > 0$. A sufficient condition for the convergence of $A = \sum_{s=t+1}^{\infty} \boldsymbol{\pi}^{s-t} \mathrm{e}^{h_u(t,s)} g(v,t,s,j)$ is $C_1 + \mu - \lambda\sigma\rho^{M,C_j} v_{\min} < -\ln(\boldsymbol{\pi})$. As a result, the series in Equation (2.25) also converges.*

Proof. By Theorem 2.6.1,

$$g(v,t,t+k,j) \leq \min(\mathrm{e}^{-\lambda\sigma\rho^{M,C_j} v_{\min} k}, u_b(v,t,t+k,j)).$$

In particular,

$$g(v,t,t+k,j) \leq \mathrm{e}^{-\lambda\sigma\rho^{M,C_j} v_{\min} k}.$$

$$\begin{aligned}
A &= \sum_{s=t+1}^{\infty} \pi^{s-t} \mathrm{e}^{C_1(s-t)+\mu(s-t)-\frac{\sigma_r^2}{4a^3}\mathrm{e}^{-2a(s-t)}+C_3(t)\mathrm{e}^{-a(s-t)}} g(v,t,s,j) \\
&= \sum_{k=1}^{\infty} \pi^k \mathrm{e}^{(C_1+\mu)k-\frac{\sigma_r^2}{4a^3}\mathrm{e}^{-2ak}+C_3(t)\mathrm{e}^{-ak}} g(v,t,t+k,j) \\
&\leq \sum_{k=1}^{\infty} \pi^k \mathrm{e}^{(C_1+\mu-\lambda\sigma\rho^{M,C_j} v_{\min})k-\frac{\sigma_r^2}{4a^3}\mathrm{e}^{-2ak}+C_3(t)\mathrm{e}^{-ak}}.
\end{aligned}$$

Let B denote the value of the series

$$\sum_{k=1}^{\infty} \pi^k \mathrm{e}^{(C_1+\mu-\lambda\sigma\rho^{M,C_j} v_{\min})k-\frac{\sigma_r^2}{4a^3}\mathrm{e}^{-2ak}+C_3(t)\mathrm{e}^{-ak}}.$$

Let $a_k = \pi^k \mathrm{e}^{(C_1+\mu-\lambda\sigma\rho^{M,C_j} v_{\min})k-\frac{\sigma_r^2}{4a^3}\mathrm{e}^{-2ak}+C_3(t)\mathrm{e}^{-ak}}$. Note that $a_k > 0\ \forall k \in \mathbb{N}$ and $a > 0$. We proceed with the ratio test.

$$\begin{aligned}
\lim_{k\to\infty} \left|\frac{a_{k+1}}{a_k}\right| &= \lim_{k\to\infty} \frac{\pi^{k+1} \mathrm{e}^{(C_1+\mu-\lambda\sigma\rho^{M,C_j} v_{\min})(k+1)-\frac{\sigma_r^2}{4a^3}\mathrm{e}^{-2a(k+1)}+C_3(t)\mathrm{e}^{-a(k+1)}}}{\pi^k \mathrm{e}^{(C_1+\mu-\lambda\sigma\rho^{M,C_j} v_{\min})k-\frac{\sigma_r^2}{4a^3}\mathrm{e}^{-2ak}+C_3(t)\mathrm{e}^{-ak}}} \\
&= \lim_{k\to\infty} \pi \mathrm{e}^{(C_1+\mu-\lambda\sigma\rho^{M,C_j} v_{\min})-\frac{\sigma_r^2}{4a^3}(\mathrm{e}^{-2a(k+1)}-\mathrm{e}^{-2ak})+C_3(t)(\mathrm{e}^{-a(k+1)}-\mathrm{e}^{-ak})} \\
&= \pi \mathrm{e}^{(C_1+\mu-\lambda\sigma\rho^{M,C_j} v_{\min})}.
\end{aligned}$$

Now,

$$\begin{aligned}
&\lim_{k\to\infty} \left|\frac{a_{k+1}}{a_k}\right| < 1 \text{ iff} \\
&\mathrm{e}^{(C_1+\mu-\lambda\sigma\rho^{M,C_j} v_{\min})} < \frac{1}{\pi} \text{ iff} \\
&(C_1+\mu-\lambda\sigma\rho^{M,C_j} v_{\min}) < -\ln(\pi).
\end{aligned}$$

(Recall that $\boldsymbol{\pi}$ is a parameter affecting project lifetimes and is a value between 0 and 1.)
By the ratio test, the series in question converges absolutely. $\square$

For all $s \geq j$ with $s, j \in \mathbb{Z}^+$, define the function

$$\begin{aligned} F_3(j,s) = (C_1+\mu)(s-j) + \overline{C} + \frac{b_2}{a} - \frac{3\sigma_r^2}{4a^3} - \frac{\lambda\sigma_r\rho^{M,r}}{a^2} \\ + (\frac{\sigma_r^2}{a^3} + \frac{\lambda\sigma_r\rho^{M,r}}{a^2} - \frac{b_2}{a})\mathrm{e}^{-a(s-j)} - \frac{\sigma_r^2}{4a^3}\mathrm{e}^{-2a(s-j)}. \end{aligned}$$

For future reference, note that

$$\begin{aligned} F_3(s,s+k) = (C_1+\mu)k + \overline{C} + \frac{b_2}{a} - \frac{3\sigma_r^2}{4a^3} - \frac{\lambda\sigma_r\rho^{M,r}}{a^2} \\ + (\frac{\sigma_r^2}{a^3} + \frac{\lambda\sigma_r\rho^{M,r}}{a^2} - \frac{b_2}{a})\mathrm{e}^{-ak} - \frac{\sigma_r^2}{4a^3}\mathrm{e}^{-2ak}. \end{aligned} \tag{2.28}$$

We now show that our model reproduces the desirable property that firms are more likely to accept new projects when the interest rate is lower rather than higher.

Lemma 2.7.4. $\frac{L_j(j)}{I(j)}$ *is monotonically decreasing as a function of the interest rate.*
Specifically, $r(j_1) < r(j_2) \Rightarrow \frac{L_{j_1}(j_1)}{I(j_1)} > \frac{L_{j_2}(j_2)}{I(j_2)}$.

Proof. By assumption, $a > 0$. For every $k \in \mathbb{Z}^+$, $\mathrm{e}^{-ak} < 1 \Rightarrow \ \mathrm{e}^{-ak} - 1 < 0 \ \forall k$.

$$r(s) > 0 \Rightarrow \tfrac{r(s)}{a}(\mathrm{e}^{-ak} - 1) < 0.$$

The dependence of $\frac{L_j(j)}{I(j)}$ on $r(j)$ arises from the terms $C_2(j) = \frac{b_2 - r(j)}{a} - \frac{\lambda\sigma_r\rho^{Mr}}{a^2} - \frac{3\sigma_r^2}{4a^3}$ and $C_3(j) = \frac{\sigma_r^2}{a^3} + \frac{\lambda\sigma_r\rho^{Mr}}{a^2} + \frac{r(j)-b_2}{a}$. So, we write $\frac{L_j(j)}{I(j)}$ as follows:

$$\frac{L_j(j)}{I(j)} = \sum_{k=1}^{\infty} \boldsymbol{\pi}^k \mathrm{e}^{F_3(j,j+k) + \frac{r(j)}{a}(\mathrm{e}^{-ak}-1)} g(v,j,j+k,j). \tag{2.29}$$

Note that for any k, $F_3(j, j+k)$ and $g(v, j, j+k, j)$ do not depend on $r(j)$. Suppose $r(j_1) < r(j_2)$. Then, since for every $k \in \mathbb{Z}^+$, $(\mathrm{e}^{-ak} - 1) < 0$, it follows that

$$\frac{r(j_1)}{a}(\mathrm{e}^{-ak} - 1) > \frac{r(j_2)}{a}(\mathrm{e}^{-ak} - 1) \ \forall k.$$

Taking the exponential of each side yields

$$\mathrm{e}^{\frac{r(j_1)}{a}(\mathrm{e}^{-ak}-1)} > \mathrm{e}^{\frac{r(j_2)}{a}(\mathrm{e}^{-ak}-1)} \;\forall k.$$

Thus, we conclude that

$$\frac{L_{j_1}(j_1)}{I(j_1)} > \frac{L_{j_2}(j_2)}{I(j_2)}.$$

□

It will be seen later that the decision of the firm to take on a project will by determined by the sign of $\frac{L_j(j)}{I(j)} - 1$. So, it's easy to see that this model reproduces the desired effect that the interest rate has on a firm's decisions regarding growth opportunities, namely that a firm is more likely to take on projects during periods of low interest rates and less likely to take on projects during periods of high interest rates.

2.7.2 Valuation of growth options

The next step in firm valuation is finding the time t value of the growth options, which is given by $L^*(t)$. Note that $I(s) > 0 \;\forall s$, so division by $I(s)$ makes sense. Thus, it follows that $(L_s(s) - I(s))^+ = I(s)(\frac{L_s(s)}{I(s)} - 1)^+$. A project arrives at every month t, and the decision of whether or not to take on the project is made at the time the project arrives. For this reason, when calculating the value of growth opportunities available at time t, the value of the growth option at time t is not included. If the project is taken on at time t, the expected value of the cash flows from that project will be included in the calculation of $L_j(t)$. Now,

$$\begin{aligned} L^*(t) &= \sum_{s=t+1}^{\infty} \mathbb{E}\,[\frac{M(s)}{M(t)}(L_s(s) - I(s))^+ | \mathcal{F}_t] \\ &= \sum_{s=t+1}^{\infty} \mathbb{E}\,[\frac{M(s)}{M(t)} I(s)(\frac{L_s(s)}{I(s)} - 1)^+ | \mathcal{F}_t]. \end{aligned}$$

For simplicity we assume the investment process is independent of all other processes in this model. Thus,

$$L^*(t) = \sum_{s=t+1}^{\infty} \mathbb{E}\,[I(s)|\mathcal{F}_t]\,\mathbb{E}\,[\frac{M(s)}{M(t)}(\frac{L_s(s)}{I(s)} - 1)^+ | \mathcal{F}_t]. \tag{2.30}$$

Assuming I satisfies Equation (2.2),

$$\begin{aligned}\mathbb{E}\,[I(s)|\mathcal{F}_t] &= I(t)\mathrm{e}^{(\mu_I-\frac{\sigma_I^2}{2})(s-t)}\,\mathbb{E}\,[\mathrm{e}^{\sigma_I W^I(s-t)}|\mathcal{F}_t]\\ &= I(t)\mathrm{e}^{(\mu_I-\frac{\sigma_I^2}{2})(s-t)}\mathrm{e}^{\frac{\sigma_I^2}{2}(s-t)}\\ &= I(t)\mathrm{e}^{\mu_I(s-t)}.\end{aligned}$$

Then, substitution into Equation (2.30) yields

$$L^*(t) = I(t)\sum_{s=t+1}^{\infty}\mathrm{e}^{\mu_I(s-t)}\,\mathbb{E}\,[\frac{M(s)}{M(t)}(\frac{L_s(s)}{I(s)}-1)^+|\mathcal{F}_t]. \tag{2.31}$$

From now on, we consider the valuation of each firm over a finite time horizon T_F. For the purpose of the simulation in the next chapter, all the infinite summations will be truncated. Let T_K be the upper limit on the summation over k. We will still often write ∞ instead of T_F and T_K, but the truncation is implied. Then, there exists r^* depending on $v(s)$ and ρ^{M,C_s}, written as $r^*(s)$, such that

$$\sum_{k=1}^{T_K}\boldsymbol{\pi}^k\mathrm{e}^{F_3(s,s+k)+\frac{r^*(s)}{a}(\mathrm{e}^{-ak}-1)}g(v,s,s+k,s) = 1. \tag{2.32}$$

This follows since the the sum in question is a continuous function of r^*. Clearly, r^* can be chosen small enough so that the sum is less than 1 and large enough so that the sum is greater than 1. Then, an application of the intermediate value theorem yields the existence of the desired r^*. This will be used in the derivation of the growth option values. We begin in this direction with a Lemma on covariances.

Lemma 2.7.5. *Formulas for the following conditional covariances (given time t information) are as follows:*

1. $\mathrm{cov}_{\mathcal{F}_t}(-\lambda X_1(t,s), r(s)) = \frac{-\lambda\sigma_r\rho^{Mr}}{a}(1-\mathrm{e}^{-a(s-t)})$,
2. $\mathrm{cov}_{\mathcal{F}_t}(-\lambda X_1(t,s), -\int_t^s r(u)\,\mathrm{d}u) = \frac{\lambda\sigma_r\rho^{Mr}}{a}(s-t+\frac{\mathrm{e}^{-a(s-t)}-1}{a})$,
3. $\mathrm{cov}_{\mathcal{F}_t}(-\int_t^s r(u)\,\mathrm{d}u, r(s)) = \frac{\sigma_r\mathrm{e}^{-a(s-t)}}{a^2}\{1-\cosh\,(a(s-t))\}$.

Proof. The conditional covariances are calculated as follows:

1. Let $\Lambda_5 = \text{cov}_{\mathcal{F}_t}(-\lambda X_1(t,s), r(s))$. Substituting for $r(s)$ yields

$$\begin{aligned}
\Lambda_5 &= -\lambda \text{cov}_{\mathcal{F}_t}((W^M(s) - W^M(t)), \sigma_r \mathrm{e}^{-as} \int_t^s \mathrm{e}^{au} \, \mathrm{d}W^r(u)) \\
&= -\lambda \sigma_r \mathrm{e}^{-as} \text{cov}_{\mathcal{F}_t}(\int_t^s \mathrm{d}W^M(u), \int_t^s \mathrm{e}^{au} \, \mathrm{d}W^r(u)) \\
&= -\lambda \sigma_r \mathrm{e}^{-as} \, \mathbb{E}\,[\int_t^s \mathrm{e}^{au} \rho^{Mr} \, \mathrm{d}u | \mathcal{F}_t] \\
&= -\lambda \sigma_r \mathrm{e}^{-as} \rho^{Mr} \int_t^s \mathrm{e}^{au} \, \mathrm{d}u \\
&= \frac{-\lambda \sigma_r \rho^{Mr}}{a} (1 - \mathrm{e}^{-a(s-t)}).
\end{aligned}$$

2. Let $\Lambda_6 = \text{cov}_{\mathcal{F}_t}(-\lambda X_1(t,s), -\int_t^s r(u) \, \mathrm{d}u)$. Since

$$r(u) = \mathrm{e}^{-a(u-t)} r(t) + ab_2 \mathrm{e}^{-au} \int_t^u \mathrm{e}^{ap} \, \mathrm{d}p + \sigma_r \mathrm{e}^{-au} \int_t^u \mathrm{e}^{ap} \, \mathrm{d}W^r(p),$$

it follows that

$$\begin{aligned}
\text{cov}_{\mathcal{F}_t}(-\lambda X_1(t,s), -\int_t^s r(u) \, \mathrm{d}u) &= \lambda \text{cov}_{\mathcal{F}_t}((W^M(s) - W^M(t)), \int_t^s r(u) \, \mathrm{d}u) \\
&= \sigma_r \lambda \text{cov}_{\mathcal{F}_t}(\int_t^s \mathrm{d}W^M(p), \int_t^s \mathrm{e}^{-au} (\int_t^u \mathrm{e}^{ap} \, \mathrm{d}W^r(p)) \, \mathrm{d}u) \\
&= \sigma_r \lambda \text{cov}_{\mathcal{F}_t}(\int_t^s \mathrm{d}W^M(p), \frac{1}{a} \int_t^s (1 - \mathrm{e}^{-a(s-p)}) \, \mathrm{d}W^r(p)) \\
&= \frac{\lambda \sigma_r}{a} \, \mathbb{E}\,[\int_t^s (1 - \mathrm{e}^{-a(s-p)}) \rho^{Mr} \, \mathrm{d}p | \mathcal{F}_t] \\
&= \frac{\lambda \sigma_r \rho^{Mr}}{a} (s - t + \frac{\mathrm{e}^{-a(s-t)} - 1}{a}).
\end{aligned}$$

3. Finally, consider

$$\begin{aligned}
\text{cov}_{\mathcal{F}_t}(-\int_t^s r(u) \, \mathrm{d}u, r(s)) &= -\text{cov}_{\mathcal{F}_t}(\int_t^s r(u) \, \mathrm{d}u, r(s)) \\
&= -\text{cov}_{\mathcal{F}_t}(\frac{1}{a} \int_t^s (1 - \mathrm{e}^{-a(s-p)}) \, \mathrm{d}W^r(p), \sigma_r \mathrm{e}^{-as} \int_t^s \mathrm{e}^{ap} \, \mathrm{d}W^r(p)) \\
&= \frac{-\sigma_r \mathrm{e}^{-as}}{a} \, \mathbb{E}\,[\int_t^s (1 - \mathrm{e}^{-a(s-p)}) \mathrm{e}^{ap} \, \mathrm{d}p | \mathcal{F}_t]
\end{aligned}$$

$$= \frac{\sigma_r \mathrm{e}^{-a(s-t)}}{a^2}\{1 - \cosh(a(s-t))\}.$$

□

Before stating our first theorem on growth options, we define a few functions. These functions will occur naturally in the proof of Theorem 2.7.6. Define the functions $B_3 : (\mathbb{Z}^+)^2 \to \mathbb{R}$, $d_1 : (\mathbb{Z}^+)^3 \to \mathbb{R}$, $d_2 : (\mathbb{Z}^+)^2 \to \mathbb{R}$, $d_3 : (\mathbb{Z}^+)^3 \to \mathbb{R}$, $K^* : (\mathbb{Z}^+)^2 \to \mathbb{R}$, and $\Psi : (\mathbb{Z}^+)^3 \to \mathbb{R}$. Also, the variance of the random variable $Y(t,s)$, which is defined in the proof below, is listed here.

$$\begin{aligned}
B_3(t,s) &= (\frac{b_2 - r(t)}{a})[1 - \mathrm{e}^{-a(s-t)}] - b_2(s-t), \\
\frac{1}{2}\mathbb{V}(Y(t,s)) &= \frac{1}{2}(\lambda^2 + \frac{\sigma_r^2}{a^2} + 2\frac{\lambda\sigma_r}{a}\rho^{Mr})(s-t) + \sigma_r^2\frac{(1-\mathrm{e}^{-2a(s-t)})}{4a^3} \\
&\quad - \frac{\lambda\sigma_r\rho^{Mr}}{a^2}(1 - \mathrm{e}^{-a(s-t)}) - \frac{\sigma_r^2}{a^3}(\mathrm{e}^{-as} - \mathrm{e}^{at-2as}), \\
d_2(t,s) &= (\frac{b_2 - r(t)}{\sigma_r} + \frac{(r^*(s) - b_2)}{\sigma_r}\mathrm{e}^{a(s-t)} + \lambda\frac{\rho^{Mr}}{a}(\mathrm{e}^{a(s-t)} - 1) \\
&\quad + \frac{\sigma_r}{2a^2}(\mathrm{e}^{a\frac{(s-t)}{2}} - \mathrm{e}^{-a\frac{(s-t)}{2}})^2)\sqrt{\frac{2a}{\mathrm{e}^{2a(s-t)} - 1}}, \\
d_1(t,s,k) &= d_2(t,s) + \frac{\sigma_r}{a}(1 - \mathrm{e}^{-ak})\sqrt{\frac{1 - \mathrm{e}^{-2a(s-t)}}{2a}}, \\
K^*(s,k) &= \frac{r^*(s)}{a}(\mathrm{e}^{-ak} - 1), \\
d_3(t,s,k) &= \frac{(r(t)\mathrm{e}^{-a(s-t)} + b_2(1 - \mathrm{e}^{-a(s-t)}))}{a}(\mathrm{e}^{-ak} - 1) + \sigma_r^2(\mathrm{e}^{-ak} - 1)^2\frac{1 - \mathrm{e}^{-2a(s-t)}}{4a^3} \\
&\quad + \frac{\sigma_r}{a}(\mathrm{e}^{-ak} - 1)(-(\frac{\lambda\rho^{Mr}}{a} + \frac{\sigma_r}{a^2})(1 - \mathrm{e}^{-a(s-t)}) + \sigma_r\frac{1 - \mathrm{e}^{-2a(s-t)}}{2a^2}), \\
\Psi(t,s,k) &= \mathrm{e}^{B_3(t,s) + \frac{1}{2}\mathbb{V}(Y(t,s))}\{\mathrm{e}^{d_3(t,s,k)}N(d_1(t,s,k)) - \mathrm{e}^{K^*(s,k)}N(d_2(t,s))\}.
\end{aligned}$$

We now state our first growth option theorem.

Theorem 2.7.6. *The time t value of the future growth options is*

$$\begin{aligned}
L^*(t) = I(t)\sum_{k=1}^{\infty}\boldsymbol{\pi}^k \sum_{s=t+1}^{\infty} &\mathrm{e}^{(\mu_I - \frac{1}{2}\lambda^2)(s-t) + F_3(s,s+k)} \\
&\times \int_{\mathcal{V}}\int_{\mathcal{P}} g(v,s,s+k,s)\Psi(t,s,k)\,\mathrm{d}F_\rho(\rho^{M,C_s})\,\mathrm{d}F_V(V(s)),
\end{aligned} \tag{2.33}$$

where F_V denotes the stationary distribution of the appropriate Jacobi process and F_ρ denotes the distribution function of the random variable ρ^{M,C_s}, which is the same for all s.

Proof. First, let $\mathcal{A}(t,s) = \mathcal{F}_t \vee V_s(s) \vee \rho^{M,C_s}$. We begin by considering the following expectation:

$$\begin{aligned}
\mathbb{E}\,[\frac{M(s)}{M(t)}(\frac{L_s(s)}{I(s)}-1)^+|\mathcal{F}_t] &= \mathrm{e}^{-\frac{1}{2}\lambda^2(s-t)}\,\mathbb{E}\,[\mathrm{e}^{-\lambda(W^M(s)-W^M(t))-\int_t^s r(u)\,\mathrm{d}u}(\frac{L_s(s)}{I(s)}-1)^+|\mathcal{F}_t] \\
&= \mathrm{e}^{-\frac{1}{2}\lambda^2(s-t)}\,\mathbb{E}\,[\mathrm{e}^{-\lambda(W^M(s)-W^M(t))-\int_t^s r(u)\,\mathrm{d}u} \\
&\times (\sum_{k=1}^{\infty}\boldsymbol{\pi}^k \mathrm{e}^{F_3(s,s+k)+\frac{r(s)}{a}(\mathrm{e}^{-ak}-1)}g(v,s,s+k,s)-1)^+|\mathcal{F}_t] \\
&= \mathrm{e}^{-\frac{1}{2}\lambda^2(s-t)}\,\mathbb{E}\,[\,\mathbb{E}\,[\mathrm{e}^{-\lambda(W^M(s)-W^M(t))-\int_t^s r(u)\,\mathrm{d}u} \\
&\times (\sum_{k=1}^{\infty}\boldsymbol{\pi}^k \mathrm{e}^{F_3(s,s+k)+\frac{r(s)}{a}(\mathrm{e}^{-ak}-1)}g(v,s,s+k,s)-1)^+|\mathcal{A}(t,s)]|\mathcal{F}_t].
\end{aligned}$$

The last equality follows by the tower property. Now, we consider the inner expectation from above and manipulate the expression, so that we can later apply properties of normal random variables. Let

$$\Lambda_7 = \mathbb{E}\,[\mathrm{e}^{-\lambda X_1(t,s)-\int_t^s r(u)du}(\sum_{k=1}^{\infty}\boldsymbol{\pi}^k \mathrm{e}^{F_3(s,s+k)+\frac{r(s)}{a}(\mathrm{e}^{-ak}-1)}g(v,s,s+k,s)-1)^+|\mathcal{A}(t,s)].$$

Below, we use the represtation given in Equation (2.32) to adjust the summation and expectation.

$$\begin{aligned}
\Lambda_7 &= \mathbb{E}\,[\mathrm{e}^{-\lambda(W^M(s)-W^M(t))-\int_t^s r(u)\,\mathrm{d}u} \times (\sum_{k=1}^{\infty}\boldsymbol{\pi}^k \mathrm{e}^{F_3(s,s+k)+\frac{r(s)}{a}(\mathrm{e}^{-ak}-1)}g(v,s,s+k,s) \\
&- \sum_{k=1}^{\infty}\boldsymbol{\pi}^k \mathrm{e}^{F_3(s,s+k)+\frac{r^*(s)}{a}(\mathrm{e}^{-ak}-1)}g(v,s,s+k,s))^+|\mathcal{A}(t,s)] \\
&= \mathbb{E}\,[\mathrm{e}^{-\lambda(W^M(s)-W^M(t))-\int_t^s r(u)\,\mathrm{d}u}\sum_{k=1}^{\infty}\boldsymbol{\pi}^k g(v,s,s+k,s)\mathrm{e}^{F_3(s,s+k)}(\mathrm{e}^{\frac{r(s)}{a}(\mathrm{e}^{-ak}-1)} \\
&- \mathrm{e}^{\frac{r^*(s)}{a}(\mathrm{e}^{-ak}-1)})^+|\mathcal{A}(t,s)] \\
&= \sum_{k=1}^{\infty}\boldsymbol{\pi}^k g(v,s,s+k,s)\mathrm{e}^{F_3(s,s+k)}\,\mathbb{E}\,[\mathrm{e}^{-\lambda(W^M(s)-W^M(t))-\int_t^s r(u)\,\mathrm{d}u}(\mathrm{e}^{\frac{r(s)}{a}(\mathrm{e}^{-ak}-1)} \\
&- \mathrm{e}^{\frac{r^*(s)}{a}(\mathrm{e}^{-ak}-1)})^+|\mathcal{A}(t,s)].
\end{aligned}$$

The goal is to find a formula for the conditional expectation in the summation above. It is defined below by $\Psi(t,s,k)$. Note that Ψ is a function of $r(t)$ and $r^*(s)$. Let

$$\Psi(t,s,k) = \mathbb{E}\,[\mathrm{e}^{-\lambda X_1(t,s)-\int_t^s r(u)\,\mathrm{d}u}(\mathrm{e}^{\frac{r(s)}{a}(\mathrm{e}^{-ak}-1)} - \mathrm{e}^{\frac{r^*(s)}{a}(\mathrm{e}^{-ak}-1)})^+|\mathcal{A}(t,s)]. \tag{2.34}$$

Recall that $X_1(t,s)$ is normally distributed with mean 0 and variance $s-t$. In the expectation above, substitute for $r(s)$ using

$$r(s) = r(t)\mathrm{e}^{-a(s-t)} + b_2(1-\mathrm{e}^{-a(s-t)}) + \sigma_r \mathrm{e}^{-as}\int_t^s \mathrm{e}^{ap}\,\mathrm{d}W^r(p).$$

The random part of $r(s)$ is $\int_t^s \mathrm{e}^{au}\,\mathrm{d}W^r(u)$, which is normally distributed with mean 0 and variance $\int_t^s \mathrm{e}^{2au}\,\mathrm{d}u = \frac{\mathrm{e}^{2as}-\mathrm{e}^{2at}}{2a}$. The following integral arises in $-\int_t^s r(u)\,\mathrm{d}u$:

$$\int_t^s \mathrm{e}^{-au}(\int_t^u \mathrm{e}^{ap}\,\mathrm{d}W^r(p))\,\mathrm{d}u = \frac{1}{a}\int_t^s (1-\mathrm{e}^{a(p-s)})\,\mathrm{d}W^r(p) = \frac{1}{a}\int_t^s \mathrm{d}W^r(p) - \frac{\mathrm{e}^{-as}}{a}\int_t^s \mathrm{e}^{ap}\,\mathrm{d}W^r(p).$$

Let $X_2(t,s)$ be the random variable $\int_t^s \mathrm{d}W^r(p)$, which is normally distributed with mean 0 and variance $s-t$. Let $X_3(t,s)$ be the random variable $\int_t^s \mathrm{e}^{ap}\,\mathrm{d}W^r(p)$, which is normally distributed with mean 0 and variance $\frac{\mathrm{e}^{2as}-\mathrm{e}^{2at}}{2a}$. The following three covariances are easy to calculate.

- $\mathrm{cov}(X_1(t,s), X_2(t,s)) = \int_t^s \rho^{Mr}\,\mathrm{d}p = \rho^{Mr}(s-t)$,
- $\mathrm{cov}(X_2(t,s), X_3(t,s)) = \int_t^s \mathrm{e}^{ap}\,\mathrm{d}p = \frac{\mathrm{e}^{as}-\mathrm{e}^{at}}{a}$,
- $\mathrm{cov}(X_1(t,s), X_3(t,s)) = \int_t^s \mathrm{e}^{ap}\rho^{Mr}\,\mathrm{d}p = \frac{\rho^{Mr}}{a}(\mathrm{e}^{as}-\mathrm{e}^{at})$.

We aim to compute Λ_8 from Equation 2.34. Note that $a>0$ and $\mathrm{e}^{-ak}-1<0$. We make a few definitions for convenience and write $-\int_t^s r(u)\,\mathrm{d}u$ in terms of B_3.

1. $A_r(t,s) = r(t)\mathrm{e}^{-a(s-t)} + b_2(1-\mathrm{e}^{-a(s-t)})$. So, $r(s) = A_r(t,s) + \sigma_r\mathrm{e}^{-as}X_3(t,s)$.
2. $B_1(t,s,k) = \frac{A_r(t,s)}{a}(\mathrm{e}^{-ak}-1)$,
3. $B_2(s,k) = \frac{\sigma_r}{a}\mathrm{e}^{-as}(\mathrm{e}^{-ak}-1)$, so $|B_2(s,k)| = \frac{\sigma_r}{a}\mathrm{e}^{-as}(1-\mathrm{e}^{-ak})$,

4. For $s-t \geq 1$, $B_3(t,s) = (\frac{b_2 - r(t)}{a})[1-\mathrm{e}^{-a(s-t)}] - b_2(s-t)$. Then, $-\int_t^s r(u)\,\mathrm{d}u = B_3(t,s) - \frac{\sigma_r}{a} X_2(t,s) + \frac{\sigma_r}{a}\mathrm{e}^{-as} X_3(t,s)$.

We now have a new representation for Ψ from Equation (2.34):

$$\Psi(t,s,k) =$$
$$\mathrm{e}^{B_3(t,s)}\,\mathbb{E}\,[\mathrm{e}^{-\lambda X_1(t,s) - \frac{\sigma_r}{a} X_2(t,s) + \frac{\sigma_r}{a}\mathrm{e}^{-as} X_3(t,s)}(\mathrm{e}^{B_1(t,s,k)+B_2(s,k)X_3(t,s)} - \mathrm{e}^{\frac{r^*(s)}{a}(\mathrm{e}^{-ak}-1)})^+|\mathcal{A}(t,s)].$$

It is easy to show that all the random variables in the expectation in Ψ are jointly normal. Thus, we can apply the standard properties of normal random variables. Let the random variable $Y(t,s)$ be defined by

$$Y(t,s) = -\lambda X_1(t,s) - \frac{\sigma_r}{a} X_2(t,s) + \frac{\sigma_r}{a}\mathrm{e}^{-as} X_3(t,s).$$

Then, $\mathbb{E}\,[Y(t,s)] = 0$ and the variance of $Y(t,s)$ is given by

$$\begin{aligned}
\mathbb{V}(Y(t,s)) &= \lambda^2\,\mathbb{V}(X_1(t,s)) + \frac{\sigma_r^2}{a^2}\,\mathbb{V}(X_2(t,s)) + \frac{\sigma_r^2}{a^2}\mathrm{e}^{-2as}\,\mathbb{V}(X_3(t,s)) \\
&+ 2\frac{\lambda\sigma_r}{a}\,\mathrm{cov}(X_1(t,s),X_2(t,s)) - 2\frac{\lambda\sigma_r}{a}\mathrm{e}^{-as}\,\mathrm{cov}(X_1(t,s),X_3(t,s)) \\
&- 2\frac{\sigma_r^2}{a^2}\mathrm{e}^{-2as}\,\mathrm{cov}(X_2(t,s),X_3(t,s)) \\
&= (\lambda^2 + \frac{\sigma_r^2}{a^2} + 2\frac{\lambda\sigma_r}{a}\rho^{Mr})(s-t) + \sigma_r^2\frac{(1-\mathrm{e}^{-2a(s-t)})}{2a^3} \\
&- 2\frac{\lambda\sigma_r\rho^{Mr}}{a^2}(1-\mathrm{e}^{-a(s-t)}) - 2\frac{\sigma_r^2}{a^3}(\mathrm{e}^{-as} - \mathrm{e}^{at-2as}).
\end{aligned}$$

We will make use of $\frac{1}{2}\,\mathbb{V}(Y(t,s))$, so we record an expression for that here.

$$\begin{aligned}
\frac{1}{2}\,\mathbb{V}(Y(t,s)) &= \frac{1}{2}(\lambda^2 + \frac{\sigma_r^2}{a^2} + 2\frac{\lambda\sigma_r}{a}\rho^{Mr})(s-t) + \sigma_r^2\frac{(1-\mathrm{e}^{-2a(s-t)})}{4a^3} \\
&- \frac{\lambda\sigma_r\rho^{Mr}}{a^2}(1-\mathrm{e}^{-a(s-t)}) - \frac{\sigma_r^2}{a^3}(\mathrm{e}^{-as} - \mathrm{e}^{at-2as}).
\end{aligned}$$

For the purpose of the simulation, it's convenient to write this as a function of $n = s - t$ and t. Letting $n = s - t$ and using $\mathrm{e}^{-as} = \mathrm{e}^{-a(s-t)-at}$, we have the following formula:

$$\begin{aligned}\frac{1}{2}\,\mathbb{V}(Y(t,n)) = \frac{1}{2}(\lambda^2 + \frac{\sigma_r^2}{a^2} + 2\frac{\lambda\sigma_r}{a}\rho^{Mr})n + \sigma_r^2\frac{(1-\mathrm{e}^{-2an})}{4a^3} \\ - \frac{\lambda\sigma_r\rho^{Mr}}{a^2}(1-\mathrm{e}^{-an}) - \frac{\sigma_r^2}{a^3}\mathrm{e}^{-an-at}(1-\mathrm{e}^{-an}).\end{aligned}$$

We record the following computations for future use.

1. $\frac{B_1(t,s,k)}{|B_2(s,k)|} = \frac{b_2 - r(t)}{\sigma_r}\mathrm{e}^{at} - \frac{b_2}{\sigma_r}\mathrm{e}^{as}$,
2. $\frac{K^*(s,k)}{|B_2(s,k)|} = -\frac{r^*(s)}{\sigma_r}\mathrm{e}^{as}$,
3. $\mathrm{cov}(X_3(t,s), Y(t,s)) = -\lambda\frac{\rho^{Mr}}{a}(\mathrm{e}^{as} - \mathrm{e}^{at}) - \sigma_r\frac{\mathrm{e}^{as}-\mathrm{e}^{at}}{a^2} + \sigma_r\mathrm{e}^{-as}\frac{\mathrm{e}^{2as}-\mathrm{e}^{2at}}{2a^2}$.

Let N be the CDF of the standard normal distribution. Our aim here is to apply Lemma B.1 of BGN to find a formula for $\Psi(t,s,k)$ from Equation (2.34). In the definition of d_2 below, the first equality arises from an application of Lemma B.1 of BGN. The following equalities are for simplification purposes. We define the functions $\forall k \in \mathbb{Z}^+ \forall s > t$ with $s,t \in \mathbb{R}^+$ as follows:

1. Note that $\mathbb{E}\left[X_3(t,s)\right] = 0$. Let d_2 be defined as follows:

$$\begin{aligned}d_2(t,s,k) &= \frac{B_1(t,s,k) - K^*(s,k) + B_2(s,k)\,\mathbb{E}\left[X_3(t,s)\right] + B_2(s,k)\,\mathrm{cov}(X_3(t,s), Y(t,s))}{|B_2(s,k)|\sqrt{\mathbb{V}(X_3(t,s))}} \\ &= (\frac{b_2 - r(t)}{\sigma_r}\mathrm{e}^{at} + \frac{(r^*(s) - b_2)}{\sigma_r}\mathrm{e}^{as} + \lambda\frac{\rho^{Mr}}{a}(\mathrm{e}^{as} - \mathrm{e}^{at}) \\ &+ \frac{\sigma_r\mathrm{e}^{as} - 2\sigma_r\mathrm{e}^{at} + \sigma_r\mathrm{e}^{2at-as}}{2a^2})\sqrt{\frac{2a}{\mathrm{e}^{2as} - \mathrm{e}^{2at}}} \\ &= \mathrm{e}^{at}(\frac{b_2 - r(t)}{\sigma_r} + \frac{(r^*(s) - b_2)}{\sigma_r}\mathrm{e}^{a(s-t)} + \lambda\frac{\rho^{Mr}}{a}(\mathrm{e}^{a(s-t)} - 1) \\ &+ (\frac{\sigma_r\mathrm{e}^{a(s-t)} - 2\sigma_r + \sigma_r\mathrm{e}^{-a(s-t)}}{2a^2}))\frac{1}{\mathrm{e}^{at}}\sqrt{\frac{2a}{\mathrm{e}^{2a(s-t)} - 1}}.\end{aligned}$$

Since d_2 does not depend on k, from now on we will write d_2 as a function of t and s alone. Thus,

$$\begin{aligned}
d_2(t,s) &= (\frac{b_2 - r(t)}{\sigma_r} + \frac{(r^*(s) - b_2)}{\sigma_r}\mathrm{e}^{a(s-t)} + \lambda\frac{\rho^{Mr}}{a}(\mathrm{e}^{a(s-t)} - 1) \\
&+ (\frac{\sigma_r \mathrm{e}^{a(s-t)} - 2\sigma_r + \sigma_r \mathrm{e}^{-a(s-t)}}{2a^2}))\sqrt{\frac{2a}{\mathrm{e}^{2a(s-t)} - 1}} \\
&= (\frac{b_2 - r(t)}{\sigma_r} + \frac{(r^*(s) - b_2)}{\sigma_r}\mathrm{e}^{a(s-t)} + \lambda\frac{\rho^{Mr}}{a}(\mathrm{e}^{a(s-t)} - 1) \\
&+ \frac{\sigma_r}{2a^2}(\mathrm{e}^{a\frac{(s-t)}{2}} - \mathrm{e}^{-a\frac{(s-t)}{2}})^2)\sqrt{\frac{2a}{\mathrm{e}^{2a(s-t)} - 1}}.
\end{aligned}$$

2. Let d_1 be defined as follows:

$$\begin{aligned}
d_1(t,s,k) &= d_2(t,s) + |B_2(s,k)|\sqrt{\mathbb{V}(X_3(t,s))} \\
&= d_2(t,s) + \frac{\sigma_r}{a}\mathrm{e}^{-as}(1 - \mathrm{e}^{-ak})\sqrt{\frac{\mathrm{e}^{2as} - \mathrm{e}^{2at}}{2a}} \\
&= d_2(t,s) + \frac{\sigma_r}{a}(1 - \mathrm{e}^{-ak})\sqrt{\frac{1 - \mathrm{e}^{-2a(s-t)}}{2a}}.
\end{aligned}$$

3. Let d_3 be defined as follows:

$$\begin{aligned}
d_3(t,s,k) &= B_1(t,s,k) + B_2(s,k)\,\mathbb{E}\left[X_3(t,s)\right] + \mathbb{E}\left[Y(t,s)\right] \\
&+ \frac{1}{2}(B_2(s,k)^2\,\mathbb{V}(X_3(t,s)) + 2B_2(s,k)\operatorname{cov}(X_3(t,s), Y(t,s))) \\
&= \frac{(r(t)\mathrm{e}^{-a(s-t)} + b_2(1 - \mathrm{e}^{-a(s-t)}))}{a}(\mathrm{e}^{-ak} - 1) \\
&+ \frac{1}{2}(\frac{\sigma_r^2}{a^2}\mathrm{e}^{-2as}(\mathrm{e}^{-ak} - 1)^2\frac{\mathrm{e}^{2as} - \mathrm{e}^{2at}}{2a} + 2\frac{\sigma_r}{a}\mathrm{e}^{-as}(\mathrm{e}^{-ak} - 1)(-\lambda\frac{\rho^{Mr}}{a}(\mathrm{e}^{as} - \mathrm{e}^{at}) \\
&- \frac{\sigma_r}{a}\frac{\mathrm{e}^{as} - \mathrm{e}^{at}}{a} + \frac{\sigma_r}{a}\mathrm{e}^{-as}\frac{\mathrm{e}^{2as} - \mathrm{e}^{2at}}{2a})) \\
&= \frac{(r(t)\mathrm{e}^{-a(s-t)} + b_2(1 - \mathrm{e}^{-a(s-t)}))}{a}(\mathrm{e}^{-ak} - 1) + \sigma_r^2(\mathrm{e}^{-ak} - 1)^2\frac{1 - \mathrm{e}^{-2a(s-t)}}{4a^3} \\
&+ \frac{\sigma_r}{a}(\mathrm{e}^{-ak} - 1)(-(\frac{\lambda\rho^{Mr}}{a} + \frac{\sigma_r}{a^2})(1 - \mathrm{e}^{-a(s-t)}) + \sigma_r\frac{1 - \mathrm{e}^{-2a(s-t)}}{2a^2}).
\end{aligned}$$

Applying Lemma B.1 of Berk, Green, and Naik [15] yields a formula for Ψ:

$$\begin{aligned}\Psi(t,s,k) &= \mathrm{e}^{B_3(t,s)}\{\mathrm{e}^{d_3(t,s,k)+\frac{1}{2}\,\mathbb{V}(Y(t,s))}N(d_1(t,s,k)) - \mathrm{e}^{K^*(s,k)+\mathbb{E}\,[Y(t,s)]+\frac{1}{2}\,\mathbb{V}(Y(t,s))}N(d_2(t,s))\}\\ &= \mathrm{e}^{B_3(t,s)+\frac{1}{2}\,\mathbb{V}(Y(t,s))}\{\mathrm{e}^{d_3(t,s,k)}N(d_1(t,s,k)) - \mathrm{e}^{K^*(s,k)}N(d_2(t,s))\}.\end{aligned}$$

We now substitute our formula for Ψ into $\mathbb{E}\,[\frac{M(s)}{M(t)}(\frac{L_s(s)}{I(s)}-1)^+|\mathcal{F}_t]$.

$$\begin{aligned}\mathbb{E}\,[\frac{M(s)}{M(t)}(\frac{L_s(s)}{I(s)}-1)^+|\mathcal{F}_t] &= \mathrm{e}^{-\frac{1}{2}\lambda^2(s-t)}\,\mathbb{E}\,[\sum_{k=1}^{\infty}\boldsymbol{\pi}^k g(v,s,s+k,s)\mathrm{e}^{F_3(s,s+k)}\Psi(t,s,k)|\mathcal{F}_t]\\ &= \mathrm{e}^{-\frac{1}{2}\lambda^2(s-t)}\sum_{k=1}^{\infty}\boldsymbol{\pi}^k\mathrm{e}^{F_3(s,s+k)}\,\mathbb{E}\,[g(v,s,s+k,s)\Psi(t,s,k)|\mathcal{F}_t]\\ &= \mathrm{e}^{-\frac{1}{2}\lambda^2(s-t)}\sum_{k=1}^{\infty}\boldsymbol{\pi}^k\mathrm{e}^{F_3(s,s+k)}\\ &\times\int_{\mathcal{V}}\int_{\mathcal{P}} g(v,s,s+k,s)\Psi(t,s,k)\,\mathrm{d}F_\rho(\rho^{M,C_s})\,\mathrm{d}F_V(v).\end{aligned}$$

Appropriately summing over s yields the final result. □

2.7.3 The firm value

Now that we have formulas for the value of a firm's assets in place and growth options, we are able to write down an expression for the value of the firm. First, note that the value of the firm's assets in place is

$$A^*(t) = \sum_{j=1}^{t} L_j(t)\chi_j(t). \tag{2.35}$$

The value of the firm is the sum of the value of the assets in place and the value of growth options. The value of the firm at month t is denoted by $P(t)$.

$$P(t) = \sum_{j=1}^{t} L_j(t)\chi_j(t) + L^*(t). \tag{2.36}$$

We are now able to calculate realized returns, which are given by $R_{t+1} = \frac{P(t+1)}{P(t)} - 1$. Analogous to BGN p. 1562 Equation (16), we have the following formula for the book value of the firm:

$$b(t) = \sum_{j=1}^{t} I(j)\chi_j(t). \tag{2.37}$$

We also desire a way to calculate the expected returns for the firm. As a first step in this direction, we now derive an expression for the expected cash flow next period, given the current information. This theorem will be particularly useful when fitting the model.

Theorem 2.7.7. *At time t, the conditional expectation, given the current information, of the cash flow next period is*

$$\mathbb{E}\,[\sum_{j=1}^{t} C_j(t+1)\chi_j(t+1)|\mathcal{F}_t] = \pi e^{\overline{C}} \sum_{j=1}^{t} \chi_j(t) I(j) e^{\mu(t+1-j)+R(j,j,t)}.$$

Proof. First, note that independence implies

$$\mathbb{E}\,[\sum_{j=1}^{t} C_j(t+1)\chi_j(t+1)|\mathcal{F}_t] = \pi \sum_{j=1}^{t} \chi_j(t)\,\mathbb{E}\,[C_j(t+1)|\mathcal{F}_t]. \tag{2.38}$$

Now, we derive an expression for the conditional expectation of cash flows next period, given the current information.

$$\begin{aligned}
\mathbb{E}\,[C_j(t+1)|\mathcal{F}_t] &= I(j)e^{\overline{C}+\mu(t+1-j)+R(j,j,t)}\,\mathbb{E}\,[e^{R(j,t,t+1)}|\mathcal{F}_t] \\
&= I(j)e^{\overline{C}+\mu(t+1-j)+R(j,j,t)}\,\mathbb{E}\,[\,\mathbb{E}\,[e^{R(j,t,t+1)}|\mathcal{F}_t \vee \mathcal{F}^j_{t,t+1}]|\mathcal{F}_t] \\
&= I(j)e^{\overline{C}+\mu(t+1-j)+R(j,j,t)}.
\end{aligned}$$

Substitution into Equation (2.38) yields the result. □

In the next section, we will derive a formula for the value of the currently alive projects next period, given the current information.

2.7.4 Value of ongoing projects next period

We desire to calculate the expected value of ongoing projects and growth options for the next period. This amounts to calculating the time $t+1$ value of the cash flows for each project given the information available at time t, and then summing up the value of each of these projects. We begin with a Lemma.

Lemma 2.7.8. *The conditional expectation of the value at time $t+1$ of the cash flows from the j-th project given the information available at time t is*

$$\mathbb{E}\left[L_j(t+1)|\mathcal{F}_t\right] = I(j)\sum_{s=t+2}^{\infty} \boldsymbol{\pi}^{s-t-1} C_4(j,t,s)\mathrm{e}^{R(j,j,t)} Q_j^*(v,t,s), \tag{2.39}$$

where

$$f_2(j,t,s) = \frac{\sigma\sigma_r}{a}(\mathrm{e}^{-as} - \mathrm{e}^{-a(t+1)})\rho^{r,C_j},$$

and

$$Q_j^*(v,t,s) = \mathbb{E}\left[g(v,t+1,s,j)\mathrm{e}^{f_2(j,t,s)\int_t^{t+1} V_j(u)\mathrm{e}^{au}\,\mathrm{d}u}|\mathcal{F}_t\right].$$

Proof. We begin the proof by defining the function Q_j, which is not the same as Q_j^*.

1. Let $Q_j(v,t,s) = \mathbb{E}\left[\mathrm{e}^{C_2(t+1)+R(j,t,t+1)+C_3(t+1)\mathrm{e}^{-a(s-t-1)}} g(v,t+1,s,j)|\mathcal{F}_t\right]$. Then, the time t conditional expectation of $L_j(t+1)$ is given as follows:

$$\begin{aligned}\mathbb{E}\left[L_j(t+1)|\mathcal{F}_t\right] &= I(j)\,\mathbb{E}\left[\mathrm{e}^{h_l(j,t+1)}\sum_{s=t+2}^{\infty}\boldsymbol{\pi}^{s-t-1}\mathrm{e}^{h_u(t+1,s)}g(v,t+1,s,j)|\mathcal{F}_t\right]\\ &= I(j)\sum_{s=t+2}^{\infty}\boldsymbol{\pi}^{s-t-1}\mathrm{e}^{\overline{C}+\mu(s-j)+C_1(s-t-1)-\frac{\sigma_r^2}{4a^3}\mathrm{e}^{-2a(s-t-1)}+R(j,j,t)}Q_j(v,t,s).\end{aligned}$$

2. We now substitute for $r(t+1)$ with the following:

$$r(t+1) = r(t)\mathrm{e}^{-a} + b_2(1-\mathrm{e}^{-a}) + \sigma_r\mathrm{e}^{-a(t+1)}\int_t^{t+1}\mathrm{e}^{au}\,\mathrm{d}W^r(u).$$

Below, instead of writing $Q_j(v,t,s)$, we simply write Q. The first equality follows by the tower property.

$$
\begin{aligned}
Q &= \mathbb{E}\,[\,\mathbb{E}\,[\mathrm{e}^{C_2(t+1)+R(j,t,t+1)+C_3(t+1)\mathrm{e}^{-a(s-t-1)}} g(v,t+1,s,j)|\mathcal{F}_t \vee \mathcal{F}^j_{t,t+1}]|\mathcal{F}_t] \\
&= \mathbb{E}\,[\mathrm{e}^{-\frac{\sigma^2}{2}\int_t^{t+1} V_j^2(u)\,\mathrm{d}u} g(v,t+1,s,j) \\
&\times \mathbb{E}\,[\mathrm{e}^{C_2(t+1)+\sigma\int_t^{t+1} V_j(u)\,\mathrm{d}W^{C_j}(u)+C_3(t+1)\mathrm{e}^{-a(s-t-1)}}|\mathcal{F}_t \vee \mathcal{F}^j_{t,t+1}]|\mathcal{F}_t] \\
&= \mathrm{e}^{(\frac{b_2}{a}-\frac{\lambda\sigma_r\rho^{Mr}}{a^2}-\frac{\sigma_r^2}{a^3})(1-\mathrm{e}^{-a(s-t-1)})+\frac{\sigma_r^2}{4a^3}}\,\mathbb{E}\,[\mathrm{e}^{-\frac{\sigma^2}{2}\int_t^{t+1} V_j^2(u)\,\mathrm{d}u} g(v,t+1,s,j) \\
&\times \mathbb{E}\,[\mathrm{e}^{\sigma\int_t^{t+1} V_j(u)\,\mathrm{d}W^{C_j}(u)+\frac{r(t+1)}{a}(\mathrm{e}^{-a(s-t-1)}-1)}|\mathcal{F}_t \vee \mathcal{F}^j_{t,t+1}]|\mathcal{F}_t] \\
&= \mathrm{e}^{(\frac{b_2}{a}-\frac{\lambda\sigma_r\rho^{Mr}}{a^2}-\frac{\sigma_r^2}{a^3}-\frac{r(t)\mathrm{e}^{-a}+b_2(1-\mathrm{e}^{-a})}{a})(1-\mathrm{e}^{-a(s-t-1)})+\frac{\sigma_r^2}{4a^3}}\,\mathbb{E}\,[\mathrm{e}^{-\frac{\sigma^2}{2}\int_t^{t+1} V_j^2(u)\,\mathrm{d}u} g(v,t+1,s,j) \\
&\times \mathbb{E}\,[\mathrm{e}^{\sigma\int_t^{t+1} V_j(u)\,\mathrm{d}W^{C_j}(u)+\frac{\sigma_r}{a}(\mathrm{e}^{-as}-\mathrm{e}^{-a(t+1)})\int_t^{t+1}\mathrm{e}^{au}\,\mathrm{d}W^r(u)}|\mathcal{F}_t \vee \mathcal{F}^j_{t,t+1}]|\mathcal{F}_t].
\end{aligned}
$$

After a calculation in the next step, we simplify the inner expectation.

3. We calculate the following conditional covariance in order to compute the inner expectation above. Let $\Lambda_9 = \mathrm{cov}_{\mathcal{F}_t\vee\mathcal{F}^j_{t,t+1}}(\sigma\int_t^{t+1} V_j(u)\,\mathrm{d}W^{C_j}(u), \frac{\sigma_r}{a}(\mathrm{e}^{-as}-\mathrm{e}^{-a(t+1)})\int_t^{t+1}\mathrm{e}^{au}\,\mathrm{d}W^r(u))$. Then, the following computation is standard.

$$
\begin{aligned}
\Lambda_9 &= \frac{\sigma\sigma_r}{a}(\mathrm{e}^{-as}-\mathrm{e}^{-a(t+1)})\,\mathrm{cov}_{\mathcal{F}_t\vee\mathcal{F}^j_{t,t+1}}(\int_t^{t+1} V_j(u)\,\mathrm{d}W^{C_j}(u), \int_t^{t+1}\mathrm{e}^{au}\,\mathrm{d}W^r(u)) \\
&= \frac{\sigma\sigma_r}{a}(\mathrm{e}^{-as}-\mathrm{e}^{-a(t+1)})(\mathbb{E}\,[\int_t^{t+1} V_j(u)\mathrm{e}^{au}\,\mathrm{d}[W^{C_j},W^r](u)|\mathcal{F}_t\vee\mathcal{F}^j_{t,t+1}] \\
&- \mathbb{E}\,[\int_t^{t+1} V_j(u)\,\mathrm{d}W^{C_j}(u)|\mathcal{F}_t\vee\mathcal{F}^j_{t,t+1}]\,\mathbb{E}\,[\int_t^{t+1}\mathrm{e}^{au}\,\mathrm{d}W^r(u)|\mathcal{F}_t\vee\mathcal{F}^j_{t,t+1}]) \\
&= \frac{\sigma\sigma_r}{a}(\mathrm{e}^{-as}-\mathrm{e}^{-a(t+1)})\rho^{r,C_j}\,\mathbb{E}\,[\int_t^{t+1} V_j(u)\mathrm{e}^{au}\,\mathrm{d}u|\mathcal{F}_t\vee\mathcal{F}^j_{t,t+1}] \\
&= \frac{\sigma\sigma_r}{a}(\mathrm{e}^{-as}-\mathrm{e}^{-a(t+1)})\rho^{r,C_j}\int_t^{t+1}\mathbb{E}\,[V_j(u)\mathrm{e}^{au}|\mathcal{F}_t\vee\mathcal{F}^j_{t,t+1}]\,\mathrm{d}u \\
&= \frac{\sigma\sigma_r}{a}(\mathrm{e}^{-as}-\mathrm{e}^{-a(t+1)})\rho^{r,C_j}\int_t^{t+1} V_j(u)\mathrm{e}^{au}\,\mathrm{d}u.
\end{aligned}
$$

The last line follows since $V_j(u)\mathrm{e}^{au}$ is $\mathcal{F}_t\vee\mathcal{F}^j_{t,t+1}$ measurable.

4. We are now ready to calculate the conditional expectation given by

$$
\Lambda_{10} = \mathbb{E}\,[\mathrm{e}^{\sigma\int_t^{t+1} V_j(u)\,\mathrm{d}W^{C_j}(u)+\frac{\sigma_r}{a}(\mathrm{e}^{-as}-\mathrm{e}^{-a(t+1)})\int_t^{t+1}\mathrm{e}^{au}\,\mathrm{d}W^r(u)}|\mathcal{F}_t\vee\mathcal{F}^j_{t,t+1}].
$$

By the properties of normal random variables, we simplify as follows:

$$\begin{aligned}
\Lambda_{10} &= \mathrm{e}^{\frac{\sigma^2}{2}\int_t^{t+1} V_j^2(u)\,\mathrm{d}u+\frac{\sigma_r^2}{2a^2}(\mathrm{e}^{-as}-\mathrm{e}^{-a(t+1)})^2\int_t^{t+1}\mathrm{e}^{2au}\,\mathrm{d}u+\frac{\sigma\sigma_r}{a}(\mathrm{e}^{-as}-\mathrm{e}^{-a(t+1)})\rho^{r,C_j}\int_t^{t+1}V_j(u)\mathrm{e}^{au}\,\mathrm{d}u} \\
&= \mathrm{e}^{\frac{\sigma^2}{2}\int_t^{t+1} V_j^2(u)\,\mathrm{d}u+\frac{\sigma_r^2}{2a^2}(\mathrm{e}^{-as}-\mathrm{e}^{-a(t+1)})^2\times\frac{\mathrm{e}^{2a(t+1)}(1-\mathrm{e}^{-2a})}{2a}+\frac{\sigma\sigma_r}{a}(\mathrm{e}^{-as}-\mathrm{e}^{-a(t+1)})\rho^{r,C_j}\int_t^{t+1}V_j(u)\mathrm{e}^{au}\,\mathrm{d}u} \\
&= \mathrm{e}^{\frac{\sigma^2}{2}\int_t^{t+1} V_j^2(u)\,\mathrm{d}u+\frac{\sigma_r^2}{4a^3}(1-\mathrm{e}^{-a(s-t-1)})^2\times(1-\mathrm{e}^{-2a})+\frac{\sigma\sigma_r}{a}(\mathrm{e}^{-as}-\mathrm{e}^{-a(t+1)})\rho^{r,C_j}\int_t^{t+1}V_j(u)\mathrm{e}^{au}\,\mathrm{d}u}.
\end{aligned}$$

5. Substituting Λ_{10} into the inner expectation of Q yields the following:

$$\begin{aligned}
Q &= \mathrm{e}^{(\frac{b_2}{a}-\frac{\lambda\sigma_r\rho^{Mr}}{a^2}-\frac{\sigma_r^2}{a^3}-\frac{r(t)\mathrm{e}^{-a}+b_2(1-\mathrm{e}^{-a})}{a})(1-\mathrm{e}^{-a(s-t-1)})+\frac{\sigma_r^2}{4a^3}+\frac{\sigma_r^2}{4a^3}(1-\mathrm{e}^{-a(s-t-1)})^2(1-\mathrm{e}^{-2a})} \\
&\quad\times\mathbb{E}\,[g(v,t+1,s,j)\mathrm{e}^{\frac{\sigma\sigma_r}{a}(\mathrm{e}^{-as}-\mathrm{e}^{-a(t+1)})\rho^{r,C_j}\int_t^{t+1}V_j(u)\mathrm{e}^{au}du}|\mathcal{F}_t].
\end{aligned}$$

Using the definitions of C_4, R, and f_2 yields the result. $\square$

Using the previous Lemma, it is now easy to derive a formula for the time t expected value of the ongoing projects next period, which we denote $V^*(t)$. We do this in the theorem below.

Theorem 2.7.9. *The time t expected value of the ongoing projects next period (ongoing at time $t+1$) is*

$$V^*(t)=\sum_{j=1}^{t}\chi_j(t)I(j)\sum_{s=t+2}^{\infty}\boldsymbol{\pi}^{s-t}C_4(j,t,s)\mathrm{e}^{R(j,j,t)}Q_j^*(v,t,s).$$

Proof. Below, we record the standard computations that lead to the result.

$$\begin{aligned}
\mathbb{E}\,[\sum_{j=1}^{t}L_j(t+1)\chi_j(t+1)|\mathcal{F}_t] &= \sum_{j=1}^{t}\mathbb{E}\,[L_j(t+1)\chi_j(t)Y_j(t+1)|\mathcal{F}_t] \\
&= \sum_{j=1}^{t}\chi_j(t)\,\mathbb{E}\,[L_j(t+1)|\mathcal{F}_t]\,\mathbb{E}\,[Y_j(t+1)|\mathcal{F}_t] \\
&= \boldsymbol{\pi}\sum_{j=1}^{t}\chi_j(t)\,\mathbb{E}\,[L_j(t+1)\mathcal{F}_t].
\end{aligned}$$

Substituting for $\mathbb{E}\,[L_j(t+1)|\mathcal{F}_t]$ from Equation (2.39) yields the result. $\square$

The final step in deriving a formula for the expected returns for a firm is finding the value of the growth options next period.

2.7.5 Value of growth opportunities next period

Let $L^{**}(t)$ denote the time $t+1$ value of the growth options given the information at time t. Explicitly, this means we calculate the time $t+1$ value of all growth opportunities that become available on or after time $t+1$. The main difference between this valuation and that of $L^{*}(t)$ is in the discounting, as the same projects are available in each case. We begin the section by defining several functions. We define the functions $d_2^* : \mathbb{Z}^2 \to \mathbb{R}$, $d_1^* : \mathbb{Z}^3 \to \mathbb{R}$, $f^{**} : \mathbb{Z}^2 \to \mathbb{R}$, $K^{**} : \mathbb{Z}^2 \to \mathbb{R}$, $d_5^* : \mathbb{Z} \to \mathbb{R}$, $d_4 : \mathbb{Z}^3 \to \mathbb{R}$, $d_6^* : \mathbb{Z}^2 \to \mathbb{R}$, and $B_4 : (\mathbb{Z}^+)^2$ below. Note that d_2^* is well defined since $s > t$ implies $\mathrm{e}^{2a(s-t)} - 1 > 0$. It's important to note that d_2^* is a function of the interest rate at time t. We also define the function $\Phi : \mathbb{Z}^3 \to \mathbb{R}$ below for $s \geq t+2$.

$$
\begin{aligned}
d_2^*(t,s) &= \Big(\frac{(b_2 - r(t))}{\sigma_r} + \frac{(r^*(s) - b_2)}{\sigma_r}\mathrm{e}^{a(s-t)} + \frac{\lambda\rho^{Mr}}{a}(\mathrm{e}^{a(s-t)} - \mathrm{e}^{a}) \\
&\quad + \frac{\sigma_r}{2a^2}(\mathrm{e}^{a(s-t)} - \mathrm{e}^{a} - \mathrm{e}^{-a} + \mathrm{e}^{-a(s-t)})\Big)\sqrt{\frac{2a}{\mathrm{e}^{2a(s-t)} - 1}}, \\
d_1^*(t,s,k) &= d_2^*(t,s) + \frac{\sigma_r}{a}(1 - \mathrm{e}^{-ak})\sqrt{\frac{1 - \mathrm{e}^{-2a(s-t)}}{2a}}, \\
f^{**}(t,k) &= \mathrm{e}^{\frac{r(t)\mathrm{e}^{-a} + b_2(1-\mathrm{e}^{-a})}{a}(\mathrm{e}^{-ak}-1) + \frac{\sigma_r^2(1-\mathrm{e}^{-2a})(1-\mathrm{e}^{-ak})^2}{4a^3}}, \\
K^{**}(s,k) &= \mathrm{e}^{\frac{r^*(s)}{a}(\mathrm{e}^{-ak}-1)}, \\
d_4(t,s,k) &= B_1(t,s,k) + \sigma_r^2(1-\mathrm{e}^{-ak})^2\frac{1 - \mathrm{e}^{-2a(s-t)}}{4a^3} + \Big(\frac{\sigma_r}{a}\mathrm{e}^{-a(s-t)}(\mathrm{e}^{-ak} - 1)\Big) \\
&\quad \times \Big(\Big[-\Big(\frac{\lambda\rho^{Mr}}{a} + \frac{\sigma_r}{a^2}\Big)(\mathrm{e}^{a(s-t)} - \mathrm{e}^{a}) \\
&\quad + \frac{\sigma_r}{2a^2}(\mathrm{e}^{-a} - \mathrm{e}^{-a(s-t)})(1 - \mathrm{e}^{2a}) + \frac{\sigma_r}{2a^2}(\mathrm{e}^{a(s-t)} - \mathrm{e}^{2a-a(s-t)})\Big]\Big), \\
d_5^*(t) &= \frac{\{-r(t)\mathrm{e}^{-a} + b_2(\mathrm{e}^{-a} - 1) + r^*(t+1)\}\sqrt{2a}}{\sigma_r\sqrt{1 - \mathrm{e}^{-2a}}}, \\
d_6^*(t,k) &= d_5^*(t) + \frac{\sigma_r\sqrt{1 - \mathrm{e}^{-2a}}(1 - \mathrm{e}^{-ak})}{\sqrt{2a^3}}, \\
B_4(n,t) &= \frac{(b_2 - r(t))\mathrm{e}^{-a}}{a}(1 - \mathrm{e}^{-an}) - b_2 n,
\end{aligned}
$$

$$\Phi(t,s,k) = \mathrm{e}^{B_4(s-t-1,t)+\frac{1}{2}\mathbb{V}(Y^*(t,s))}\{\mathrm{e}^{d_4(t,s,k)}N(d_1^*(t,s,k) - \mathrm{e}^{K^*(s,k)}N(d_2^*(t,s))\}.$$

Let the random variable $Y^*(t,s)$ be defined by

$$\begin{aligned}Y^*(t,s) &= -\lambda X_1(t+1,s) - \frac{\sigma_r}{a}(\mathrm{e}^{-at-a} - \mathrm{e}^{-as})\int_t^{t+1} \mathrm{e}^{ap}\,\mathrm{d}W^r(p) \\ &\quad - \frac{\sigma_r}{a}\int_{t+1}^{s} \mathrm{d}W^r(p) + \frac{\sigma_r \mathrm{e}^{-as}}{a}\int_{t+1}^{s} \mathrm{e}^{ap}\,\mathrm{d}W^r(p).\end{aligned}$$

It is easy to see that $\mathbb{E}[Y^*(t,s)] = 0$. Below, we calculate $\mathbb{V}[Y^*(t,s)]$.

$$\begin{aligned}\mathbb{V}[Y^*(t,s)] &= -\lambda X_1(t+1,s) - \frac{\sigma_r}{a}(\mathrm{e}^{-at-a} - \mathrm{e}^{-as})\int_t^{t+1} \mathrm{e}^{ap}\,\mathrm{d}W^r(p) - \frac{\sigma_r}{a}\int_{t+1}^{s} \mathrm{d}W^r(p) \\ &\quad + \frac{\sigma_r \mathrm{e}^{-as}}{a}\int_{t+1}^{s} \mathrm{e}^{ap}\,\mathrm{d}W^r(p) \\ &= \lambda^2(s-t-1) + \frac{\sigma_r^2}{a^2}(\mathrm{e}^{-at-a} - \mathrm{e}^{-as})^2 \mathrm{e}^{2at}\frac{\mathrm{e}^{2a}-1}{2a} + \frac{\sigma_r^2}{a^2}(s-t-1) \\ &\quad + \frac{\sigma_r^2 \mathrm{e}^{-2as}}{a^2}\frac{\mathrm{e}^{2as} - \mathrm{e}^{2at+2a}}{2a} + 2\frac{\lambda\sigma_r}{a}\rho^{M,r}(s-t-1) - 2\frac{\lambda\sigma_r\rho^{M,r}\mathrm{e}^{-as}}{a^2}(\mathrm{e}^{as} - \mathrm{e}^{at+a}) \\ &\quad - 2\frac{\sigma_r^2 \mathrm{e}^{-as}}{a^3}(\mathrm{e}^{as} - \mathrm{e}^{at+a}).\end{aligned}$$

Rearranging yields the following formula.

$$\begin{aligned}\mathbb{V}[Y^*(t,s)] &= (\lambda^2 + \frac{\sigma_r^2}{a^2} + 2\frac{\lambda\sigma_r}{a}\rho^{M,r})(s-t-1) + \frac{\sigma_r^2}{a^2}(\mathrm{e}^{-a} - \mathrm{e}^{-a(s-t)})^2\left(\frac{\mathrm{e}^{2a}-1}{2a}\right) \\ &\quad + \sigma_r^2\frac{1-\mathrm{e}^{-2a(s-t)+2a}}{2a^3} - 2(\frac{\lambda\sigma_r\rho^{M,r}}{a^2} + \frac{\sigma_r^2}{a^3})(1 - \mathrm{e}^{-a(s-t)+a}).\end{aligned}$$

The following standard lemma is recorded here for use in the second growth option theorem.

Lemma 2.7.10. *Let X be a normal random variable with $\mathbb{E}[X] = \mu_x$ and $\mathbb{V}[X] = \sigma_x^2$. Let the constants A and K be positive. Then,*

$$\mathbb{E}[(A\mathrm{e}^X - K)^+] = A\mathrm{e}^{\mu_x + \frac{\sigma_x^2}{2}}N(\frac{\ln(A) - \ln(K) + \mu_x + \sigma_x^2}{\sigma_x}) - KN(\frac{\ln(A) - \ln(K) + \mu_x}{\sigma_x}).$$

Proof. First,

$$(A\mathrm{e}^x - K)^+ = \begin{cases} A\mathrm{e}^x - K & \text{iff } x > \ln(\frac{K}{A}) \\ 0 & \text{iff } A\mathrm{e}^x - K \leq 0 \end{cases}$$

Below, we will use the transformation $z = \frac{x-(\mu_x+\sigma_x^2)}{\sigma_x}$, with of course $\mathrm{d}z = \frac{\mathrm{d}x}{\sigma_x}$. First, we have

$$\begin{aligned}
A\int_{\ln(\frac{K}{A})}^{\infty} \mathrm{e}^x \frac{1}{\sigma_x\sqrt{2\pi}}\mathrm{e}^{-\frac{1}{2}(\frac{x-\mu_x}{\sigma_x})^2}\,\mathrm{d}x &= A\mathrm{e}^{\mu_x+\frac{\sigma_x^2}{2}}\int_{\ln(\frac{K}{A})}^{\infty} \frac{1}{\sigma_x\sqrt{2\pi}}\mathrm{e}^{-\frac{1}{2}(\frac{x-(\mu_x+\sigma_x^2)}{\sigma_x})^2}\,\mathrm{d}x \\
&= A\mathrm{e}^{\mu_x+\frac{\sigma_x^2}{2}}\int_{\frac{\ln(\frac{K}{A})-(\mu_x+\sigma_x^2)}{\sigma_x}}^{\infty} \frac{1}{\sqrt{2\pi}}\mathrm{e}^{-\frac{1}{2}z^2}\,\mathrm{d}z \\
&= A\mathrm{e}^{\mu_x+\frac{\sigma_x^2}{2}}\{1-N(\frac{\ln(\frac{K}{A})-(\mu_x+\sigma_x^2)}{\sigma_x})\} \\
&= A\mathrm{e}^{\mu_x+\frac{\sigma_x^2}{2}}N(\frac{\ln(A)-\ln(K)+\mu_x+\sigma_x^2}{\sigma_x}).
\end{aligned}$$

Also,

$$\begin{aligned}
-K\int_{\ln(\frac{K}{A})}^{\infty} \frac{1}{\sigma_x\sqrt{2\pi}}\mathrm{e}^{-\frac{1}{2}(\frac{x-\mu_x}{\sigma_x})^2}\,\mathrm{d}x &= -K\int_{\frac{\ln(K)-\ln(A)-\mu_x}{\sigma_x}}^{\infty} \frac{1}{\sqrt{2\pi}}\mathrm{e}^{-\frac{1}{2}z^2}\,\mathrm{d}z \\
&= -KN(\frac{\ln(A)-\ln(K)+\mu_x}{\sigma_x}).
\end{aligned}$$

Finally,

$$\begin{aligned}
\mathbb{E}\left[(A\mathrm{e}^X - K)^+\right] &= \int_{\ln(\frac{K}{A})}^{\infty}(A\mathrm{e}^x - K)\frac{1}{\sigma_x\sqrt{2\pi}}\mathrm{e}^{-\frac{1}{2}(\frac{x-\mu_x}{\sigma_x})^2}\,\mathrm{d}x \\
&= A\mathrm{e}^{\mu_x+\frac{\sigma_x^2}{2}}N(\frac{\ln(A)-\ln(K)+\mu_x+\sigma_x^2}{\sigma_x}) - KN(\frac{\ln(A)-\ln(K)+\mu_x}{\sigma_x}).
\end{aligned}$$

□

We are now prepared to state and prove our theorem on the value of growth options next period.

Theorem 2.7.11. *The time $t+1$ value of the growth opportunities available beginning next period conditional on the information available at time t is given by*

$$L^{**}(t) = I(t)\mathrm{e}^{\mu_I-\frac{1}{2}\lambda^2}\int_{\mathcal{V}}\int_{\mathcal{P}}\sum_{k=1}^{\infty}\pi^k\mathrm{e}^{F_3(t+1,1+t+k)}g(v,t+1,t+1+k,t+1)$$

$$
\begin{aligned}
&\times \{f^{**}(t,k)N(d_6^*(t,k)) - K^{**}(t+1,k)N(d_5^*(t))\}\,\mathrm{d}F_\rho(\rho^{M,C_{t+1}})\,\mathrm{d}F_V(V_{t+1}(t+1))\\
&+ I(t)\sum_{s=t+2}^{\infty} \mathrm{e}^{(\mu_I-\frac{1}{2}\lambda^2)(s-t)}\int_{\mathcal{V}}\int_{\mathcal{P}}\sum_{k=1}^{\infty}\boldsymbol{\pi}^k\mathrm{e}^{F_3(s,s+k)}\\
&\times g(v,s,s+k,s)\Phi(t,s,k)\,\mathrm{d}F_\rho(\rho^{M,C_s})\,\mathrm{d}F_V(V_s(s)),
\end{aligned}
$$

where F_V denotes the stationary distribution of the Jacobi process and F_ρ denotes the distribution function of the random variable ρ^{M,C_s}, which is the same for all s.

Proof. The value of growth opportunities at month $t+1$ given the information at time t is

$$
\begin{aligned}
L^{**}(t) &= \mathbb{E}\,[L^*(t+1) + (V_{t+1}(t+1) - I(t+1))^+|\mathcal{F}_t]\\
&= \sum_{s=t+1}^{\infty}\mathbb{E}\,[\frac{M(s)}{M(t+1)}(L_s(s)-I(s))^+|\mathcal{F}_t]\\
&= \sum_{s=t+1}^{\infty}\mathbb{E}\,[I(s)|\mathcal{F}_t]\,\mathbb{E}\,[\frac{M(s)}{M(t+1)}(\frac{L_s(s)}{I(s)}-1)^+|\mathcal{F}_t]\\
&= I(t)\sum_{s=t+1}^{\infty}\mathrm{e}^{\mu_I(s-t)}\,\mathbb{E}\,[\frac{M(s)}{M(t+1)}(\frac{L_s(s)}{I(s)}-1)^+|\mathcal{F}_t].
\end{aligned}
$$

Observe that by Equation (2.9), we have

$$
\frac{M(s)}{M(t+1)} = \mathrm{e}^{-\frac{\lambda^2}{2}(s-t-1)-\lambda X_1(t+1,s)-\int_{t+1}^{s} r_u\,\mathrm{d}u}.
$$

We now focus on the calculation of the conditional expectation defined by Λ_{11}:

$$
\Lambda_{11}(t,s) = \mathbb{E}\,[\frac{M(s)}{M(t+1)}(\frac{L_s(s)}{I(s)}-1)^+|\mathcal{F}_t] = \mathbb{E}\,[\,\mathbb{E}\,[\frac{M(s)}{M(t+1)}(\frac{L_s(s)}{I(s)}-1)^+|\mathcal{A}(t,s)]|\mathcal{F}_t].
$$

As before, there exists $r^*(s)$ such that

$$
\sum_{k=1}^{\infty}\boldsymbol{\pi}^k\mathrm{e}^{F_3(s,s+k)+\frac{r^*(s)}{a}(\mathrm{e}^{-ak}-1)}g(v,s,s+k,s) = 1.
$$

Let the function $G:[v_{\min},v_{\max}]\times(\mathbb{Z}^+)^2\to\mathbb{R}$ be defined as follows:

$$
G(v,t,s) = \mathbb{E}\,[\mathrm{e}^{-\lambda X_1(t+1,s)-\int_{t+1}^{s}r(u)\,\mathrm{d}u}(\sum_{k=1}^{\infty}\boldsymbol{\pi}^k\mathrm{e}^{F_3(s,s+k)+\frac{r(s)}{a}(\mathrm{e}^{-ak}-1)}g(v,s,s+k,s)
$$

$$-\sum_{k=1}^{\infty}\boldsymbol{\pi}^k \mathrm{e}^{F_3(s,s+k)+\frac{r^*(s)}{a}(\mathrm{e}^{-ak}-1)}g(v,s,s+k,s))^+|\mathcal{A}(t,s)].$$

We split this up into two cases. The first case is for $s=t+1$, and the second is for $s \geq t+2$. For the case $s=t+1$, we have

$$\begin{aligned}
G(v,t,t+1) = \mathbb{E}\,[(&\sum_{k=1}^{\infty}\boldsymbol{\pi}^k \mathrm{e}^{F_3(t+1,1+t+k)+\frac{r(t+1)}{a}(\mathrm{e}^{-ak}-1)}g(v,t+1,t+1+k,t+1) \\
&-\sum_{k=1}^{\infty}\boldsymbol{\pi}^k \mathrm{e}^{F_3(t+1,t+1+k)+\frac{r^*(t+1)}{a}(\mathrm{e}^{-ak}-1)}\times \\
&g(v,t+1,t+1+k,t+1))^+|\mathcal{A}(t,t+1)] \\
&=\sum_{k=1}^{\infty}\boldsymbol{\pi}^k \mathrm{e}^{F_3(t+1,1+t+k)}g(v,t+1,t+1+k,t+1)\times \\
&\mathbb{E}\,[(\mathrm{e}^{\frac{r(t+1)}{a}(\mathrm{e}^{-ak}-1)}-\mathrm{e}^{\frac{r^*(t+1)}{a}(\mathrm{e}^{-ak}-1)})^+|\mathcal{A}(t,t+1)].
\end{aligned}$$

Now, we aim to derive a formula for

$$\Lambda_{12}=\mathbb{E}\,[(\mathrm{e}^{\frac{r(t+1)}{a}(\mathrm{e}^{-ak}-1)}-\mathrm{e}^{\frac{r^*(t+1)}{a}(\mathrm{e}^{-ak}-1)})^+|\mathcal{A}(t,t+1)].$$

Recall that $r(t+1)=r(t)\mathrm{e}^{-a}+b_2(1-\mathrm{e}^{-a})+\sigma_r\mathrm{e}^{-a(t+1)}\int_t^{t+1}\mathrm{e}^{ap}\,\mathrm{d}W^r(p)$. Now, note that the random variable $X_3(t,t+1)$ is normally distributed with mean 0 and variance $\frac{\mathrm{e}^{2at}(\mathrm{e}^{2a}-1)}{2a}$. So, the random variable $\frac{\sigma_r\mathrm{e}^{-a(t+1)}\int_t^{t+1}\mathrm{e}^{ap}\,\mathrm{d}W^r(p)}{a}(\mathrm{e}^{-ak}-1)$ is normally distributed with mean 0 and variance $\frac{\sigma_r^2\mathrm{e}^{-2a(t+1)}(\mathrm{e}^{-ak}-1)^2}{a^2}\frac{\mathrm{e}^{2at}(\mathrm{e}^{2a}-1)}{2a}=\frac{\sigma_r^2(1-\mathrm{e}^{-2a})(\mathrm{e}^{-ak}-1)^2}{2a^3}$. So, the standard deviation of $X_3(t,t+1)$ is given by

$$\sigma_{X_3(t,t+1)}=\frac{\sigma_r\sqrt{1-\mathrm{e}^{-2a}}(1-\mathrm{e}^{-ak})}{\sqrt{2a^3}}.$$

Substituting the above and an application of Lemma 2.7.10 yields

$$\begin{aligned}
\Lambda_{12}&=\mathbb{E}\,[(\mathrm{e}^{\frac{r(t)\mathrm{e}^{-a}+b_2(1-\mathrm{e}^{-a})}{a}(\mathrm{e}^{-ak}-1)}\mathrm{e}^{\frac{\sigma_r\mathrm{e}^{-a(t+1)}\int_t^{t+1}\mathrm{e}^{ap}\,\mathrm{d}W^r(p)}{a}(\mathrm{e}^{-ak}-1)}-K^{**}(t+1,k))^+|\mathcal{A}(t,t+1)] \\
&=f^{**}(t,k)N(d_6^*(t,k))-K^{**}(t+1,k)N(d_5^*(t)).
\end{aligned}$$

Thus, for the case $s = t+1$, we have an expression for $\Lambda_{11}(t,s)$.

$$\begin{aligned}\Lambda_{11}(t,t+1) = &\int_{\mathcal{V}}\int_{\mathcal{P}}\sum_{k=1}^{\infty}\boldsymbol{\pi}^k \mathrm{e}^{F_3(t+1,1+t+k)} g(v,t+1,t+1+k,t+1)\\ &\times \{f^{**}(t,k)N(d_6^*(t,k)) - K^{**}(t+1,k)N(d_5^*(t))\}\,\mathrm{d}F_\rho(\rho^{M,C_{t+1}})\,\mathrm{d}F_v(v(t+1)).\end{aligned}$$

For all $s \geq t+2$,

$$\begin{aligned}G(v,t,s) = &\sum_{k=1}^{\infty}\boldsymbol{\pi}^k \mathrm{e}^{F_3(s,s+k)} g(v,s,s+k,s)\\ &\times \mathbb{E}\,[\mathrm{e}^{-\lambda X_1(t+1,s)-\int_{t+1}^{s} r(u)\,\mathrm{d}u}(\mathrm{e}^{\frac{r(s)}{a}(\mathrm{e}^{-ak}-1)} - \mathrm{e}^{\frac{r^*(s)}{a}(\mathrm{e}^{-ak}-1)})^+|\mathcal{A}(t,s)].\end{aligned}$$

Recall again that

$$r(u) = r(t)\mathrm{e}^{-a(u-t)} + b_2(1-\mathrm{e}^{-a(u-t)}) + \sigma_r \mathrm{e}^{-au}\int_t^u \mathrm{e}^{ap}\,\mathrm{d}W^r(p),$$

so

$$\begin{aligned}-\int_{t+1}^{s} r(u)\,\mathrm{d}u = &-r(t)\frac{\mathrm{e}^{-a}-\mathrm{e}^{-a(s-t)}}{a} - b_2(s-t-1) + b_2\frac{\mathrm{e}^{-a}-\mathrm{e}^{-a(s-t)}}{a}\\ &-\sigma_r\int_{t+1}^{s}\left(\mathrm{e}^{-au}\int_t^u \mathrm{e}^{ap}\,\mathrm{d}W^r(p)\right)\mathrm{d}u.\end{aligned} \tag{2.40}$$

Now, we calculate $\Lambda_{13} = \sigma_r\int_{t+1}^{s}(\mathrm{e}^{-au}\int_t^u \mathrm{e}^{ap}\,\mathrm{d}W^r(p))\,\mathrm{d}u$.

$$\begin{aligned}\Lambda_{13} &= \sigma_r\int_{t+1}^{s}(\mathrm{e}^{-au}\int_t^{t+1}\mathrm{e}^{ap}\,\mathrm{d}W^r(p))\,\mathrm{d}u + \sigma_r\int_{t+1}^{s}(\mathrm{e}^{-au}\int_{t+1}^{u}\mathrm{e}^{ap}\,\mathrm{d}W^r(p))\,\mathrm{d}u\\ &= \frac{\sigma_r}{a}(\mathrm{e}^{-at-a}-\mathrm{e}^{-as})\int_t^{t+1}\mathrm{e}^{ap}\,\mathrm{d}W^r(p) + \sigma_r\int_{t+1}^{s}(\mathrm{e}^{-au}\int_{t+1}^{u}\mathrm{e}^{ap}\,\mathrm{d}W^r(p))\,\mathrm{d}u\\ &= \frac{\sigma_r}{a}(\mathrm{e}^{-at-a}-\mathrm{e}^{-as})\int_t^{t+1}\mathrm{e}^{ap}\,\mathrm{d}W^r(p) + \frac{\sigma_r}{a}\int_{t+1}^{s}\mathrm{d}W^r(p) - \frac{\sigma_r\mathrm{e}^{-as}}{a}\int_{t+1}^{s}\mathrm{e}^{ap}\,\mathrm{d}W^r(p).\end{aligned}$$

By substitution of Λ_{13} into Equation (2.40), we have

$$\begin{aligned}-\int_{t+1}^{s} r(u)\,\mathrm{d}u = &B_4(n,t) - \frac{\sigma_r}{a}(\mathrm{e}^{-at-a}-\mathrm{e}^{-as})\int_t^{t+1}\mathrm{e}^{ap}\,\mathrm{d}W^r(p)\\ &-\frac{\sigma_r}{a}\int_{t+1}^{s}\mathrm{d}W^r(p) + \frac{\sigma_r\mathrm{e}^{-as}}{a}\int_{t+1}^{s}\mathrm{e}^{ap}\,\mathrm{d}W^r(p).\end{aligned}$$

Let the function $\Phi : (\mathbb{Z}^+)^3 \to \mathbb{R}$ be defined by

$$\begin{aligned}\Phi(t,s,k) &= \mathbb{E}\,[\mathrm{e}^{-\lambda X_1(t+1,s)-\int_{t+1}^{s} r(u)\,\mathrm{d}u}(\mathrm{e}^{\frac{r(s)}{a}(\mathrm{e}^{-ak}-1)} - \mathrm{e}^{\frac{r^*(s)}{a}(\mathrm{e}^{-ak}-1)})^+|\mathcal{A}(t,s)] \\ &= \mathrm{e}^{B_4(s-t-1,t)}\,\mathbb{E}\,[\mathrm{e}^{Y^*(t,s)}(\mathrm{e}^{B_1(t,s,k)}\mathrm{e}^{B_2(s,k)X_3(t,s)} - \mathrm{e}^{K^*(s,k)})^+|\mathcal{A}(t,s)],\end{aligned}$$

where $B_1(t,s,k), B_2(s,k), K^*(s,k)$ and $X_3(t,s)$ were defined previously. We now calculate the covariance of $Y^*(t,s)$ and $X_3(t,s)$.

$$\begin{aligned}\mathrm{cov}(Y^*(t,s),X_3(t,s)) &= -\lambda\mathrm{cov}(\int_t^s \mathrm{e}^{ap}\,\mathrm{d}W^r(p), \int_{t+1}^s \mathrm{d}W^M(p)) \\ &- \frac{\sigma_r}{a}(\mathrm{e}^{-at-a} - \mathrm{e}^{-as})\,\mathrm{cov}(\int_t^s \mathrm{e}^{ap}\,\mathrm{d}W^r(p), \int_t^{t+1} \mathrm{e}^{ap}\,\mathrm{d}W^r(p)) \\ &- \frac{\sigma_r}{a}\,\mathrm{cov}(\int_t^s \mathrm{e}^{ap}\,\mathrm{d}W^r(p), \int_{t+1}^s \mathrm{d}W^r(p)) \\ &+ \frac{\sigma_r\mathrm{e}^{-as}}{a}\,\mathrm{cov}(\int_t^s \mathrm{e}^{ap}\,\mathrm{d}W^r(p), \int_{t+1}^s \mathrm{e}^{ap}\,\mathrm{d}W^r(p)) \\ &= -\frac{\lambda\rho^{Mr}}{a}(\mathrm{e}^{as} - \mathrm{e}^{a(t+1)}) - \frac{\sigma_r}{2a^2}(\mathrm{e}^{-at-a} - \mathrm{e}^{-as})(\mathrm{e}^{2a(t+1)} - \mathrm{e}^{2at}) \\ &- \frac{\sigma_r}{a^2}(\mathrm{e}^{as} - \mathrm{e}^{a(t+1)}) + \frac{\sigma_r\mathrm{e}^{-as}}{2a^2}(\mathrm{e}^{2as} - \mathrm{e}^{2a(t+1)}) \\ &= -(\frac{\lambda\rho^{Mr}}{a} + \frac{\sigma_r}{a^2})(\mathrm{e}^{as} - \mathrm{e}^{a(t+1)}) + \frac{\sigma_r}{2a^2}(\mathrm{e}^{-at-a} - \mathrm{e}^{-as})\mathrm{e}^{2at}(1 - \mathrm{e}^{2a}) \\ &+ \frac{\sigma_r}{2a^2}(\mathrm{e}^{as} - \mathrm{e}^{2a(t+1)-as}) \\ &= \mathrm{e}^{at}[-(\frac{\lambda\rho^{Mr}}{a} + \frac{\sigma_r}{a^2})(\mathrm{e}^{a(s-t)} - \mathrm{e}^{a}) + \frac{\sigma_r}{2a^2}(\mathrm{e}^{-a} - \mathrm{e}^{-a(s-t)})(1 - \mathrm{e}^{2a}) \\ &+ \frac{\sigma_r}{2a^2}(\mathrm{e}^{a(s-t)} - \mathrm{e}^{2a-a(s-t)})].\end{aligned}$$

We will make use of the following calculations:

1. $\mathbb{E}\,[B_2(s,k)X_3(t,s)] = 0$,

2. $\mathbb{V}(B_2(s,k)X_3(t,s)) = B_2^2(s,k)\frac{\mathrm{e}^{2as}-\mathrm{e}^{2at}}{2a}$,

3. $|B_2(s,k)| = \frac{\sigma_r}{a}\mathrm{e}^{-as}(1-\mathrm{e}^{-ak})$,

4. $\frac{B_1(t,s,k)}{|B_2(s,k)|} = \frac{(b_2-r(t))}{\sigma_r}\mathrm{e}^{at} - \frac{b_2}{\sigma_r}\mathrm{e}^{as}$,

5. $\frac{K^*(s,k)}{|B_2(s,k)|} = -\frac{r^*(s)}{\sigma_r}\mathrm{e}^{as}$.

We define the following functions and proceed to apply Lemma B.1 of Berk, Green, and Naik [15]. Note that t, s, k are positive integers and $s \geq t+1$.

$$
\begin{aligned}
d_1^*(t,s,k) &= \frac{B_1(t,s,k) - K^*(s,k) + B_2^2(s,k)\frac{\mathrm{e}^{2as}-\mathrm{e}^{2at}}{2a} + B_2(s,k)\operatorname{cov}(Y^*(t,s), X_3(t,s))}{|B_2(s,k)|\sqrt{\frac{\mathrm{e}^{2as}-\mathrm{e}^{2at}}{2a}}} \\
&= \frac{B_1(t,s,k)}{|B_2(s,k)|}\sqrt{\frac{2a}{\mathrm{e}^{2as}-\mathrm{e}^{2at}}} - \frac{K^*(s,k)}{|B_2(s,k)|}\sqrt{\frac{2a}{\mathrm{e}^{2as}-\mathrm{e}^{2at}}} + |B_2(s,k)|\sqrt{\frac{\mathrm{e}^{2as}-\mathrm{e}^{2at}}{2a}} \\
&- \operatorname{cov}(Y^*(t,s), X_3(t,s))\sqrt{\frac{2a}{\mathrm{e}^{2as}-\mathrm{e}^{2at}}} \\
&= \left(\frac{B_1(t,s,k)}{|B_2(s,k)|} - \frac{K^*(s,k)}{|B_2(s,k)|} - \operatorname{cov}(Y^*(t,s), X_3(t,s))\right)\sqrt{\frac{2a}{\mathrm{e}^{2as}-\mathrm{e}^{2at}}} \\
&+ |B_2(s,k)|\sqrt{\frac{\mathrm{e}^{2as}-\mathrm{e}^{2at}}{2a}} \\
&= (\frac{(b_2 - r(t))}{\sigma_r} - \frac{b_2}{\sigma_r}\mathrm{e}^{a(s-t)} + \frac{r^*(s)}{\sigma_r}\mathrm{e}^{a(s-t)} \\
&+ (\frac{\lambda\rho^{Mr}}{a} + \frac{\sigma_r}{a^2})(\mathrm{e}^{a(s-t)} - \mathrm{e}^{a}) + \frac{\sigma_r}{2a^2}(\mathrm{e}^{-a} - \mathrm{e}^{-a(s-t)})(\mathrm{e}^{2a} - 1) \\
&+ \frac{\sigma_r}{2a^2}(\mathrm{e}^{2a-a(s-t)} - \mathrm{e}^{a(s-t)}))\sqrt{\frac{2a}{\mathrm{e}^{2a(s-t)} - 1}} + \frac{\sigma_r}{a}(1 - \mathrm{e}^{-ak})\sqrt{\frac{1 - \mathrm{e}^{-2a(s-t)}}{2a}}, \\
d_2^*(t,s) &= d_1^*(t,s,k) - \frac{\sigma_r}{a}(1 - \mathrm{e}^{-ak})\sqrt{\frac{1 - \mathrm{e}^{-2a(s-t)}}{2a}}.
\end{aligned}
$$

We now have a formula for $\Lambda_{14} = E[\mathrm{e}^{Y^*(t,s)}(\mathrm{e}^{B_1(t,s,k)}\mathrm{e}^{B_2(s,k)X_3(t,s)} - \mathrm{e}^{K^*(s,k)})^+ | \mathcal{A}(t,s)]$.

$$
\begin{aligned}
\Lambda_{14} = \exp\{&\frac{1}{2}\,\mathbb{V}(Y^*(t,s)) + B_1(t,s,k) + \sigma_r^2(1 - \mathrm{e}^{-ak})^2\frac{1 - \mathrm{e}^{-2a(s-t)}}{4a^3} \\
&+ (\frac{\sigma_r}{a}\mathrm{e}^{-a(s-t)}(\mathrm{e}^{-ak} - 1))([-(\frac{\lambda\rho^{Mr}}{a} + \frac{\sigma_r}{a^2})(\mathrm{e}^{a(s-t)} - \mathrm{e}^{a}) \\
&+ \frac{\sigma_r}{2a^2}(\mathrm{e}^{-a} - \mathrm{e}^{-a(s-t)})(1 - \mathrm{e}^{2a}) + \frac{\sigma_r}{2a^2}(\mathrm{e}^{a(s-t)} - \mathrm{e}^{2a-a(s-t)})])\}N(d_1^*(t,s,k)) \\
&- \mathrm{e}^{K^*(s,k) + \frac{1}{2}\,\mathbb{V}(Y^*(t,s))}N(d_2^*(t,s)).
\end{aligned}
$$

So, for $s \geq t+2$,

$$
\Phi(t,s,k) = \mathrm{e}^{B_4(s-t-1,t) + \frac{1}{2}\,\mathbb{V}(Y^*(t,s))}\{\mathrm{e}^{d_4(t,s,k)}N(d_1^*(t,s,k) - \mathrm{e}^{K^*(s,k)}N(d_2^*(t,s))\}.
$$

Thus, for a fixed $s \geq t+2$, we have

$$\Lambda_{11}(t,s) = \int_{\mathcal{V}} \int_{\mathcal{P}} \sum_{k=1}^{\infty} \boldsymbol{\pi}^k \mathrm{e}^{F_3(s,s+k)} g(v,s,s+k,s) \Phi(t,s,k) \, \mathrm{d}F_\rho(\rho^{M,C_s}) \, \mathrm{d}F_v(v(s)).$$

For the final result, we sum this over all $s \geq t+2$, and then add this to $\Lambda(t, t+1)$. $\square$

We are now able to write down a formula for the expected rate of return for holding a claim on the firm for exactly 1 month starting at time t. The formula is given by $E[R_{t+1}|\mathcal{F}_t] = \frac{E[P(t+1)|\mathcal{F}_t]}{P(t)} - 1$. Thus, the expected rate of return for holding a claim on the firm for exactly one month starting at time t is given by

$$E[R_{t+1}|\mathcal{F}_t] = \frac{V^*(t) + L^{**}(t)}{\sum_{j=1}^{t} L_j(t)\chi_j(t) + L^*(t)} - 1.$$

Having derived the necessary formulas for firm valuation, we turn our attention to the simulation in the next chapter.

3. SIMULATION

In this chapter, we present the parameter estimation procedure and the simulation results. The Jacobi process parameters and the cash flow growth rate will be estimated from Compustat data using a regression method. The initial value of the cash flow process for each firm is determined using yearly S&P500 returns as a returns proxy. After estimating the parameters, we analyze the effect of different parameters on growth option values for both the Jacobi process and the CIR process. Differences become clear. We then study the effects of these parameters on returns. We begin with parameter estimation.

3.1 Parameter estimation

In this section, we describe our method of parameter estimation. The parameters for the interest rate process and the Bernoulli random variables determining project lifetimes are chosen to be the same as those of BGN. As mentioned before, the Jacobi process parameters are firm specific. We apply the "indirect inference method" of Gourieroux and Valery [14] to estimate parameters for the Jacobi process. Recall the dynamics of the Jacobi process, which can be found in Equations (2.5) and (2.6). Discretization of Equation (2.6) (for the j-th project) yields

$$\begin{aligned} V_j(t+1) &= V_j(t) + \kappa(\theta - V_j(t)) + \sigma_V \sqrt{Q(V_j(t))}\xi(t+1) \\ &= (1-\kappa)V_j(t) + \kappa\theta + \sigma_V \sqrt{Q(V_j(t))}\xi(t+1), \end{aligned} \tag{3.1}$$

where the random variables $\xi(t)$ are standard normal for all t. For this section only, we let $\alpha = 1-\kappa$ and $\beta = \kappa\theta$. Then, division by $\sqrt{Q(V_j(t))}$ in Equation (3.1) yields

$$\frac{V_j(t+1)}{\sqrt{Q(V_j(t))}} = \alpha \frac{V_j(t)}{\sqrt{Q(V_j(t))}} + \beta \frac{1}{\sqrt{Q(V_j(t))}} + \sigma_V \xi(t+1). \tag{3.2}$$

We now consider the cash flow process and demonstrate the validity of our proceeding procedure. First, we apply Ito's lemma to the logarithm of the cash flows from Equation (2.3) (recall that we assume $\sigma = 1$):

$$\mathrm{d}\left(\log(C_j(t)\right) = \left(\mu - \frac{1}{2}V_j^2(t)\right)\mathrm{d}t + V_j(t)\,\mathrm{d}W^{C_j}(t).$$

As a discrete-time analogue, we have

$$\log(C_j(t+1)) = \log(C_j(t)) + \mu - \frac{1}{2}V_j^2(t) + V_j(t)\left(W^{C_j}(t+1) - W^{C_j}(t)\right).$$

Taking the conditional variance of each side given the time t information yields:

$$\mathbb{V}(\log(C_j(t+1))|\mathcal{F}_t) = V_j^2(t).$$

We estimate the conditional cash flow variance, $\mathbb{V}(\log(C_j(t+1))|\mathcal{F}_t)$, by taking the variance of the natural logarithm of each of the prior twenty cash flow observations. Note that it may have been better to use the variance of the differences of the logarithm of the cash flows. The resulting parameter estimates in this case are similar to simply taking the logarithm of the cash flows, except using the difference yields more outlier estimates. Our estimates still allow us to address the questions at hand, so we proceed with using the variance of the logarithm of the cash flows and not the difference of the logarithms of the cash flows. We implicitly assume the time t information consists of the prior twenty cash flow observations. We use the standard deviation of the logarithm of each of the prior twenty cash flow data points to estimate $V_j(t)$ at each time t. Then, we apply the regression method mentioned above. Lastly, we need to mention how $V_j(j)$, the value of the Jacobi process for the j-th project when the project becomes available, is determined. Since the Jacobi process is stationary with a Beta distribution, for every j, $V_j(j)$ will be drawn from a Beta distribution depending on the parameters of the specific Jacobi process. We now turn our attention to the cash flow proxy.

We follow the procedures of Keefe and Yaghoubi [28] to deal with the cash flow data. We describe this process now. We use OIBDPQ (Operating Income Before Depreciation

Quarterly) as a proxy for the cash flow. For each firm, we scale OIBDPQ by CSHOQ (Common Shares Outstanding Quarterly), ACTQ (Total Assets Quarterly), and net assets. We have calculated nets assets as ACTQ minus LCTQ, where LCTQ is Total Liabilities Quarterly. If the Compustat footnote of REVTQ is 'AB', then the associated observation is deleted. If the common equity for a quarter (CEQQ) is negative, then this observation is deleted. Utility firms are deleted, and there are no financial services firms. If ACTQ or REVTQ are negative, then the associated observation is deleted. All observations with missing data are deleted. If a firm has one or more negative values for OIBDPQ, then the firm is removed from the data set. We delete firms with less than 90 OIBDPQ data points.

Since firms with negative values of OIBDPQ are dropped and our model assumes positive cash flows, it makes sense to take the natural logarithm of the scaled OIBDPQ values. We chose to scale OIBDPQ by ACTQ, and we will discuss differences in the scaling later. Cash flow volatility is estimated using a rolling standard deviation of the past 20 scaled OIBDPQ data points. Thus, the first 20 data points for each firm are deleted. Parameters are estimated using the regression method. After running the regressions, firms with a p-value associated with the estimates for θ or κ greater than or equal to .01 are deleted. We use the root mean square error as an estimator of σ_V. The parameters $v_{\max}$ and $v_{\min}$ are determined by taking the largest and smallest values of $V_j(t)$ for each specific firm, respectively. Obviously, we ensure that $v_{\min} \leq \theta \leq v_{\max}$ for each firm when the Jacobi process is used. We now describe the aforementioned cash flow scaling.

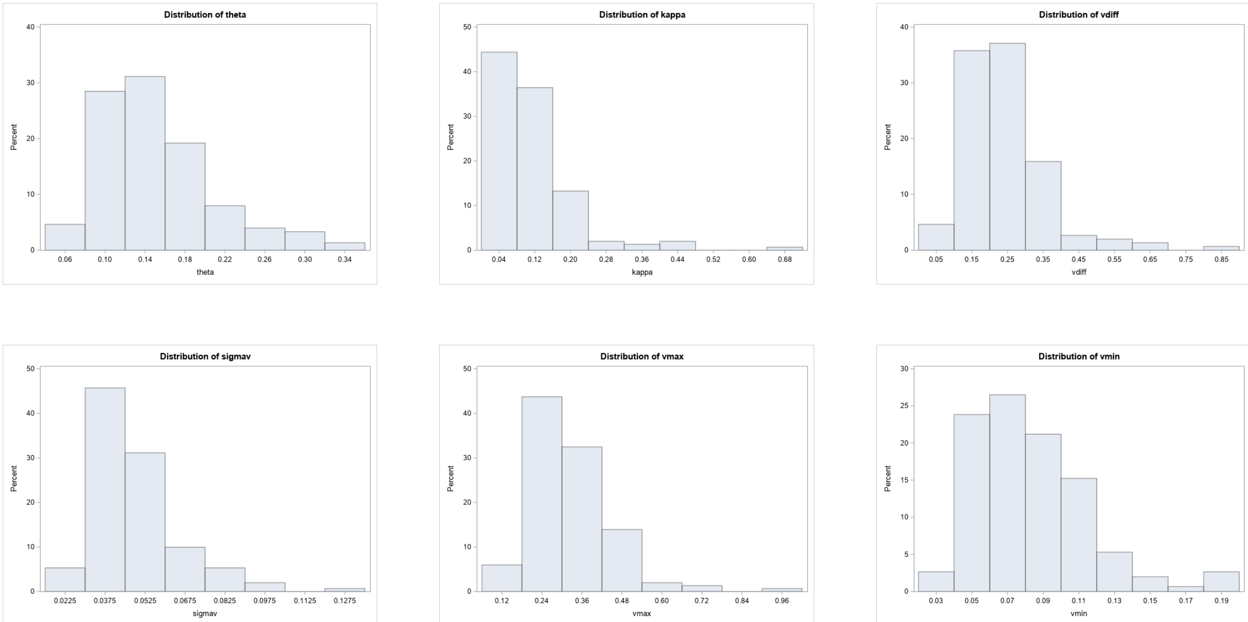

Figure 3.1. Jacobi parameter estimates for OIBDPQ scaled by CSHOQ

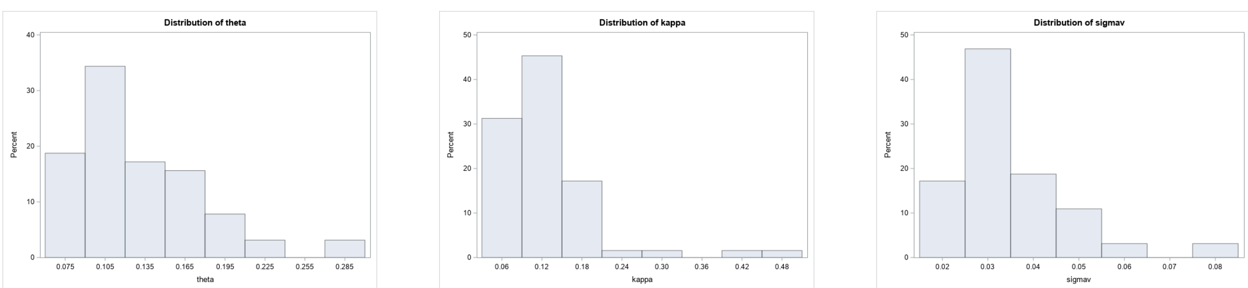

Figure 3.2. CIR parameter estimates for OIBDPQ scaled by CSHOQ

We present the distribution of the parameter estimates when OIBDPQ was scaled by CSHOQ in Figure 3.1 for the Jacobi process and in Figure 3.2 for the CIR process. The procedures above yield 151 firms for the Jacobi process and 64 firms for the CIR process. When OIBDPQ is scaled by ACTQ, the parameter estimation procedures yield 153 firms for the Jacobi process and 87 firms for the CIR process. The distribution of parameter estimates when OIBDPQ is scaled by ACTQ is presented in Figure 3.3 for the Jacobi process and in Figure 3.4 for the CIR process. Not all firms satisfy the condition for convergence in Lemma

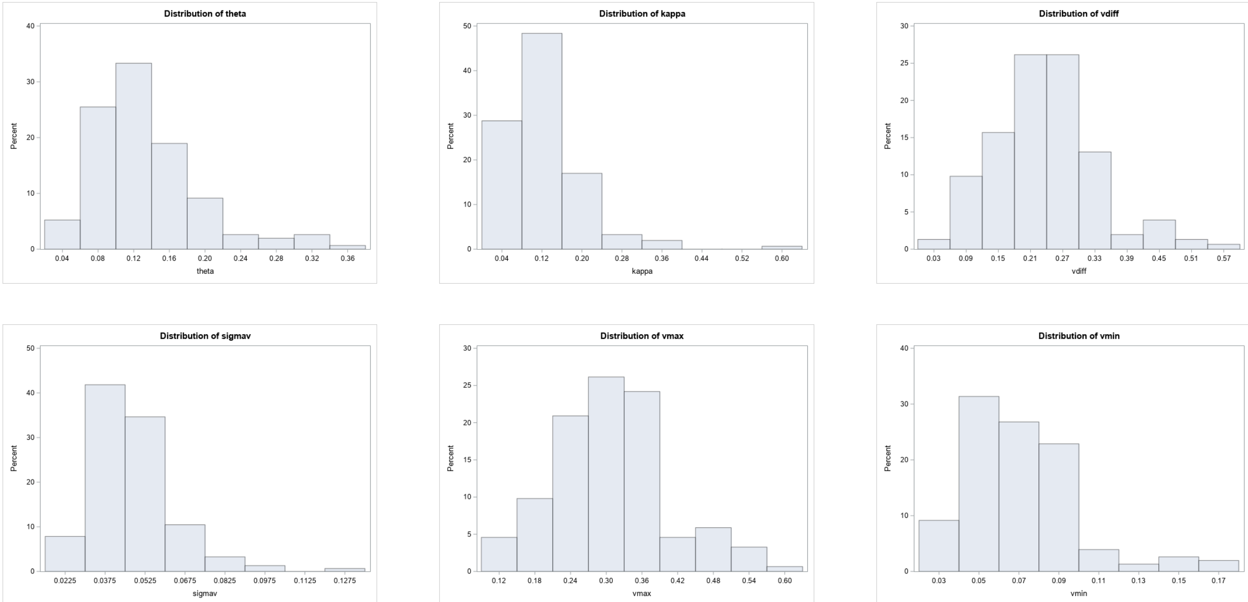

Figure 3.3. Jacobi parameter estimates for OIBDPQ scaled by ACTQ

2.7.3. Furthermore, the convergence depends on ρ^{M,C_j}. For the Jacobi process, we allow ρ^{M,C_j} to be drawn from a uniform discrete distribution, and ρ^{M,C_j} takes six values linearly spaced between .0001 and .2. As ρ^{M,C_j} increases, it is more likely for a firm to satisfy the convergence condition. For example, in one of our runs, we found that for the smallest value of ρ^{M,C_j}, 75 of 153 firms meet the convergence criterion, but for the largest value of ρ^{M,C_j}, 106 of 153 firms meet the criterion. It is obvious that this always holds, due to the convergence criterion. Finally, when OIBDPQ is scaled by net assets, the parameter estimation procedures yield 122 firms for the Jacobi process and 40 firms for the CIR process.

Tables 3.1, 3.2, 3.3, 3.4, 3.5, and 3.6 present the minimum, maximum, mean, standard deviation, skewness, and excess kurtosis of the parameters estimated for use in the Jacobi and CIR processes. Each plot is labelled by what factor scales OIBDPQ. This concludes the volatility parameter estimation, and we turn our attention to cash flow growth.

We now consider parameter estimation for the cash flow growth rate. Discretization of Equation (2.12) with the assumption that $\sigma = 1$ yields

$$C_j(t+1) = C_j(t) + C_j(t)\hat{\mu} + C_j(t)V_j(t)\left(W^{C_j}(t+1) - W^{C_j}(t)\right). \tag{3.3}$$

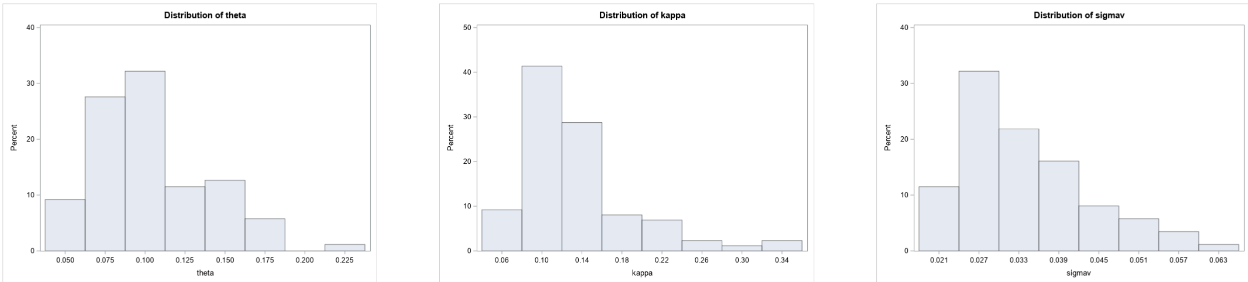

Figure 3.4. CIR parameter estimates for OIBDPQ scaled by ACTQ

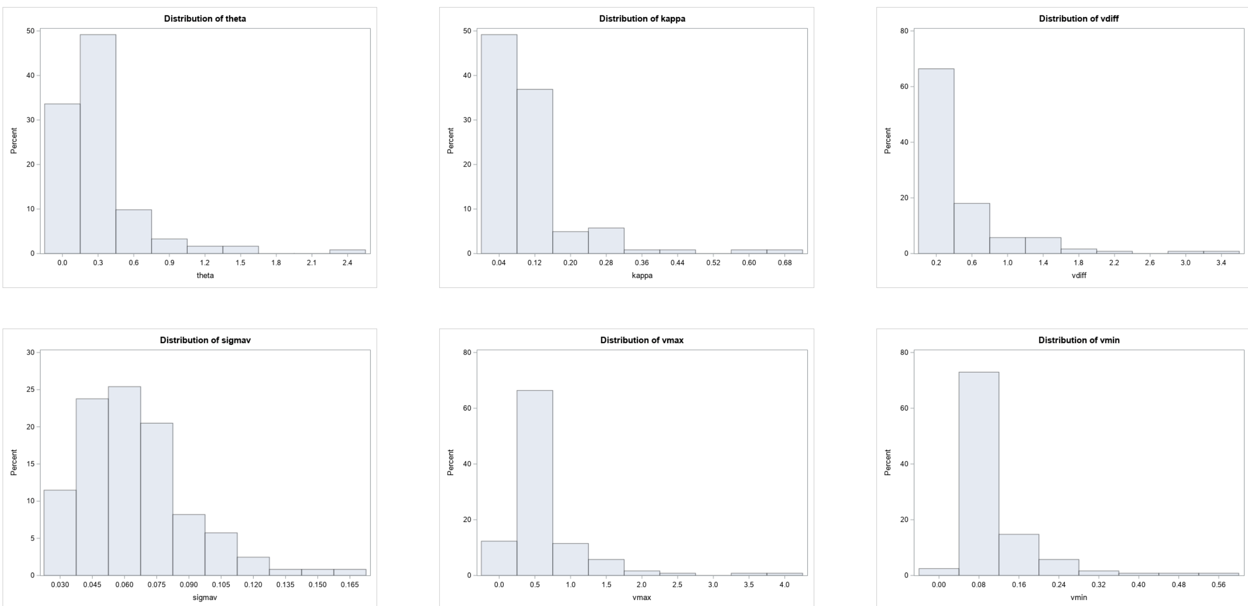

Figure 3.5. Jacobi parameter estimates for OIBDPQ scaled by net assets

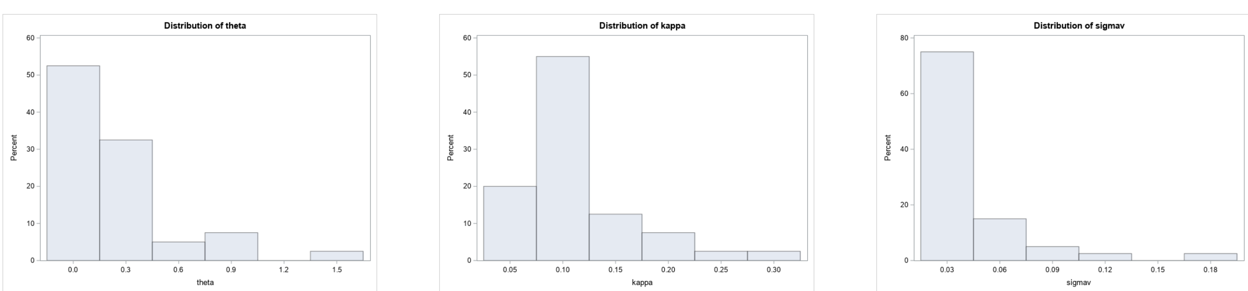

Figure 3.6. CIR parameter estimates for OIBDPQ scaled by net assets

Table 3.1.
Jacobi parameter statistics (scaled by CSHOQ)

	θ	κ	σ_V	$v_{\min}$	$v_{\max}$
min	0.046788	0.023796	0.022332	0.020137	0.12751
max	0.33841	0.6898	0.13004	0.19246	0.98935
mean	0.15237	0.11665	0.047842	0.08286	0.32115
median	0.14574	0.084999	0.044846	0.077799	0.30099
std	0.057192	0.091707	0.016534	0.032004	0.11962
skew	1.0335	2.8683	1.6223	1.1372	1.7403
ex.kurt	1.0732	11.4374	3.9922	1.7631	6.033

Table 3.2.
CIR parameter statistics (scaled by CSHOQ)

	θ	κ	σ_V
min	0.061905	0.052325	0.0174
max	0.29702	0.48261	0.084019
mean	0.12945	0.12897	0.03518
median	0.11875	0.11741	0.031951
std	0.048333	0.07594	0.012529
skew	1.1971	2.6491	1.6031
ex. kurt	1.7143	8.5795	3.2504

Table 3.3.

Jacobi parameter statistics (scaled by ACTQ)

	θ	κ	σ_V	$v_{\min}$	$v_{\max}$
min	0.044917	0.022081	0.019554	0.025608	0.10479
max	0.36776	0.62619	0.12482	0.17853	0.62093
mean	0.1328	0.12645	0.046946	0.071289	0.30904
median	0.11879	0.11143	0.045257	0.067339	0.30831
std	0.060825	0.077913	0.015836	0.028664	0.096582
skew	1.4637	2.4164	1.6392	1.291	0.43324
ex. kurt	2.4872	10.6915	4.3761	2.2987	0.28834

Table 3.4.

CIR parameter statistics (scaled by ACTQ)

	θ	κ	σ_V
min	0.047354	0.056137	0.018207
max	0.22371	0.33941	0.063786
mean	0.1041	0.13522	0.033871
median	0.098241	0.11905	0.031569
std	0.034907	0.055721	0.0096284
skew	0.79468	1.5727	0.85079
ex. kurt	0.49894	2.7616	0.36164

Table 3.5.
Jacobi parameter statistics (scaled by net assets)

	θ	κ	σ_V	$v_{\min}$	$v_{\max}$
min	0.046788	0.023796	0.022332	0.020137	0.12751
max	0.33841	0.6898	0.13004	0.19246	0.98935
mean	0.15237	0.11665	0.047842	0.08286	0.32115
median	0.14574	0.084999	0.044846	0.077799	0.30099
std	0.057192	0.091707	0.016534	0.032004	0.11962
skew	1.0335	2.8683	1.6223	1.1372	1.7403
ex. kurt	1.0732	11.4374	3.9922	1.7631	6.033

Table 3.6.
CIR parameter statistics (scaled by net assets)

	θ	κ	σ_V
min	0.062936	0.029879	0.020264
max	1.5734	0.31727	0.18982
mean	0.26889	0.11121	0.045374
median	0.14267	0.09771	0.037774
std	0.31739	0.057981	0.029476
skew	2.5514	1.6348	3.2898
ex. kurt	6.1561	2.9414	12.2827

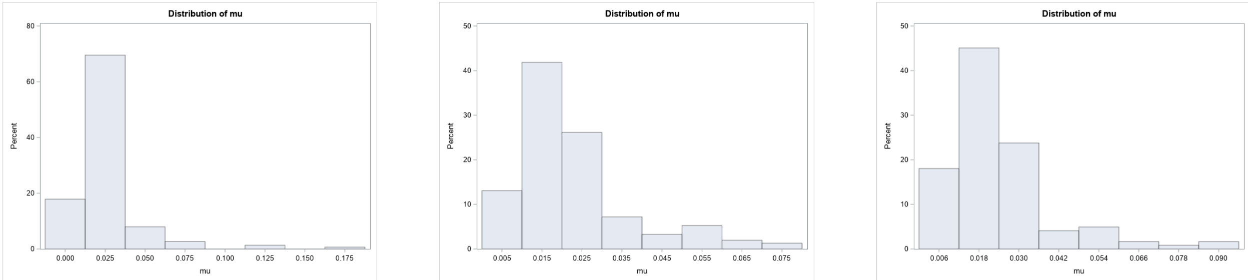

(a) CSHOQ (b) ACTQ (c) net assets

Figure 3.7. Parameter estimates cash flow growth (Jacobi)

Taking conditional expectations yields

$$\mathbb{E}\left[C_j(t+1)|\mathcal{F}_t\right] = C_j(t) + C_j(t)\hat{\mu},$$

which implies

$$\hat{\mu} = \frac{\mathbb{E}\left[C_j(t+1)|\mathcal{F}_t\right] - C_j(t)}{C_j(t)}. \tag{3.4}$$

Figures 3.7 and 3.8 present histograms of estimated values of μ when scaled values of OIBDPQ are used to estimate μ. An estimate for μ is obtained by taking the average of $\hat{\mu}$ in Equation (3.4) for each firm. The parameter μ has a significant effect on firm value, cash flow growth, and returns. In fact, μ may be the most important parameter in regards to returns. The simulation may be run for the scenario in which all firms have their own value for μ. In this case, it is no longer possible to discern the effects of the volatility process parameters. Therefore, we opt to keep μ the same across firms. We now turn our attention to the estimation of $\overline{C}$.

We now derive two more equations to assist in parameter estimation. Assuming the j-th project is alive at time t, i.e. $\chi_j(t) = 1$, then the expected cash flow at time $t+k$ is given by:

$$\begin{aligned}\mathbb{E}\left[C_j(t+k)\chi_j(t+k)|\mathcal{F}_t\right] &= \boldsymbol{\pi}^k\,\mathbb{E}\left[I(j)\mathrm{e}^{\overline{C}+\mu(t+k-j)+\sigma\int_j^{t+k} V_j(u)dW^{C_j}(u)-\frac{\sigma^2}{2}\int_j^{t+k} V_j^2(u)du}|\mathcal{F}_t\right]\\ &= I(j)\boldsymbol{\pi}^k\mathrm{e}^{\overline{C}+\mu(t+k-j)}\mathrm{e}^{\int_j^t V_j(u)dW^{C_j}(u)-\frac{1}{2}\int_j^t V_j^2(u)du}.\end{aligned}$$

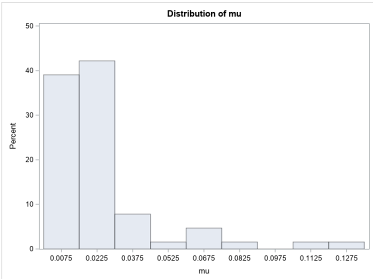

(a) CSHOQ

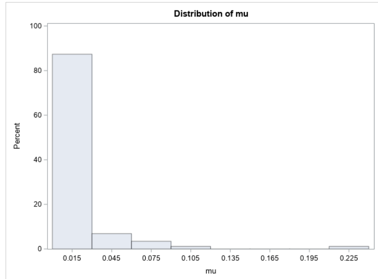

(b) ACTQ

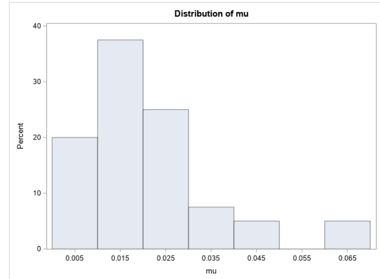

(c) net assets

Figure 3.8. Parameter estimates cash flow growth (CIR)

We also have

$$\begin{aligned}\mathbb{E}\left[C_j(t)\chi_j(t)|\chi_j(j)=1\right] &= \pi^{t-j}\,\mathbb{E}\left[I(j)\mathrm{e}^{\overline{C}+\mu(t-j)+\sigma\int_j^t V_j(u)dW^{C_j}(u)-\frac{\sigma^2}{2}\int_j^t V_j^2(u)du}\right]\\ &= I(j)\pi^{t-j}\mathrm{e}^{\overline{C}+\mu(t-j)}.\end{aligned} \tag{3.5}$$

We use $\pi = .99$, which yields average project life spans of 100 months. We use Equation (3.5) to estimate $\overline{C}$. We sum over $t = j+1$ to $t = j+100$ in Equation (3.5) and think of the left hand side as being the average return on the asset, which we denote by ROA. Then, we solve for $\overline{C}$. Thus, we estimate $\overline{C}$ through the equation

$$\overline{C} = -\log\left(\frac{1}{\mathrm{ROA}}\sum_{l=1}^{100}\pi^l\mathrm{e}^{\mu l}\right). \tag{3.6}$$

Now that we have described the parameter estimation procedure, we proceed with the simulation in the next section.

3.2 The case of no cash flow growth

In this section, we examine the effects of κ, σ_V, $v_{\max}$, $v_{\min}$, θ, $v_{\max}-v_{\min}$, and $\frac{v_{\max}+v_{\min}}{2}$ from Equation (2.6) on the value of the growth options when a Jacobi process is used to model cash flow volatility. For comparison, we also consider the analogous case in which a CIR process is used in place of the Jacobi process. In this case, we examine the effects of the parameters κ, θ, and σ_V, along with the empirical max in certain cases, on the growth option values. We use the phrase "value of future growth options" to mean the value at a specific month of all the projects that will be available after that month, namely the value of $L^*(t)$ at month t. The formula used to calculate this quantity is Equation (2.33). "Mean value of all future growth options" refers to the average value of $L^*(t)$ taken over all of the values of t for each firm individually. The time-frame is usually 1750 months, but the first 140 observations are dropped in some cases. Results from several simulations are presented. We now begin for the case of $\mu = 0$ and $\overline{C} = -3.7$. Following the procedure outlined in Section 3.1, we are left with 155 firms for the Jacobi process and 103 firms for the CIR process. We arbitrarily reduce the number of firms to 150 and 100, respectively.

Figure 3.9a presents a plot of the mean value of all future growth options as a function of θ for the full set of 150 firms, and it shows that the value of growth options decreases as the value of θ increases. On the surface, this appears contrary to the standard results in which a geometric Brownian motion (with constant volatility) is used, such as in McDonald and Siegel [16], who use a GBM to model the project values. Our project values are calculated after modeling the cash flows by stochastic processes. On the other hand, it is also known that investors value smooth cash flows, as seen in Rountree, Weston, and Allayannis [29]. The cash flow volatility should fluctuate around θ. As θ increases, the long run mean of the cash flow volatility increases, making the project cash flows less smooth and thus less valuable to investors. Investment in projects becomes less likely as θ increases. Equation (2.12) gives some insight into why our model produces these results, for the Jacobi process, from a mathematical perspective. Interestingly, when a CIR process is used in place of a Jacobi process, the long run mean of the cash flow volatility does not have the same effect. From the plot, it is not clear whether growth option values increase as a function of θ or there are simply less firms possessing a larger θ parameter. On the other hand, as the rate of mean-reversion increases, the growth option values trend downward for the CIR process. Interestingly, Figure 3.9c displays growth option values as a function of the rate of mean reversion, and the effect of this parameter is not conclusive. Finally, Figures 3.9e and 3.9f display growth option values as a function of the VoV constant coefficient.

Since it is not possible to discern a pattern in all of the plots above, we will investigate special cases in which some of the parameters are held constant while others are allowed to vary. First, we consider the effect of individually changing the value of each of the bounds

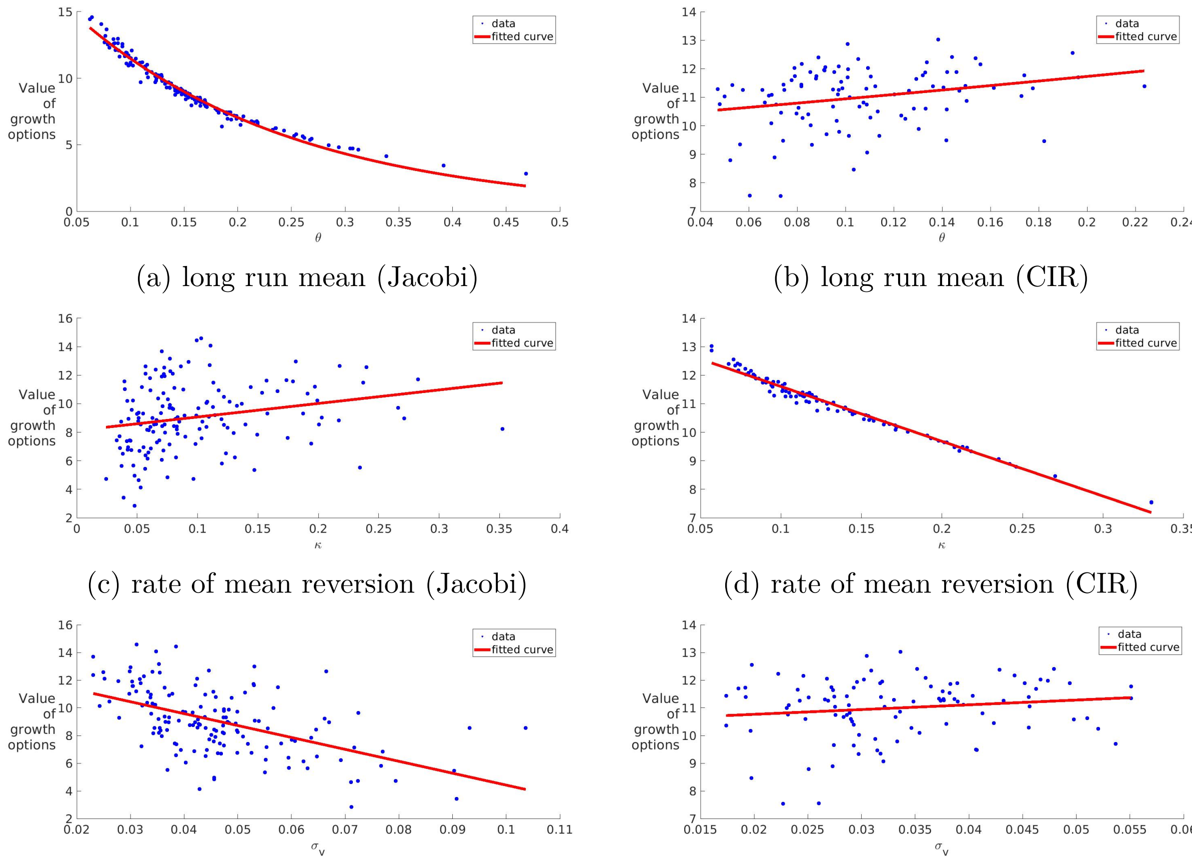

(a) long run mean (Jacobi)

(b) long run mean (CIR)

(c) rate of mean reversion (Jacobi)

(d) rate of mean reversion (CIR)

(e) VoV constant (Jacobi)

(f) VoV constant (CIR)

Figure 3.9. Growth option values

Notes. This figure plots the mean value of growth options as a function of different parameters from our two separate cash flow volatility models. There are 150 firms for the Jacobi process and 100 firms for the CIR process. “Mean value of growth options” refers to taking the mean of the growth option values for each firm over all of the 1750 months. In (a), (c), and (e) a Jacobi process is used, and in (b), (d), and (f) a CIR process is used to model cash flow volatility. Plots (a) and (b) concern the long run mean. The fitted curve in (a) is given by $f(x) = 18.71\mathrm{e}^{-4.885x}$, with 95% confidence intervals $(18.34, 19.07)$ and $(-5.026, -4.744)$. The fitted line in (b) is given by $f(x) = 7.797x + 10.17$ with 95% confidence intervals $(2.072, 13.52)$ and $(9.522, 10.81)$. Plots (c) and (d) concern the rate of mean reversion. The equation for the fitted line in (c) is given by $f(x) = 9.498x + 8.119$ with 95% confidence bounds given by $(3.192, 15.8)$ and $(7.398, 8.839)$. The equation of the fitted line in (d) is $f(x) = -19.23x + 13.53$ with 95% confidence intervals $(-19.82, -18.63)$ and $(13.44, 13.61)$. Figures (e) and (f) concern the VoV constant coefficient. The fitted line in (e) is given by $f(x) = -86.03x + 13.02$ with 95% confidence intervals $(-108.1, -63.93)$ and $(11.95, 14.09)$. The fitted line in (f) is given by $f(x) = 17.16x + 10.42$ with 95% confidence intervals $(-5.925, 40.25)$ and $(9.622, 11.22)$.

on the value of the growth options. To this aim, we select three values of θ and run three simulations. In each simulation, the parameter $v_{\min}$ or $v_{\max}$ varies. Figures 3.10a and 3.10b show three plots of the mean value of growth options for $\theta = .075$, $\theta = .16$, and $\theta = .25$ for varying $v_{\max}$ and $v_{\min}$, respectively. Note that as $v_{\min}$ increases $u_M = \frac{v_{\min}+v_{\max}}{2}$ also increases, and the same is true of $v_{\max}$. As expected, a lower value for $v_{\min}$ leads to higher growth option values, and the relationship appears to be linear. Intuitively, we view a decrease in the lower bound as a good type of uncertainty for two reasons. First, it allows for the possibility of periods of lower cash flow volatility, and second, it yields a lower max uncertainty. Note that the effect of $v_{\min}$ is quantitatively negligible. One plausible reason for this is that the range of possible lower bound values is small, as it must be within the long run mean and zero. We remark on the necessity of obtaining an accurate estimate of $v_{\min}$ from a risk management perspective. If the estimate for $v_{\min}$ is lower than it should be, the project will be overvalued and riskier. The risk stems not only from the lower bound itself being incorrect but also from an inaccurate estimate of u_M, which will be lower than the true value. If the true $v_{\min}$ is larger than the estimate, it will not allow for periods of low cash flow volatility, and the true max uncertainty will be higher than the estimate. We now turn our attention to the upper bound. In addition, the lack of knowledge of the volatility should be reflected in the growth option value. It is interesting to see that when the volatility is not known, an increase in the long run mean of the volatility yields a decrease in the growth option value.

In Figure 3.10a, we plot the value of growth options as a function of $v_{\max}$. Clearly, as θ increases, the growth option values decrease. For each value of θ, as $v_{\max}$ increases, the growth option values decrease. An increase in the upper bound $v_{\max}$ allows for higher cash flow volatility and higher max uncertainty. Thus, we consider an increase in $v_{\max}$ to be an increase in bad uncertainty. A higher $v_{\max}$ means that project investment is less likely, and if the project is accepted, cash flows will most likely be less smooth. Let us now investigate the effect of the constant VoV coefficient.

We plot growth option values as a function of σ_V with the other Jacobi and CIR process parameters left unchanged in Figure 3.11. These plots show an upward trend for the Jacobi process but no clear trend for the CIR process. In the graphs, the maximum difference in growth option values as σ_V changes is .0122 for the Jacobi process and .0046 for the CIR

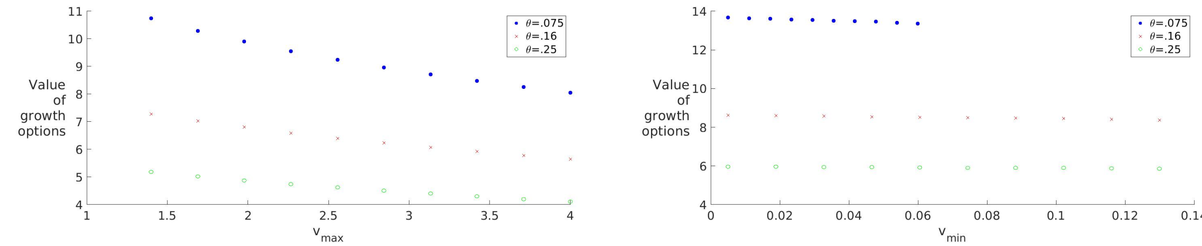

(a) Upper bound

(b) Lower bound

Figure 3.10. Growth option values (the bounds)

Notes. This figure plots the mean value of growth options as a function of $v_{\max}$ in (a) and $v_{\min}$ in (b) when a Jacobi process is used to model cash flow volatility. The length of time is 1610 months, and there are 10 firms for three different values of θ. "Mean value of growth options" refers to taking the mean for each firm over the 1610 months. We give equations for fitted lines, but we leave the lines off of the plot for visual clarity. The fitted lines in (a) correspond to three different θ values. For $\theta = .075$ (represented by blue dots), the fitted line is $f(x) = -1.02x + 12.0$ with 95% confidence intervals $(-1.13, -.91)$ and $(11.7, 12.3)$. For $\theta = .16$ (represented by red dots), the fitted line is $f(x) = -.62x + 8.1$ with 95% confidence intervals $(-.67, -.57)$ and $(7.9, 8.2)$. For $\theta = .25$ (represented by green dots), the fitted line is $f(x) = -.41x + 5.7$ with 95% confidence intervals $(-.44, -.38)$ and $(5.6, 5.8)$. The fitted lines in (b) are given as follows: For $\theta = .075$ (represented by blue dots), $f(x) = -5.36x + 13.7$ with 95% confidence intervals $(-5.83, -4.90)$ and $(13.68, 13.72)$. For $\theta = .16$ (represented by red dots), $f(x) = -1.87x + 8.64$ with 95% confidence intervals $(-2.00, -1.74)$ and $(8.63, 8.65)$. For $\theta = .25$ (represented by green dots), $f(x) = -.86x + 5.98$ with 95% confidence intervals $(-.899, -.822)$ and $(5.97, 5.98)$. Note that the blue dots in Figure (b) do not extend as far as the other dots due to restrictions on the parameters of the Jacobi process, namely Inequality (2.7).

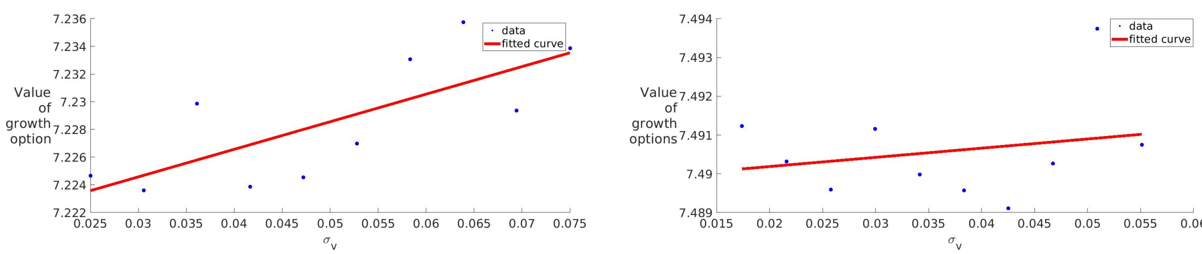

(a) vol-of-vol constant

(b) vol-of-vol constant

Figure 3.11. Growth option values (vol-of-vol constant)

Notes. This figure plots the mean value of growth options as a function of σ_V for the Jacobi process in (a) and for the CIR process in (b). In each case, we consider ten linearly spaced values of σ_V. "Mean value of growth options" refers to taking the mean for each firm over all of the 1750 months. In (a), the equation of the fitted line is $f(x) = .1991x + 7.219$ with 95% confidence intervals $(0.05279, 0.3454)$ and $(7.211, 7.226)$. The equation of the fitted line in (b) is $f(x) = .0237x + 7.49$ with 95% confidence intervals $(-.05829, .1057)$ and $(7.487, 7.493)$.

process. Because of Equation (2.6.1) and the Feller condition, the range of possible σ_V values is limited, and this may hinder our ability to discern the effect of σ_V. Quantitatively, the effect of the constant VoV coefficient is small compared to the effect of the other parameters in these models.

Recall that Figure 3.9 presents plots of the mean growth option values versus σ_V for the full set of firms for both the Jacobi and CIR processes. Since θ dominates the growth option values in the Jacobi process and κ dominates the growth option values in the CIR process, we consider the effect of the VoV constant when the firms are separated based on the dominant parameter for the respective process. Figure 3.12 displays the effect of σ_V on growth option values for three different groups based on the parameter θ for the Jacobi process and the parameter κ for the CIR process. Again, these parameters were chosen because they have a prominent effect on growth option values, as seen in Figures 3.9. We struggle to find a pattern in all of the figures concerning σ_V, except for the pattern observed in Figure 3.11a. This pattern is puzzling because we would expected a larger VoV to yield lower project values. Nevertheless, it is clear that σ_V is not a dominant parameter in either model, especially when compared to κ in the CIR process or θ and u_M in the Jacobi process. Let us now investigate the other important parameter u_M.

Figure 3.13 shows growth option values as a function of $u_M = \frac{v_{\max}+v_{\min}}{2}$ in (a) and the empirical max in (b), when κ and σ_V are fixed. As the square root in the diffusion term is not bounded, there is no direct analog in the CIR process corresponding to the max uncertainty of the Jacobi process. Thus, we consider the empirical max of the observations for the CIR process. Recall that u_M is where the max of $Q(v)$ from Equation (2.6) occurs. Note that the empirical max takes the value .6 six times, but the growth option values are different in these cases. The difference in growth option value is due to the difference in the corresponding θ values. As u_M increases, the growth option values decrease. More data is required to make conclusions regarding the empirical max, but the very small data set that we have does trend down as the empirical max increases. In Figures 3.14a and 3.14b, we present plots of the value of growth options as a function of u_M and the empirical max for the full set of firms when the Jacobi process and CIR process are used, respectively. It is clear that an increase

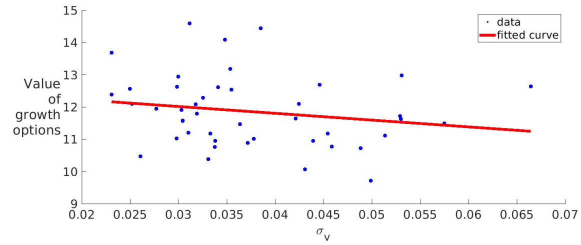

(a) VoV constant (Jacobi)

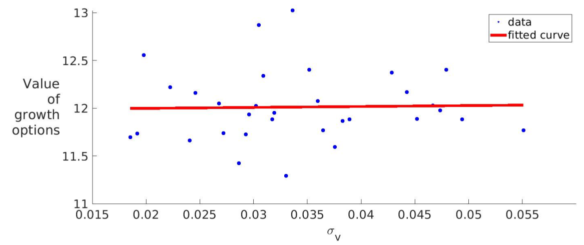

(b) VoV constant (CIR)

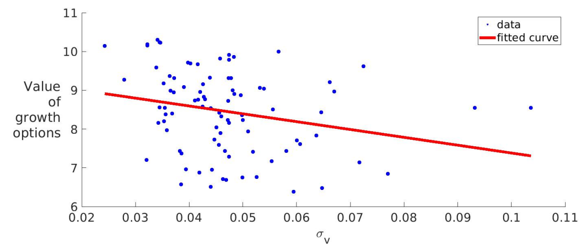

(c) VoV constant (Jacobi)

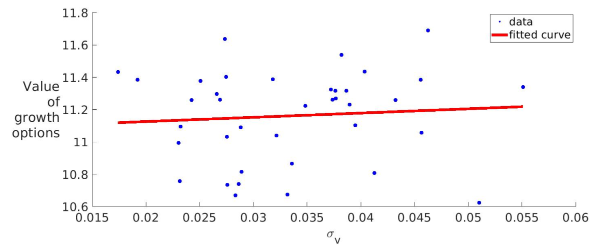

(d) VoV constant (CIR)

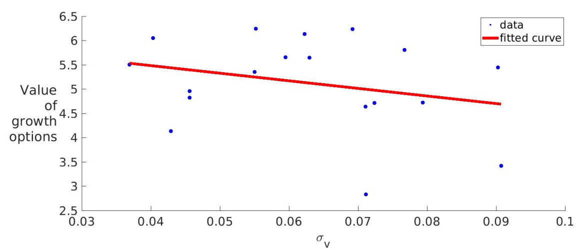

(e) VoV constant (Jacobi)

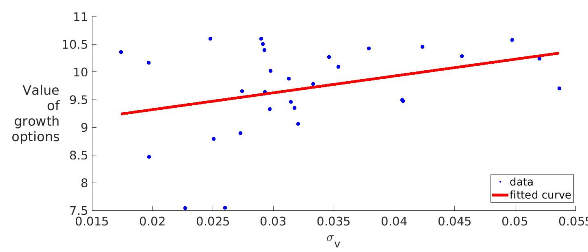

(f) VoV constant (CIR)

Figure 3.12. Growth option values (grouped by certain parameters)

Notes. Plots (a), (c), and (e) display the mean value of growth options as a function of σ_V when a Jacobi process is used to model volatility for firms that meet the criterion $\theta < .12$, $.12 < \theta < .22$, and $.22 < \theta$, respectively. Plots (b), (d), and (f) display the mean value of growth options as a function of σ_V when a Jacobi process is used to model volatility for firms that meet the criterion $\kappa < .1$, $.1 < \kappa < .15$, and $.15 < \kappa$, respectively. In (a), the equation of the fitted line is given by $f(x) = -21.08 + 12.65$ with 95% confidence intervals given by $(-55.04, 12.89)$ and $(11.33, 13.96)$. In (b), the equation of the fitted line in (b) is $f(x) = 0.9628x + 11.98$ with 95% confidence intervals $(-13.86, 15.79)$ and $(11.45, 12.5)$. In (c), the equation of the fitted line is given by $f(x) = -20.22x + 9.403$ with 95% confidence intervals given by $(-37.24, -3.207)$ and $(8.573, 10.23)$. The equation of the fitted line in (d) is $f(x) = 2.628x + 11.07$ with 95% confidence intervals $(-8.131, 13.39)$ and $(10.7, 11.45)$. In (e), the equation of the fitted line is given by $f(x) = -15.64x + 6.109$ with 95% confidence intervals given by $(-45.37, 14.08)$ and $(4.189, 8.03)$. The equation of the fitted line in (f) is $f(x) = 30.32x + 8.712$ with 95% confidence intervals given by $(-1.941, 62.57)$ and $(7.619, 9.805)$. In (a), (c), and (e) there are 150 firms. In (b), (d), and (f) there are 100 firms. "Mean value of growth options" refers to taking the mean of all growth option values for each firm over all of the 1750 months.

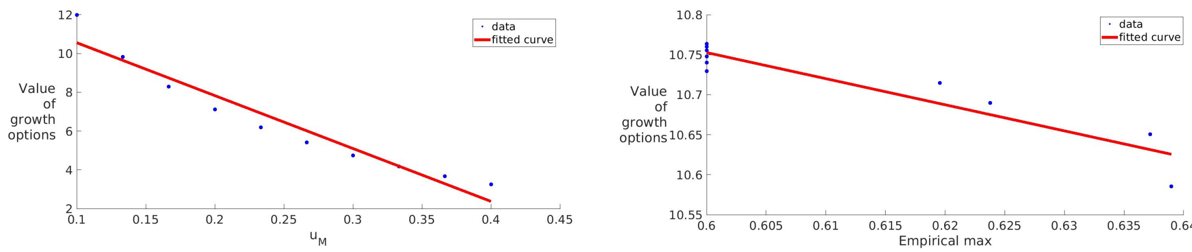

(a) Max uncertainty (Jacobi)

(b) Empirical max (CIR)

Figure 3.13. Growth option values (max uncertainty)

Notes. This figure plots the mean value of growth options as a function of u_M when a Jacobi process is used in (a) and as a function of the empirical max when a CIR process is used in (b) to model volatility. In both cases, $\kappa = .15$, $\sigma_V = .04$, and θ takes 10 values linearly spaced between .1 and .4. For the Jacobi process, $v_{\min}$ varies between .03 and .33, and $v_{\max}$ varies between .17 and .47. The values increase along with θ for the Jacobi process. The equation of the fitted line is given by $f(x) = -27.39x + 13.34$ with 95% confidence intervals given by $(-33.29, -21.49)$ and $(11.76, 14.92)$. The equation of the fitted line in (b) is $f(x) = -3.263x + 12.71$ with 95% confidence intervals $(-4.279, -2.247)$ and $(12.09, 13.33)$. In (a), there are 150 firms. In (b), there are 100 firms. "Mean value of growth options" refers to taking the mean for each firm over all of the 1750 months.

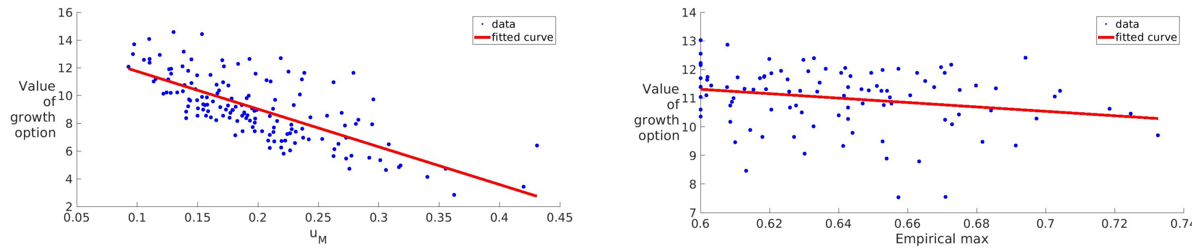

(a) Max uncertainty (Jacobi) (b) Empirical max (CIR)

Figure 3.14. Growth option values (max uncertainty)

Notes. This figure plots the mean value of growth options as a function of u_M when a Jacobi process is used in (a) and as a function of the empirical max when a CIR process is used in (b) to model volatility. In (a), 150 firms are used. In (b), 100 firms are used. The equation of the fitted line is given by $f(x) = -27.2x + 14.46$ with 95% confidence intervals given by $(-31.41, -22.99)$ and $(13.58, 15.34)$. The equation of the fitted line in (b) is $f(x) = -7.705x + 15.93$ with 95% confidence intervals $(-14.3, -1.108)$ and $(11.7, 20.16)$. "Mean value of growth options" refers to taking the mean for each firm over a period of 1750 months.

in u_M yields a decrease in growth option values, but there is no discernible effect for the empirical max of the CIR process.

Finally, we remark that firm value decreases in an exponential manner as θ increases for the Jacobi process. Also, firm value trends downward as u_M increases. This is expected since firm value is the sum of future growth options and expected cash flows from projects that are still alive. So, in our model smaller firms tend to be those with higher volatility.

Now, we consider what determines the project acceptance rate. The parameter $\overline{C}$ plays a large role in the acceptance or rejection of a project. If $\overline{C}$ is too low, all projects will be rejected, and if $\overline{C}$ is too large, all projects will be accepted, though this does depend on the other parameters. In our model, the other main factors that determine the acceptance or rejection of a project are the interest rate, the value of ρ^{M,C_j} (which becomes know at the time the project becomes available), and the Jacobi process parameters. In the case of the Jacobi process, the projects that are rejected are associated with firms that have higher uncertainty and long run mean. Only 3 firms out of 150 with parameters fitted from Compustat have projects being rejected. Out of 1750 months (so 1750 projects), a firm with $\theta = .3048$ and $u_M = .3555$ had 10 projects rejected. A firm with $\theta = .3917$ and $u_M = .4200$ had 125 projects rejected. A firm with $\theta = .4682$ and $u_M = .3624$ had 85 projects rejected.

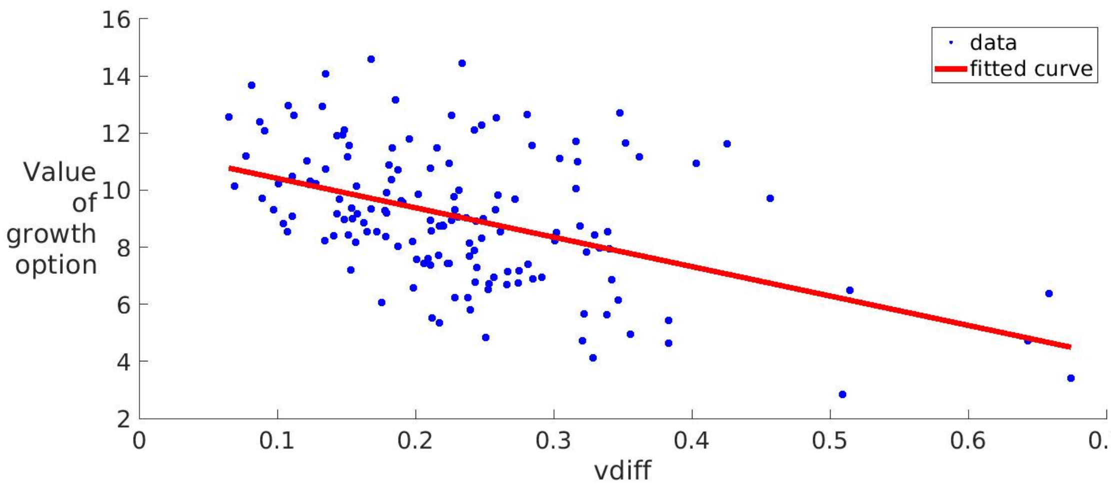

Figure 3.15. Growth option values (vdiff)

Notes. This figure plots the mean value of growth options as a function of the difference in bounds when a Jacobi process is used to model volatility. The equation of the fitted line is given by $f(x) = -10.3x + 11.44$ with 95% confidence intervals given by $(-13.51, -7.101)$ and $(10.63, 12.26)$. There are 150 firms. "Mean value of growth options" refers to taking the mean for each firm over the 1750 months.

The last two firms had the two largest theta values of all firms. Note that $\theta = .3917$ has a larger associated u_M than $\theta = .4682$ does, and we believe this is why more projects are rejected for the firm with $\theta = .3917$. We also note that $\theta = .3048$ is the sixth largest θ value if θ values are ranked from our sample set of 150 parameters, but its value of u_M is higher than the u_M value for firms that have a θ value of third, fourth, or fifth in the ranking of θ values. We view this as further evidence of the importance of the max uncertainty u_M in the decision to take on a project.

Now, we consider the case of no cash flow growth, that is the case of $\mu = 0$, but using Equation (3.6), the parameter $\overline{C}$ is estimated to be -4.3. When there is no cash flow growth, a minor change in the parameter $\overline{C}$ can mean the difference between all projects being accepted and all projects being rejected. Since $\mu = 0$, the future cash flows are less valuable because they are multiplied by the appropriate value from the function g, which is monotonically decreasing. For the case $\overline{C} = -4.3$, all projects are rejected, and for the case $\overline{C} = -3.7$ (seen previously), almost all projects are accepted. In these cases, we only consider the growth option values, as we would like to study returns when not all projects are accepted or rejected.

Figure 3.16 presents the mean value of growth options as a function of the parameters θ, κ, and σ_V from the CIR process. In Figure 3.16a, the equation of the fitted curve is $f(x) = 1.4865 * 10^{-6} * \mathrm{e}^{-18.5406x}$ with 95% confidence bounds given by $(1.378 * 10^{-6}, 1.5949 * 10^{-6})$ and $(-19.3147, -17.7665)$. The bounds correspond to the coefficients in the same order as they appear in $f(x)$. As before, we notice that as the rate of mean reversion increases, the value of growth options decreases exponentially.

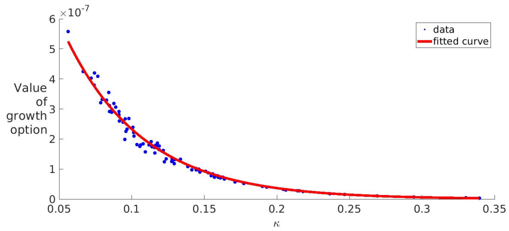

(a) rate of mean reversion, CIR

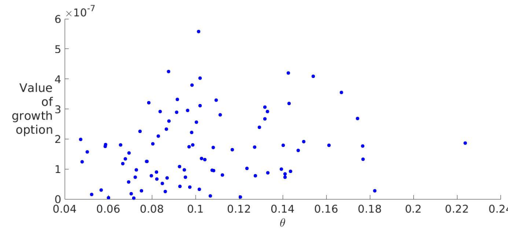

(b) long run mean, CIR

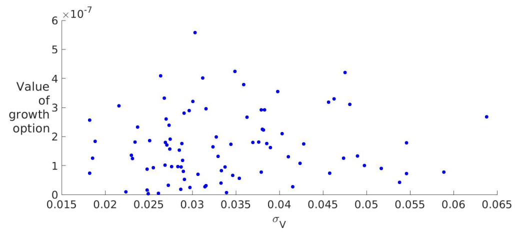

(c) VoV constant, CIR

Figure 3.16. Growth option values (CIR, no cash flow growth)

Now, in Figure 3.17 we turn our attention to the same scenario, except the CIR process is replaced by the Jacobi process. In (b), the equation of the fitted curve is $f(x) = 1.9195 * 10^{-6} * \mathrm{e}^{-19.1885x}$ with 95% confidence bounds given by $(1.8405 * 10^{-6}, 1.9986 * 10^{-6})$ and $(-19.6878, -18.6893)$. The bounds correspond to the coefficients in the same order as they appear in $f(x)$. The most discernible trend is due to the parameter θ. Due to confounding effects, we will also run simulations in which most parameters are held constant while we investigate individual parameters.

Along these lines, let us now investigate several special cases in which certain parameters are allowed to vary while others are held constant for the case of the Jacobi process. In Figure 3.18, we present special cases when different parameters of the Jacobi process are allowed to vary while others are held constant. In Figure 3.18a, the case of the upper bound is presented, and the fitted lines, which are not displayed, have the following equations: The equation of the fitted line for $\theta = .075$ is $f(x) = -1.0576x + 12.0116$ with 95% confidence bounds given by $(-1.1662, -0.949)$ and $(11.7049, 12.3183)$. The equation of the fitted line for $\theta = .16$ is $f(x) = -0.63539x + 8.0944$ with 95% confidence bounds given by $(-0.68744, -0.58335)$ and $(7.9474, 8.2414)$. The equation of the fitted line for $\theta = .25$ is $f(x) = -0.4179x + 5.7288$ with 95% confidence bounds given by $(-0.44679, -0.389)$ and $(5.6472, 5.8104)$. In Figure 3.18b, we present a plot concerning the lower bound. Equations of the fitted line are as

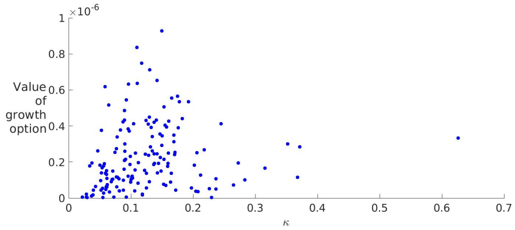

(a) rate of mean reversion, Jacobi

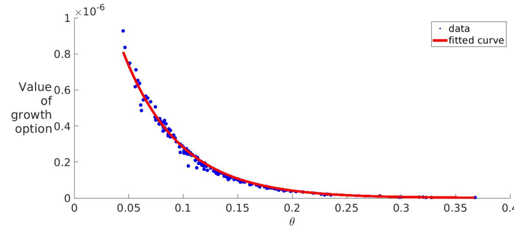

(b) long run mean, Jacobi

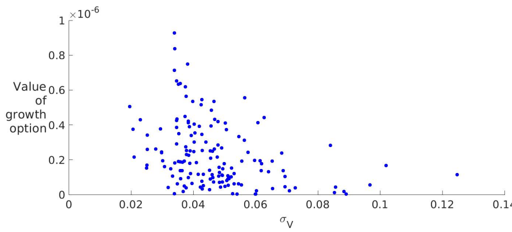

(c) VoV constant, Jacobi

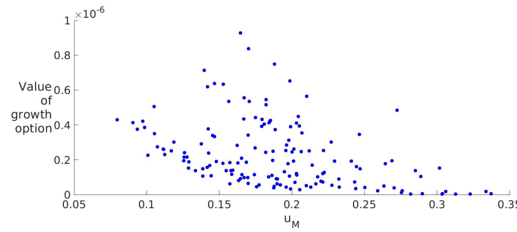

(d) max uncertainty, Jacobi

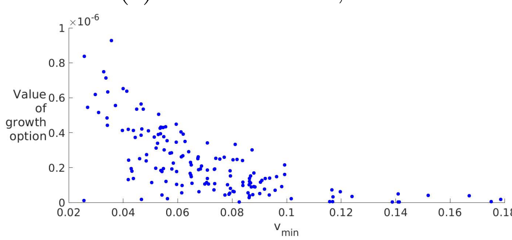

(e) lower bound, Jacobi

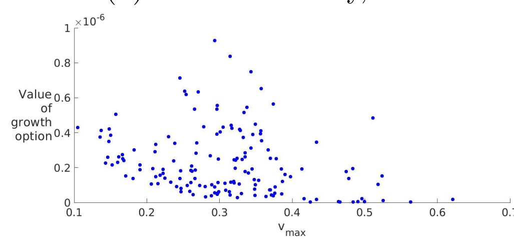

(f) upper bound, Jacobi

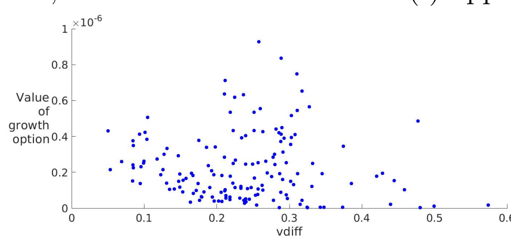

(g) bounds difference, Jacobi

Figure 3.17. Growth option values (Jacobi, no cash flow growth)

follows: The equation of the fitted line for $\theta = .075$ is $f(x) = -5.5361x + 13.8245$ with 95% confidence bounds given by $(-6.0299, -5.0422)$ and $(13.8063, 13.8427)$. The equation of the fitted line for $\theta = .16$ is $f(x) = -1.9183x + 8.7258$ with 95% confidence bounds given by $(-2.0551, -1.7816)$ and $(8.7151, 8.7365)$. The equation of the fitted line for $\theta = .25$ is $f(x) = -0.88189x + 6.0374$ with 95% confidence bounds given by $(-0.91913, -0.84465)$ and $(6.0345, 6.0404)$. The blue dots corresponding to $\theta = .075$ do not extend as far as the others due to the restraint from Inequality (2.7). In 3.18c, the equation of the fitted line is $f(x) = 18.1066\mathrm{e}^{-4.51x}$ with 95% confidence bounds given by $(16.9476, 19.2657)$ and

(−4.8398, −4.1803). In 3.18d, the equation of the fitted line is $f(x) = 0.11816x + 7.0414$ with 95% confidence bounds given by $(-0.037736, 0.27405)$ and $(7.0332, 7.0496)$. In 3.18e, the equation of a fitted exponential curve would be $f(x) = 7.714\mathrm{e}^{-0.15171x}$ with 95% confidence bounds given by $(7.5543, 7.8737)$ and $(-0.24896, -0.054453)$, though we do not display it since it looks more like a line. The bounds correspond to the coefficients in the same order as they appear in $f(x)$. In 3.18e, why does an increase in the rate of mean reversion yield lower growth option values? We suggest that a lower rate of mean reversion yields lower uncertainty on average over large periods. If κ is relatively small and the Jacobi process is near one of the bounds, then on average it will take longer to return to the long run mean, which is also usually near the location of max uncertainty. By the same logic, a large rate of mean reversion quickly brings the volatility back near the location of max uncertainty, in most cases. This in turn leads to a higher volatility of volatility of cash flows.

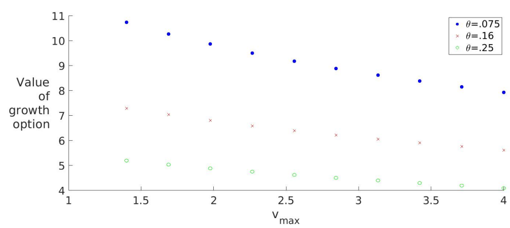

(a) upper bound, Jacobi

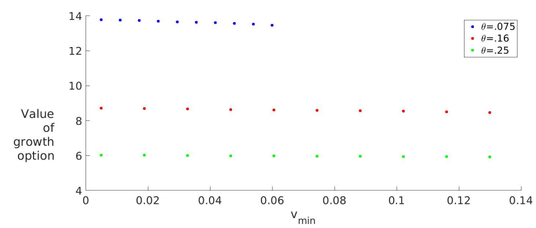

(b) lower bound, Jacobi

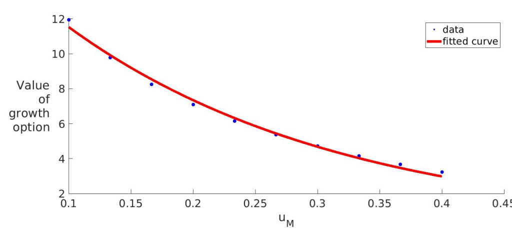

(c) max uncertainty, Jacobi

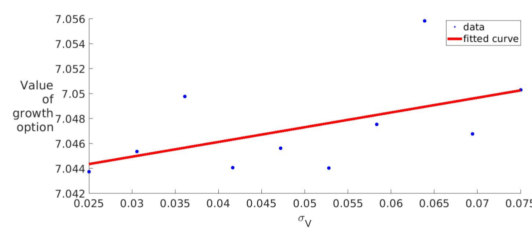

(d) VoV, Jacobi

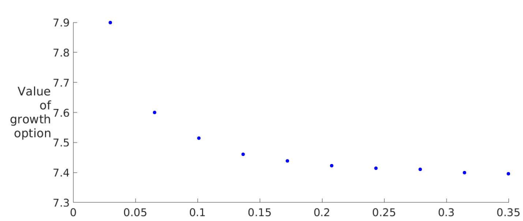

(e) rate of mean reversion, Jacobi

Figure 3.18. Growth option values (Jacobi, no cash flow growth)

We now turn our attention to returns for the same case. Figure 3.19 presents plots regarding the realized returns. In Figure 3.19a, we present a plot concerning the upper bound for three different values of θ. The equation of the fitted line for the case $\theta = .075$ is $f(x) = 9.1289*10^{-6}x+0.00017227$ with 95% confidence bounds given by $(4.4344*10^{-7}, 1.7814*10^{-5})$ and $(0.00014774, 0.0001968)$. The equation of the fitted line for the case $\theta = .16$ is $f(x) = 3.2093*10^{-5}x+0.00054616$ with 95% confidence bounds given by $(8.7347*10^{-6}, 5.5451*10^{-5})$ and $(0.00048018, 0.00061214)$. The equation of the fitted line for the case $\theta = .25$ is $f(x) = 9.9844*10^{-5}x + 0.0023205$ with 95% confidence bounds given by $(5.2104*10^{-5}, 0.00014758)$ and $(0.0021857, 0.0024554)$. The number of projects rejected in each case of θ are as follows: 119.1340 for $\theta = .075$, 586.6340 for $\theta = .16$, and 883.9180 for $\theta = .25$. In Figure 3.19b, we present a plot concerning the lower bound for three different values of θ. The equation of the fitted line for the case of $\theta = .075$ is $f(x) = -0.00010367x + 0.00014763$ with 95% confidence bounds given by $(-0.00028415, 7.6808*10^{-5})$ and $(0.00014097, 0.0001543)$. The equation of the fitted line for the case of $\theta = .16$ is $f(x) = 0.00021469x+0.0004988$ with 95% confidence bounds given by $(-0.00022247, 0.00065184)$ and $(0.00046453, 0.00053308)$. The equation of the fitted line for the case of $\theta = .25$ is $f(x) = 0.00034624x + 0.0021529$ with 95% confidence bounds given by $(-0.00034926, 0.0010417)$ and $(0.0020984, 0.0022074)$. In 3.19c, the equation of the fitted line is $f(x) = 0.0001708e^{10.6014x}$ with 95% confidence bounds given by $(0.00010104, 0.00024056)$ and $(9.4993, 11.7034)$. We now turn our attention to the rate of project acceptance.

Figure 3.20 contains plots of the number of projects rejected versus the value of the upper bound for three different values of the long run mean, namely $\theta = .075, .16, .25$. In the case of $\theta = .075$, as the upper bound increases, there is a clear decrease in the number of projects rejected. The case of a medium long run mean displays an increase and then a decrease in projects rejected as the upper bound increases. Finally, the case of the largest long run mean shows an increase in the projects rejected as the upper bound increases followed by a short decrease in rejected projects.

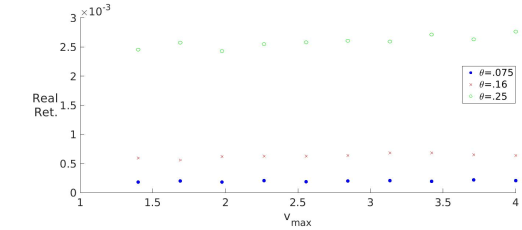

(a) upper bound, Jacobi

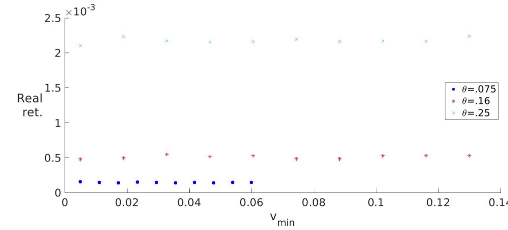

(b) lower bound, Jacobi

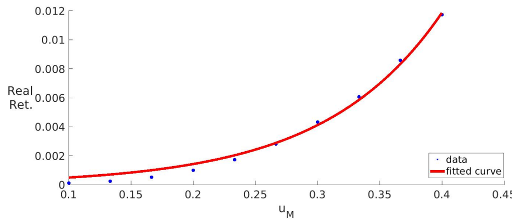

(c) max uncertainty, Jacobi

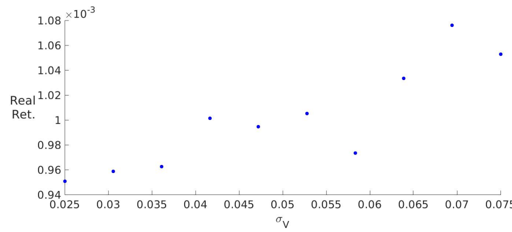

(d) VoV, Jacobi

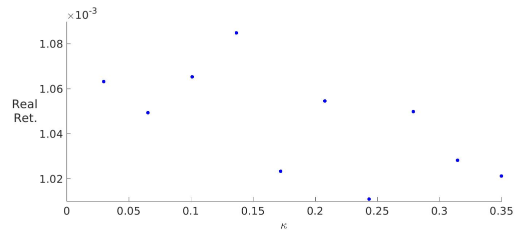

(e) rate of mean reversion, Jacobi

Figure 3.19. Realized returns (Jacobi, no cash flow growth)

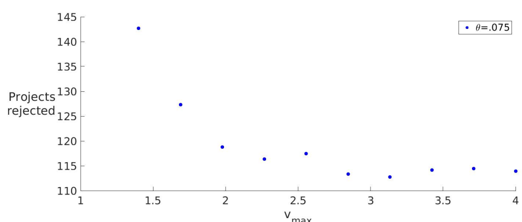

(a) low long run mean

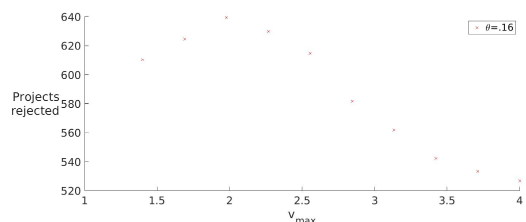

(b) medium long run mean

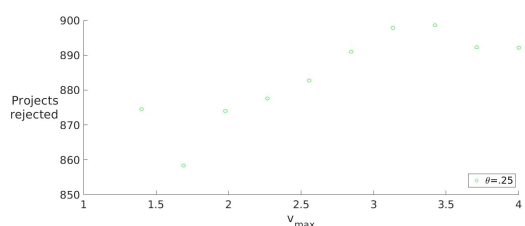

(c) high long run mean

Figure 3.20. Rejected projects, upper bound, Jacobi

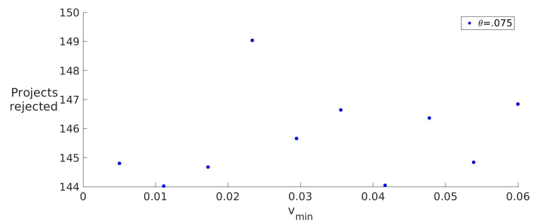

(a) low long run mean

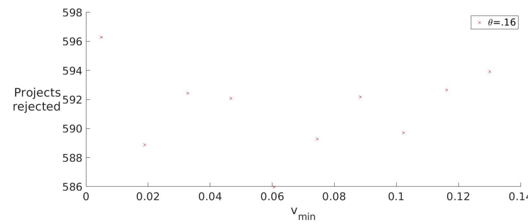

(b) medium long run mean

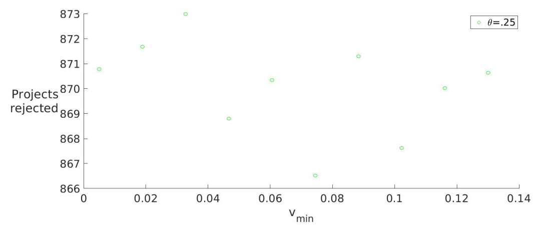

(c) high long run mean

Figure 3.21. Rejected projects, lower bound, Jacobi

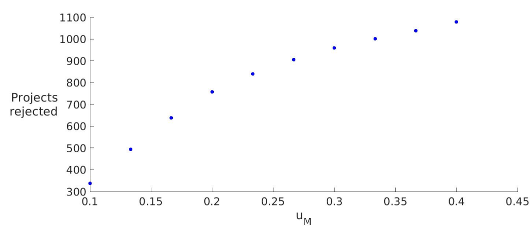

(a) max uncertainty

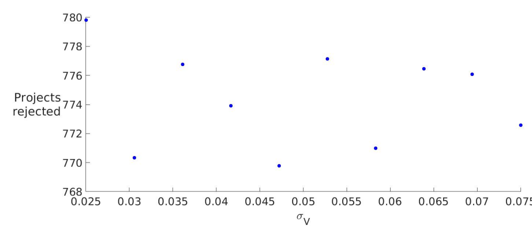

(b) VoV constant

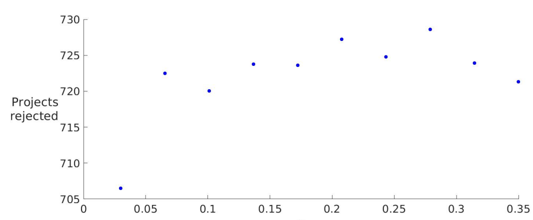

(c) rate of mean reversion

Figure 3.22. Rejected projects, Jacobi

Figure 3.21 shows the average number of projects rejected as a function of the lower bound for three different values of the long run mean, and Figure 3.22 shows plots of the average number of rejected projects versus the max uncertainty, the VoV constant, and the rate of mean reversion. Clearly, as the max uncertainty increases, the average number of projects rejected increases. Otherwise, the results are mostly inconclusive but recorded for completeness. This concludes our investigation of the case in which there is no cash flow growth. Now, we turn our attention to the case of positive cash flow growth.

3.3 Positive cash flow growth

In this section, we present simulation results for the case of positive cash flow growth, using a monthly cash flow growth rate of $\mu = .0124$ for all firms. The parameter μ plays such a dominant role in the model, that fixing μ is the best way to inspect the effects of the uncertainty measures arising from the volatility process. As usual, the parameter $\boldsymbol{\pi} = .99$ controls the project lifetimes. The value of $\overline{C}$, which was estimated by Equation (3.6), is -4.91 for both the case of the Jacobi process and the CIR process. The cash flow volatility parameters are firm specific, and they were estimated using the procedures previously discussed for the case of OIBDPQ scaled by ACTQ. We will first consider growth options, and then, we will consider returns.

3.3.1 Growth option values (positive cash flow growth)

We now consider the growth option values for the cases when cash flow volatility is modeled by a Jacobi process and a CIR process. We begin first with the Jacobi process.

Figure 3.23 presents plots of the mean value of growth option values as a function of relevant parameters. The "mean value of growth option values" refers to taking the mean for each firm type over fifty realizations of that firm type over a period of 1750 months. In (a), the equation of the fitted curve is $f(x) = 3.763\mathrm{e}^{-16.396x}$ with 95% confidence bounds given by $(3.437, 4.089)$ and $(-17.3958, -15.3962)$. In (b), the equation of the fitted line is $f(x) = 0.62958x + 0.52393$ with 95% confidence bounds given by $(-0.21192, 1.4711)$ and $(0.39894, 0.64892)$. In (c), the equation of the fitted line is $f(x) = -8.9607x + 1.0242$ with 95% confidence bounds given by $(-12.874, -5.0475)$ and $(0.83033, 1.2181)$. In (d), the equation of the fitted curve is $f(x) = 2.5054\mathrm{e}^{-22.1801x}$ with 95% confidence bounds given by $(1.9947, 3.0161)$ and $(-26.008, -18.3522)$. In (e), the equation of the fitted line is $f(x) = -0.98382x + 0.90758$ with 95% confidence bounds given by $(-1.649, -0.31864)$ and $(0.69221, 1.123)$. In (f), the equation of the fitted line is $f(x) = -2.9812x + 1.1705$

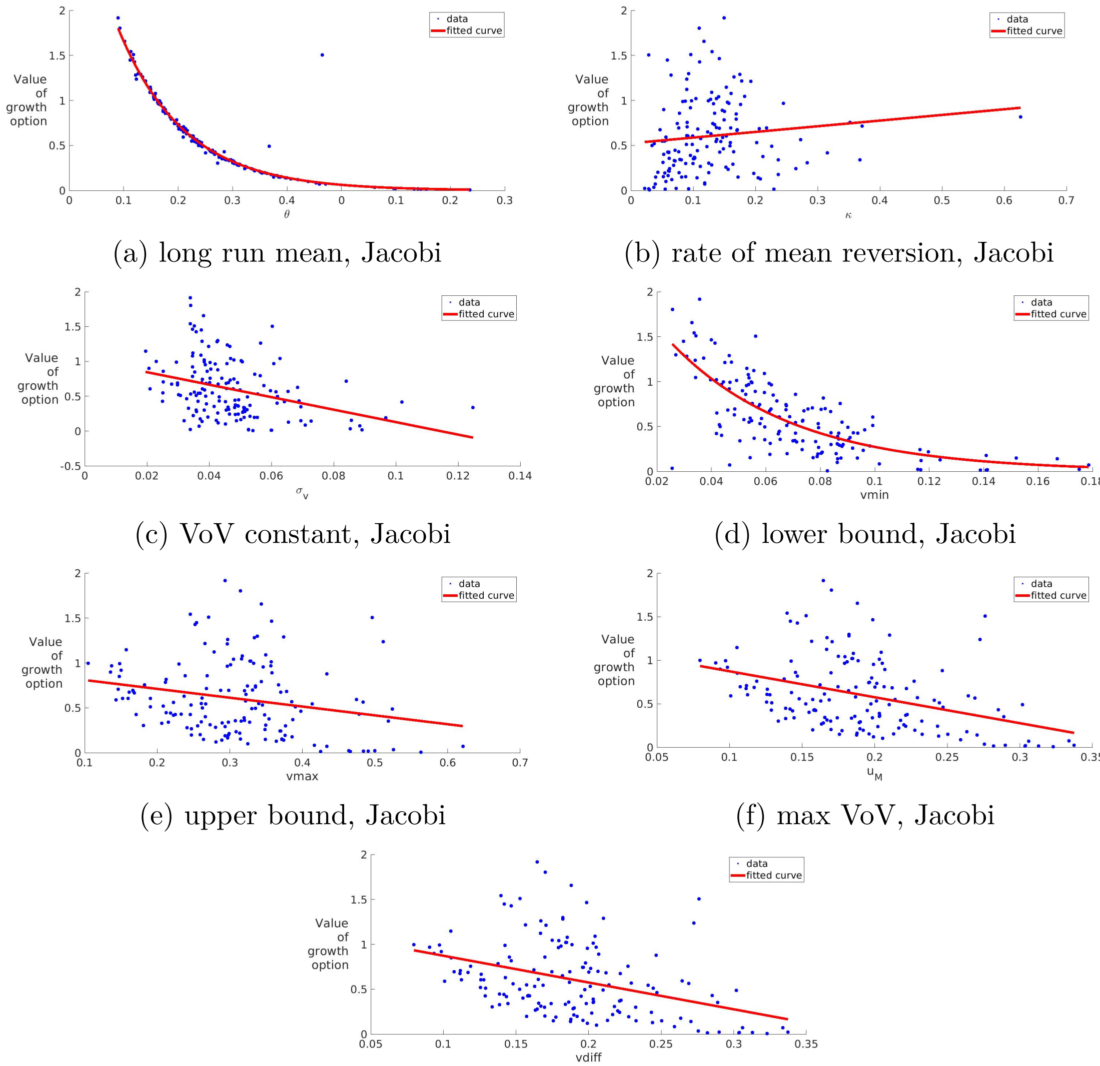

(a) long run mean, Jacobi

(b) rate of mean reversion, Jacobi

(c) VoV constant, Jacobi

(d) lower bound, Jacobi

(e) upper bound, Jacobi

(f) max VoV, Jacobi

(g) vdiff, Jacobi

Figure 3.23. Growth option values (Jacobi)

with 95% confidence bounds given by $(-4.1147, -1.8477)$ and $(0.9465, 1.3944)$. In (g), the equation of the fitted line is $f(x) = -2.9812x + 1.1705$ with 95% confidence bounds given by $(-4.1147, -1.8477)$ and $(0.9465, 1.3944)$. In each case, the bounds correspond to the coefficients in the same order as they appear in $f(x)$.

In Figure 3.23, notice that as θ and u_M increase, the mean value of growth options decreases. We will see later that firms with the largest values of θ and u_M experience the largest returns. Why is the value of the growth option low and the returns high for firms with large θ and u_M? One plausible explanation is that the firm does not know when the large cash flows will occur. Assuming all other factors are equal, an increase in θ implies higher cash flow volatility on average in the long run, but we do not know for certain what the volatility will be in the future. Thus, a project with a relatively large value of θ may indeed experience large cash flows, but these large cash flows may be in the future, when they would be comparatively less valuable due to discounting. Later, we will see a long right tail in the returns of firms with a larger value of θ. We postulate that the firm does not know if or when these large cash flows will occur, making the growth option less valuable. Our result agrees with the observation that investors value smooth cash flows, as seen in Rountree, Weston, and Allayannis [29]. We note that the only truly discernible trend is associated with the parameter θ. We believe we can make some hypotheses based on trends regarding the other parameters, but the trends are not as noticeable due to confounding factors from the other parameters not being held constant. For example, the true effect of κ, in the case of the Jacobi process, is best seen when all of the other parameters are held constant. In a similar vein, as the parameter $v_{\min}$ increases, the value of growth options tends to decrease. As mentioned previously, this is likely due to two reasons. First, periods in which the cash flow volatility is less than or equal to the lower bound are precluded, so the firm is guaranteed cash flow volatility which is greater than the lower bound. Secondly, increasing the lower bound requires an increase in the max uncertainty u_M, and larger values of max uncertainty are correlated with lower growth option values and the possibility of higher returns. Now, consider the effect of the rate of mean reversion κ. A higher rate of mean reversion means that the cash flows would spend less time in both the lower and higher volatility states prior to reverting back toward the long run mean, which is often near the location of max uncertainty. When the volatility is at or near the long run mean, the contribution of the drift term is relatively small compared to that of the diffusion term, and the volatility may tend towards a state of higher or lower volatility rather quickly. Again, it is not only that the drift term makes a small contribution near the long run mean but also that the quadratic function of the diffusion term is usually close to its max here. To show this, in Table 3.7, we present the statistics regarding the magnitude of the difference of the long run mean and and the location of max uncertainty. UTdiff refers to the absolute value of the difference of θ and u_M, and the relative difference is calculated by dividing UTdiff by v_{diff}. The net result of having a larger rate of mean reversion is a higher overall cash flow volatility of volatility. Next, an increase in the parameter σ_V may lead to a decrease in the growth option values, further signifying the importance of the magnitude of the VoV, but this result is not entirely clear without more data. Figure 3.23c displays very weak evidence that an increase in the VoV coefficient precludes large growth option values, and more data would be necessary to settle this. A trend for the upper bound is not very clear, but we believe that as the upper bound increases, growth options are more likely to go down. An increase in the upper bound of cash flow volatility yields a decrease in growth option values for two reasons. First, it allows for periods of higher cash flow volatility, and second, it implies a higher max uncertainty since $u_M = \frac{v_{\min}+v_{\max}}{2}$. Similarly, notice that larger values of v_{diff} appear to lead to lower growth option values. It makes sense that this trend is not very clear, because a decrease in the lower bound is actually good uncertainty. Thus, it is important to realize that an increase in the magnitude of v_{diff} is not as important as the change in the individual upper and lower bounds. It is interesting to compare these trends to those of the CIR process.

Table 3.7.

Difference in max uncertainty and long run mean (Jacobi)

Stats	UTdiff	relative difference
min	0.0010453	0
max	0.21067	0.36687
mean	0.060927	0.00069347
median	0.054028	0
std	0.047146	0.010811
skew	0.56539	18.6169
ex. kurt	−0.52685	385.3111

Figure 3.24 contains plots of growth option values as a function of different parameters. This figure plots the mean value of growth options as a function of the long run mean, θ, in (a), as a function of κ, the rate of mean reversion, in (b), as a function of the coefficient in the diffusion term in (c), and as a function of the empirical max in (d), when a CIR process is

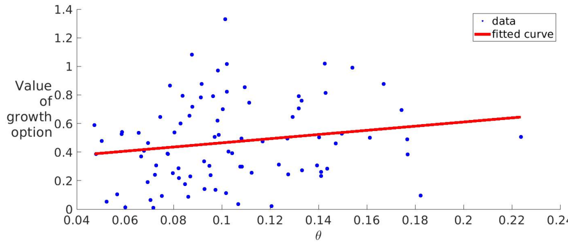

(a) GO and long run mean (CIR)

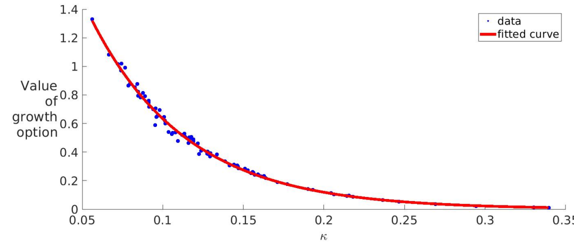

(b) Value of growth options (CIR)

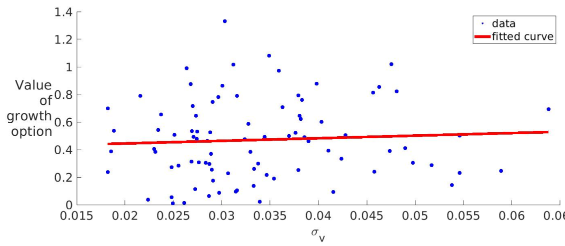

(c) GO and diffusion coefficient (CIR)

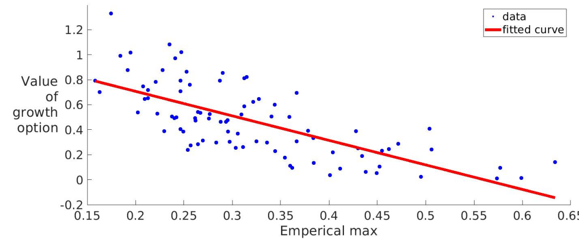

(d) GO and empirical max (CIR)

Figure 3.24. Growth option values (CIR)

used to model cash flow volatility. In (a), the equation of the fitted line is $f(x) = 1.4587x + 0.31856$ with 95% confidence bounds given by $(-0.28043, 3.1977)$ and $(0.12762, 0.5095)$, and there is no obvious trend. On the other hand, in (b), the equation of the fitted curve is $f(x) = 3.3845\mathrm{e}^{-16.7603x}$ with 95% confidence bounds given by $(3.2558, 3.5132)$ and $(-17.1548, -16.3657)$. In (c), the equation of the fitted line is $f(x) = 1.8887x + 0.40643$ with 95% confidence bounds given by $(-4.5055, 8.283)$ and $(0.18127, 0.63159)$. In (d), the equation of the fitted line is $f(x) = -1.9617x + 1.0991$ with 95% confidence bounds given by $(-2.385, -1.5385)$ and $(0.95664, 1.2416)$. The bounds correspond to the coefficients in the same order as they appear in $f(x)$. For the empirical max, we calculated the maximum value observed after sampling the CIR process 1000 times over a time frame of 1750 months for each firm. Thus, each firm had 1000×1750 total observations.

In Figure 3.24, the two main trends concern the rate of mean reversion and the empirical max. Contrary to what we see when the Jacobi process is used to model cash flow volatility, in the case of the CIR process, an increase in the rate of mean reversion yields exponential decay in the growth option values. Thus, it is natural to see if there is a relationship between the rate of mean reversion and the empirical max. As previously mentioned, we calculated the maximum value observed after sampling the CIR process 1000 times over a time frame of 1750 months for each firm. Thus, each firm had 1000×1750 total observations. In Figure 3.25, we present the results of plotting the empirical max as a function of the long run mean in (a), the rate of mean reversion in (b), and the VoV constant in (c). In (a), the equation of the fitted line is $f(x) = -0.88778x + 0.41292$ with 95% confidence bounds given by $(-1.4952, -0.28036)$ and $(0.34623, 0.47961)$. In (b), the equation of the fitted line is $f(x) = 1.3932x + 0.13211$ with 95% confidence bounds given by $(1.1306, 1.6557)$ and $(0.093722, 0.17051)$. In (c), the equation of the fitted line is $f(x) = 4.7604x + 0.15926$ with 95% confidence bounds given by $(2.6922, 6.8285)$ and $(0.086436, 0.23209)$. In each case, the bounds correspond to the coefficients in the same order as they appear in $f(x)$. The most obvious trend is that an increase in the rate of mean reversion yields a larger empirical max. We now turn our attention to the returns and determine if the rate of mean reversion is the dominant parameter there as well.

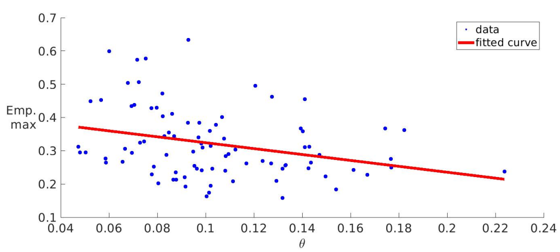

(a) Emp. max and long run mean (CIR)

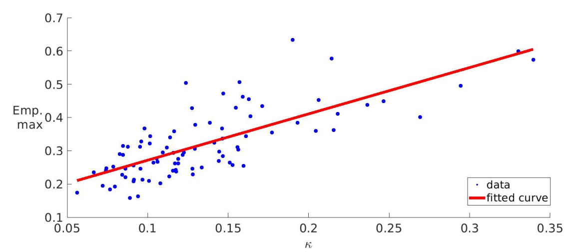

(b) Emp. max and rate of mean reversion (CIR)

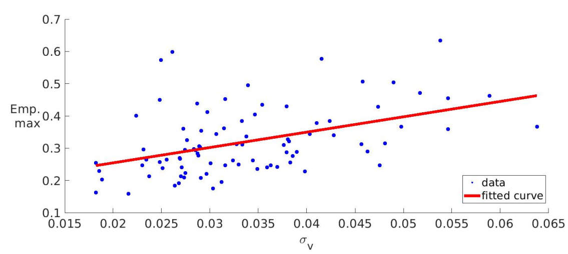

(c) Emp. max and diffusion coefficient (CIR)

Figure 3.25. Growth option values (CIR)

We now consider the returns from holding a claim on the firm. We mainly focus on realized returns because we believe the expected returns are not a good predictor of realized returns. We explain our reasoning for this now. Expected returns are lower, often negative, and skewed to the left in this simulation. The opposite may be true if other parameters are selected. This is due to the method of valuation used for assets in place. First, the month t expected value of future cash flows from all alive projects is calculated, given the current information. Then, the month $t+1$ expected value of future cash flows from all alive projects is calculated, given the current information. Two interesting effects arise. In the case presented below, the negative expected returns arise from the cash flows having more value at the current time period than at the next time period. On the other hand, it is possible to adjust parameters in such a way that expected returns are positive and too large. In this case, the expected returns do not "see" the projects that will be terminated during the next period and thus overestimate the realized returns. We begin by examining the returns when the Jacobi process is used to model cash flow volatility.

Table 3.8.
Jacobi realized returns

	Stats
min	0.0014248
max	0.010001
mean	0.0030773
median	0.0024213
std	0.0017001
skew	1.7733
ex. kurt	3.257

Table 3.9.
Jacobi expected returns

	Stats
min	−0.059398
max	0.0041917
mean	0.00068055
median	0.0019826
std	0.006587
skew	−6.1649
ex. kurt	46.7235

Table 3.10.
Jacobi realized returns

	Stats
min	0.0012329
max	0.47628
mean	0.014624
median	0.0018815
std	0.058334
skew	5.4607
ex. kurt	32.2629

Table 3.11.
Jacobi expected returns

	Stats
min	-0.059296
max	0.0041936
mean	0.00065744
median	0.0019792
std	0.0066133
skew	-6.0871
ex. kurt	45.6403

Tables 3.8 and 3.9 present winsorized realized and expected returns, respectively, when a Jacobi process is used to model cash flow volatility. In each case, the returns for the simulation of each realization of each firm are winsorized at the 5% and 95% level. This affects the firms with large values of the long run mean and max uncertainty the most. Tables 3.10 and 3.11 present results when the returns have not been winsorized. We believe one of the reasons for the negative skewness in the expected returns is that due to discounting, assuming all else is equal, cash flows today are more valuable than cash flows tomorrow. Obviously, this statement depends on the growth rate of the cash flows. In any case, we believe the method of calculating expected returns is not accurate, and this was discussed previously in the thesis. In regards to the realized returns, the mean is more in line with true market observations for the data that is not winsorized than for the data that is winsorized. On the other hand, the excess kurtosis of the winsorized realized returns is more in line with market observations than that of the realized returns that were not winsorized. We now consider which parameters

yield the largest and smallest realized and expected returns for the case of the Jacobi process. In order to truly understand the effects of the parameters, we do not winsorize the data. In Tables 3.12 and 3.13, we present the parameters corresponding to the top ten largest mean realized and expected returns, respectively. In Tables 3.14, and 3.15, we present the parameters corresponding to the top ten smallest mean realized and expected returns, respectively. In each case, the average is taken over fifty realizations for each parameter set and a time frame of 1550 for expected returns and 1549 for realized returns. These tables suggest that a combination of the long run mean and the max uncertainty dramatically affect realized returns. We now investigate further by way of Figure 3.26, which presents plots of the realized returns as a function of different parameters. The trend concerning the plot of real returns versus the long run mean is not clear when wisorized returns are presented. Thus, for the long run mean, we also present a plot in which the returns are not winsorized. Figure 3.26a is a plot of winsorized realized returns versus the long run mean. Figure 3.26h presents the corresponding plot when the returns are not winsorized. We will present more details in the next paragraph.

Table 3.12.

Jacobi realized returns (largest)

returns	θ	κ	σ_V	$v_{\min}$	$v_{\max}$	u_M	v_{diff}
0.47628	0.36776	0.029695	0.05407	0.08262	0.56304	0.32283	0.48042
0.29194	0.328	0.055243	0.060078	0.14094	0.46595	0.30344	0.32502
0.28356	0.32277	0.2295	0.05989	0.13883	0.42491	0.28187	0.28608
0.23522	0.31688	0.092607	0.089128	0.14141	0.48419	0.3128	0.34278
0.22864	0.32015	0.028625	0.052687	0.11689	0.49048	0.30368	0.37359
0.15511	0.29975	0.072539	0.052621	0.11581	0.4637	0.28975	0.34789
0.1362	0.29782	0.022081	0.033884	0.17511	0.49949	0.3373	0.32438
0.075572	0.28044	0.036596	0.085378	0.025608	0.5252	0.27541	0.4996
0.018101	0.23563	0.1183	0.036823	0.17853	0.43335	0.30594	0.25482
0.015114	0.22968	0.03902	0.088456	0.046699	0.62093	0.33382	0.57423

Table 3.13.

Jacobi expected returns (largest)

returns	θ	κ	σ_V	$v_{\min}$	$v_{\max}$	u_M	v_{diff}
0.0041936	0.082893	0.12432	0.023026	0.054581	0.10479	0.079684	0.050206
0.0038788	0.08415	0.24527	0.06072	0.043726	0.13726	0.090494	0.093537
0.0038412	0.074323	0.15297	0.019554	0.053002	0.15741	0.1052	0.1044
0.0037681	0.092683	0.62619	0.054613	0.081052	0.21237	0.14671	0.13132
0.0037114	0.06587	0.17521	0.037685	0.046565	0.37395	0.21026	0.32739
0.0037066	0.044917	0.14988	0.033941	0.035617	0.29337	0.16449	0.25775
0.0036444	0.088274	0.052862	0.020661	0.051392	0.13572	0.093557	0.08433
0.0036329	0.070079	0.17783	0.039819	0.047341	0.26574	0.15654	0.21839
0.0036055	0.070148	0.19257	0.046702	0.044894	0.29615	0.17052	0.25126
0.0035861	0.0791	0.16067	0.034629	0.053547	0.31688	0.18521	0.26333

Table 3.14.

Jacobi realized returns (smallest)

returns	θ	κ	σ_V	$v_{\min}$	$v_{\max}$	u_M	v_{diff}
0.0014248	0.134	0.1426	0.045257	0.093704	0.22477	0.15924	0.13107
0.0014611	0.132	0.061025	0.024964	0.086762	0.17067	0.12872	0.08391
0.001486	0.12776	0.14843	0.032749	0.09636	0.39787	0.24712	0.30151
0.0014918	0.12146	0.2022	0.034069	0.079174	0.24636	0.16277	0.16718
0.0015315	0.1378	0.21223	0.048447	0.090948	0.35364	0.22229	0.26269
0.0015504	0.14221	0.076841	0.043228	0.083997	0.23308	0.15854	0.14908
0.0015596	0.13771	0.095435	0.039093	0.086378	0.31968	0.20303	0.23331
0.0015711	0.12217	0.1222	0.05234	0.079426	0.52395	0.30169	0.44452
0.0015771	0.11913	0.088918	0.030757	0.099198	0.39	0.2446	0.2908
0.0015794	0.13312	0.059243	0.036418	0.070909	0.24535	0.15813	0.17444

Table 3.15.

Jacobi expected returns (smallest)

returns	θ	κ	σ_V	$v_{\min}$	$v_{\max}$	u_M	v_{diff}
−0.059398	0.36776	0.029695	0.05407	0.08262	0.56304	0.32283	0.48042
−0.023975	0.32015	0.028625	0.052687	0.11689	0.49048	0.30368	0.37359
−0.023894	0.328	0.055243	0.060078	0.14094	0.46595	0.30344	0.32502
−0.02018	0.32277	0.2295	0.05989	0.13883	0.42491	0.28187	0.28608
−0.017031	0.31688	0.092607	0.089128	0.14141	0.48419	0.3128	0.34278
−0.012628	0.28044	0.036596	0.085378	0.025608	0.5252	0.27541	0.4996
−0.012156	0.29975	0.072539	0.052621	0.11581	0.4637	0.28975	0.34789
−0.010979	0.29782	0.022081	0.033884	0.17511	0.49949	0.3373	0.32438
−0.0077127	0.22968	0.03902	0.088456	0.046699	0.62093	0.33382	0.57423
−0.0022856	0.10469	0.056151	0.049966	0.054214	0.4746	0.26441	0.42039

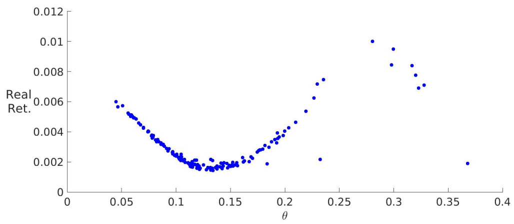

(a) Real Return (long run mean, Jacobi)

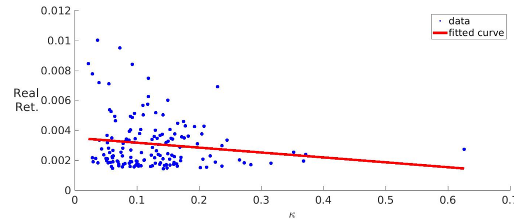

(b) Real Return (rate of mean reversion, Jacobi)

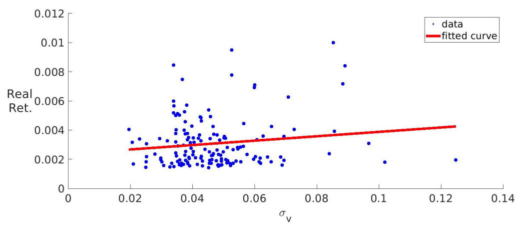

(c) Real Return (VoV constant, Jacobi)

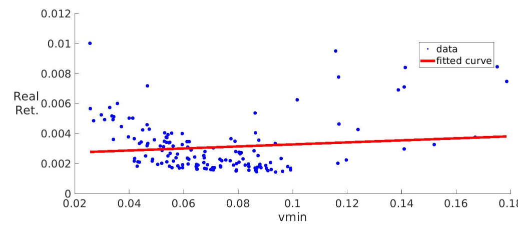

(d) Real Return (lower bound, Jacobi)

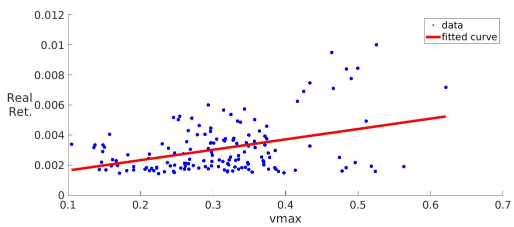

(e) Real Return (upper bound, Jacobi)

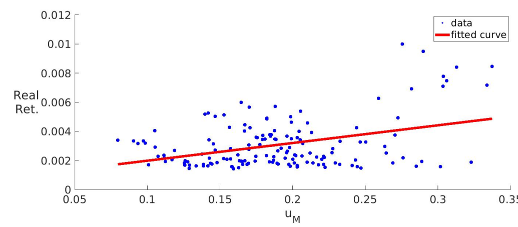

(f) Real Return (max VoV, Jacobi)

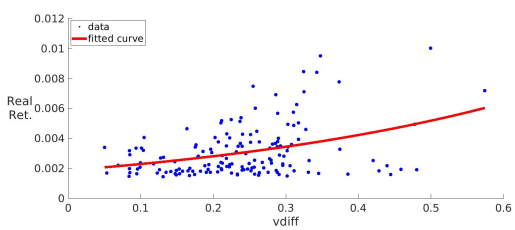

(g) Real Return (vdiff, Jacobi)

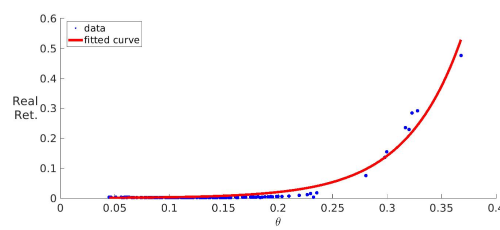

(h) Real Return (not winsorized, Jacobi)

Figure 3.26. Real Return (Jacobi)

Figure 3.26 presents mean realized returns as a function of the parameters of the Jacobi process. In Figures (a)-(g), the realized returns of each realization of each firm over a time period of 1549 are winsorized at the 5% and 95% levels. Figure (h) is not winsorized, and the result is noticeably different from Figure (a). In (b), the equation of the fitted line is $f(x) = -0.0032715x + 0.003491$ with 95% confidence bounds given by $(-0.0067286, 0.00018567)$ and $(0.0029775, 0.0040044)$. In (c), the equation of the fitted line is $f(x) = 0.015077x + 0.0023695$ with 95% confidence bounds given by $(-0.0019564, 0.03211)$ and $(0.0015255, 0.0032134)$. In (d), the equation of the fitted line is $f(x) = 0.0067405x + 0.0025967$ with 95% confidence bounds given by $(-0.0027027, 0.016184)$ and $(0.0018712, 0.0033223)$. In (e), the equation of the fitted line is $f(x) = 0.0069135x + 0.00094074$ with 95% confidence bounds given by $(0.0043208, 0.0095062)$ and $(0.00010127, 0.0017802)$. In (f), the equation of the fitted line is $f(x) = 0.01216x + 0.00076481$ with 95% confidence bounds given by $(0.0074745, 0.016846)$ and $(-0.00016108, 0.0016907)$. In (g), the equation of the fitted curve is $f(x) = 0.001854\mathrm{e}^{2.0501x}$ with 95% confidence bounds given by $(0.0014356, 0.0022723)$ and $(1.2932, 2.807)$. In Figure (h), the equation of the fitted line is $f(x) = 0.00040949\mathrm{e}^{19.4779x}$ with 95% confidence bounds given by $(0.00029014, 0.00052883)$ and $(18.6269, 20.3289)$. In all cases, the bounds correspond to the coefficients in the same order as they appear in $f(x)$.

Table 3.16.
CIR realized returns

	Stats
min	0.0082618
max	0.011448
mean	0.0091387
median	0.0089771
std	0.00068605
skew	1.6431
ex. kurt	2.8766

Table 3.17.
CIR expected returns

	Stats
min	−0.023372
max	0.006728
mean	−0.0015324
median	−0.00035033
std	0.0056801
skew	−1.4694
ex. kurt	2.8474

Tables 3.16 and 3.17 present realized and expected return, respectively, when a CIR process is used. In each case, the returns are winsorized at the 4% and 96% level.

In Tables 3.18 and 3.19, we present the parameters corresponding to the top ten largest mean realized and expected returns, respectively. In Tables 3.20 and 3.21, we present the parameters corresponding to the top ten smallest mean realized and expected returns, respectively. In these four tables, we did not winsorize the returns. In each case, the average is taken over fifty realizations for each parameter set and a time frame of 1550 for expected returns and 1549 for realized returns. Interestingly, the parameter κ seems to have the most significant effect on realized returns when the CIR process is used to

Table 3.18.

CIR realized returns (largest)

returns	θ	κ	σ_V
0.19757	0.07174	0.33941	0.024932
0.13377	0.060133	0.33031	0.0261
0.048904	0.12058	0.29433	0.033933
0.025542	0.10676	0.26914	0.022374
0.0091088	0.052397	0.24644	0.024813
0.0081535	0.070422	0.23649	0.028663
0.0057442	0.08615	0.21804	0.029713
0.0055764	0.18235	0.21556	0.031454
0.005286	0.10175	0.20433	0.027252
0.0051355	0.075258	0.21424	0.041549

Table 3.19.

CIR expected returns (largest)

returns	θ	κ	σ_V
0.0068029	0.15403	0.076578	0.026356
0.0059055	0.16696	0.084112	0.03979
0.0059022	0.13182	0.08884	0.021595
0.005419	0.22371	0.11774	0.025087
0.0045703	0.14257	0.074424	0.047555
0.0043609	0.14965	0.11348	0.027477
0.0042946	0.14291	0.087658	0.045649
0.0042608	0.17676	0.11905	0.038571
0.004115	0.16129	0.11753	0.036965
0.0041095	0.17445	0.098108	0.063786

Table 3.20.

CIR realized returns (smallest)

returns	θ	κ	σ_v
0.0033036	0.10209	0.072002	0.031213
0.0033204	0.13187	0.095536	0.036297
0.0033288	0.086706	0.096819	0.023701
0.0033346	0.096464	0.086217	0.031573
0.0033372	0.16696	0.084112	0.03979
0.0033454	0.1014	0.056137	0.030323
0.0033469	0.09139	0.086297	0.029632
0.0033472	0.082866	0.10145	0.040335
0.0034125	0.13182	0.08884	0.021595
0.0034342	0.17445	0.098108	0.063786

Table 3.21.

CIR expected returns (smallest)

returns	θ	κ	σ_v
−0.023567	0.07174	0.33941	0.024932
−0.022764	0.060133	0.33031	0.0261
−0.014553	0.048018	0.12256	0.023139
−0.013739	0.047354	0.095252	0.032758
−0.013061	0.052397	0.24644	0.024813
−0.011275	0.050298	0.10949	0.02742
−0.010382	0.056656	0.2063	0.031569
−0.009103	0.058504	0.10571	0.028793
−0.0083572	0.070422	0.23649	0.028663
−0.0082259	0.058814	0.10368	0.023422

model cash flow volatility. We now further investigate in Figure 3.27. Figure (a) plots the mean of realized returns as a function of the long run mean θ. The equation of the fitted line is $f(x) = -0.0027572x + 0.0094257$ with 95% confidence bounds given by $(-0.006929, 0.0014147)$ and $(0.0089676, 0.0098837)$. Figure (b) plots the mean of realized returns as a function of σ_V. The equation of the fitted line is $f(x) = -0.010507x + 0.0094945$ with 95% confidence bounds given by $(-0.025616, 0.0046019)$ and $(0.0089625, 0.010027)$. Figure (c) plots the rate of mean reversion of realized returns as a function of the rate of mean reversion, κ, when the realized returns of each realization of each firm are winsorized at the 4% and 96% levels. The equation of the fitted line is $f(x) = 0.011929x + 0.0075256$ with 95% confidence bounds given by $(0.011336, 0.012521)$ and $(0.0074389, 0.0076123)$. Figure (d) plots the mean of realized returns as a function of κ, when the realized returns are not winsorized. The equation of the fitted curve is $f(x) = 9.6762 * 10^{-6}\mathrm{e}^{28.9693x}$ with 95% confidence bounds given by $(2.9069\mathrm{e}-06, 1.6446\mathrm{e}-05)$ and $(26.8694, 31.0693)$. Figure (e) plots the mean of realized returns as a function of the empirical max of simulated CIR data points. The equation of the fitted line is $f(x) = 0.0046156x + 0.0076594$ with 95% confidence bounds given by $(0.0035931, 0.005638)$ and $(0.0073151, 0.0080036)$. In each case, the bounds correspond to the coefficients in the same order as they appear in $f(x)$. In all cases, a CIR process was used. The length of time is 1549 months. In both cases, 87 firms are used with 50 realizations of each type of firm, and the mean value of realized returns is taken over the 1549 months and 50 realizations.

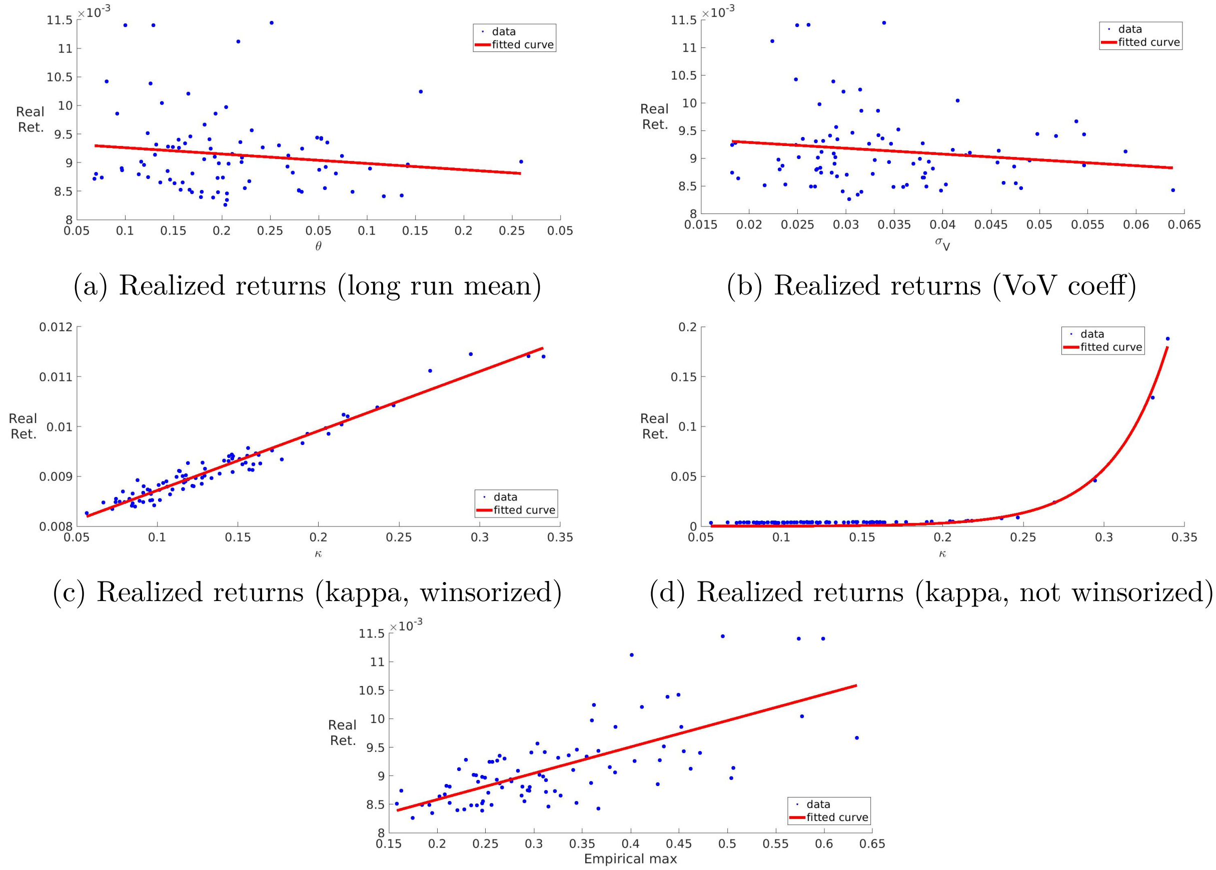

(a) Realized returns (long run mean)

(b) Realized returns (VoV coeff)

(c) Realized returns (kappa, winsorized)

(d) Realized returns (kappa, not winsorized)

(e) Realized returns (empirical max)

Figure 3.27. Realized returns (CIR)

Finally, consider the projects rejected for both the Jacobi and CIR processes. In Figure 3.29, we plot the mean number of projects rejected as a function of the long run mean, the VoV constant, and the rate of mean reversion. There is no clear trend for the long run mean or the VoV constant. On the other hand, as the rate of mean reversion increases, the number of projects rejected increases. This is what we should expect, since the rate of mean reversion is the dominant parameter in growth option values and realized returns in the case of the CIR process.

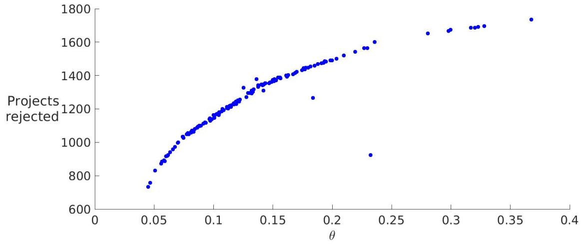

(a) Projects rejected (long run mean)

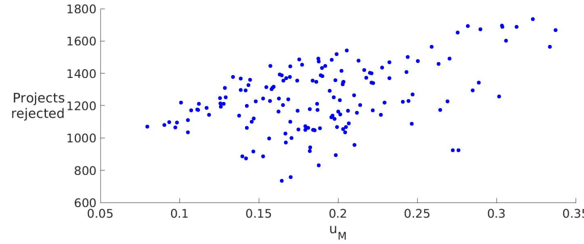

(b) Projects rejected (max uncertainty)

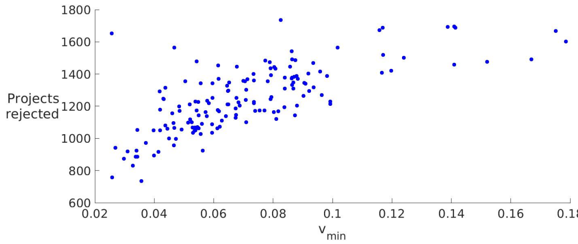

(c) Projects rejected (lower bound)

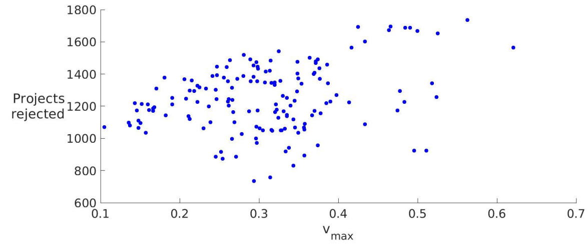

(d) Projects rejected (upper bound)

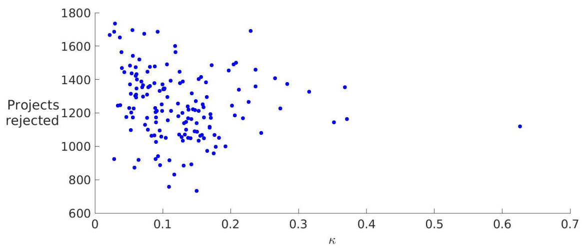

(e) Projects rejected (rate of mean reversion)

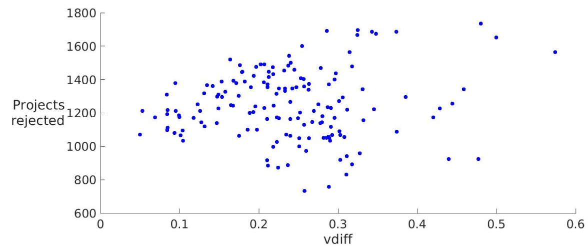

(f) Projects rejected (difference of bounds)

Figure 3.28. Projects rejected (Jacobi)

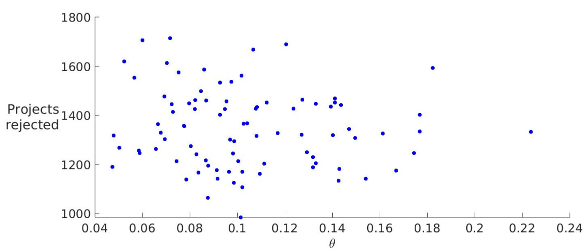

(a) Projects rejected (long run mean)

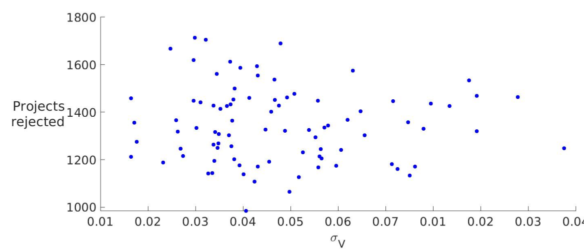

(b) Projects rejected (VoV coeff)

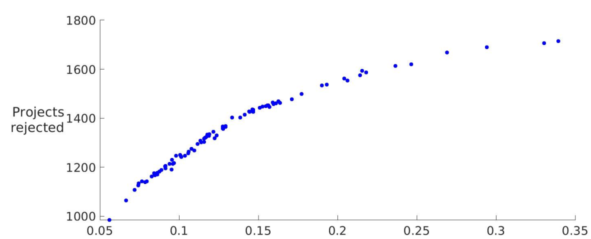

(c) Projects rejected (rate of mean reversion)

Figure 3.29. Projects rejected (CIR)

4. CONCLUSION

In this thesis, we have developed a growth option and asset pricing model that incorporates stochastic cash flow volatility, and we have used two separate diffusion processes to investigate the manner in which different measures of uncertainty affect growth option values, realized returns, and the rate of project acceptance.

Our first model for cash flow volatility was the Jacobi process, a bounded mean reverting quadratic diffusion. Since there are confounding factors, we study the effects of some parameters individually. We study both the lower and upper bound for three separate values of the long run mean, namely $\theta = .075, .16, .25$. We find that in all cases increasing the lower bound yields lower growth option values. As θ increases, the magnitude of this relationship decreases. That is to say that the slope of the regression line for growth option values plotted as a function of the lower bound remains negative but decreases in magnitude. Intuitively, increasing the lower bound removes the possibility for periods of lower cash flow volatility, and these periods of low cash flow volatility are desirable to both the firm and investors. As the long run mean increases, this effect still holds but is less prominent since over the long run the cash flow volatility will be larger. We also find that increasing the upper bound yields lower growth option values. Again this effect becomes less prominent as the long run mean increases. Intuitively, an increase in the upper bound yields the possibility of periods with larger cash flow volatility. We call the local max of the quadratic function in the diffusion term the max uncertainty. We find that an increase in the max uncertainty yields a decrease in growth option values. The same is true of the long run mean. Although the max uncertainty and long run mean are not necessarily the same, they are typically near each other. The effect of a large long run mean is that over long periods of time, the volatility will be large on average. The effect of a large max uncertainty is a large cash flow volatility of volatility. The effect of these two parameters compounds and affects growth option values, as mentioned previously. The effect of the VoV constant coefficient in the diffusion term is not immediately clear. Although an increase in this constant seems to yield an increase in growth option values when all other factors are held constant, the effect is minuscule. The effect of the rate of mean reversion is also negligible until it is investigated when all other parameters are held constant. In this case, an increase in the rate of mean reversion yields rapid exponential decay initially but this levels off quickly. We also consider realized returns and the rate of project acceptance.

We now consider returns for the Jacobi process. For the case concerning only the upper bound, realized returns increase as the upper bound increases. The increase becomes more pronounced as the long run mean increases. In the case of the lower bound, the results are mixed. When the long run mean takes the smallest of three chosen values, realized returns decrease slightly as the lower bound increases. On the other hand, for the two larger values of the long run mean, realized returns increase slightly as the lower bound increases. Realized returns increase exponentially as a function of the max uncertainty. The results for the VoV constant and rate of mean reversion are not so obvious, but realized returns generally increase as a function of the VoV constant and decrease as a function of the rate of mean reversion. The results regarding project rejection are mixed, except for the case of max uncertainty. As the max uncertainty increases, the average number of projects rejected increases. Of the trends just mentioned, the only noticeable one is that of the max uncertainty when the full set of firms is used. When the full set of firms with parameters fitted by financial data are used, the combination of the long run mean and the max uncertainty together yield the most noticeable trend. As the long run mean and the max uncertainty increase, both the realized returns increase and the number of projects rejected increase. The realized returns increase at the expense of higher cash flow volatility and uncertainty, and firms are thus less likely to accept these projects.

We now turn our attention to the case in which cash flow volatility is modeled by a CIR process. First, consider growth option values. As the rate of mean reversion increases, the mean value of growth options decreases exponentially. Also, as the empirical max of observed values from the CIR process increases, the growth option values tend to decrease. Recall that as the rate of mean reversion increases, the empirical max trends upwards. On the other hand, there is no discernible trend when plotting the mean growth option values as a function of the long run mean or the VoV constant. In regards to the realized returns, the perceptible trends are associated with the rate of mean reversion and the empirical max. As the rate of mean reversion increases, the realized returns increase exponentially. As the empirical max increases, the realized returns also increase, but not exponentially. Finally, the mean number of projects rejected increases as the rate of mean reversion increases. This is what we expect, since this parameter has such a dominant impact on the growth option values and realized returns. There is no clear trend between the long run mean and the VoV coefficient. Again, we notice a difference in which parameters are dominant when the Jacobi process is used as opposed to the CIR process.

The most obvious distinction between the two cash flow volatility models is that the rate of mean reversion is the dominant parameter when the CIR process is used, while the combination of the long run mean and max uncertainty are the dominant parameters when the Jacobi process is used. Indeed, when considering growth options and realized returns, the long run mean yields exponential trends for the case of the Jacobi process, and the rate of mean reversion yields exponential trends for the case of the CIR process. Why is this? We believe the answer lies in the diffusion term of the volatility process. Investors and firms prefer stable cash flows. Consider the Jacobi process. Investors naturally prefer a smaller long run mean of cash flow volatility. It makes sense that as this parameter increases, the project value will decrease. Furthermore, we can intuitively consider a competition between the diffusion term and the drift term. In the Jacobi process, as the state of the volatility drifts away from the location of max uncertainty, which is usually near the long run mean, the diffusion term becomes less prominent and the drift term takes over. For the purpose of this thought experiment, let us assume that the location of max uncertainty is relatively near the long run mean of volatility. A large max uncertainty then quickly pushes the state of volatility towards the bounds, where the drift term pulls the volatility back towards the long run mean. Near the long run mean, the drift term is small, especially compared to the diffusion term. Thus, firms with a high max uncertainty near the long run mean are shifting volatility states frequently, leading to a high cash flow volatility of volatility. Investors do not like a high VoV. Thus, the combination of increasing long run mean and the max uncertainty yield lower growth option values, though these projects occasionally yield massive returns, and they exhibit better than average returns. Due to the nature of the diffusion term in the Jacobi process, the job of the rate of mean reversion as a scaling factor is not so important. Interestingly, the opposite is true when the CIR process is used. As the state of the cash flow volatility increases in the case of the CIR process, the diffusion term increases, since the square root is not bounded. Thus, a large rate of mean reversion is required to compete with the diffusion term, especially when the state of volatility is larger than the long run mean. A large rate of mean reversion will pull the state of volatility back to the long run mean faster compared to a smaller rate of mean reversion. Once the state of volatility is near the long run mean, the drift term becomes negligible again. Thus, the key difference between the two models is the VoV risk. The effects of these key differences could be studied in time series and cross sectional regressions since we have significantly reduced the computation time for the simulation. Our next goal is to study cash flow volatility and cash flow VoV in the cross section of returns through the framework of this model. In conclusion, we developed a growth option model with stochastic volatility, studied the effects of cash flow volatility uncertainty through two different volatility models, and set up a computationally feasible framework to study cash flow VoV and volatility uncertainty from the perspective of firm investment.

5. APPENDIX

In the Appendix, we present the main components of the Matlab code used to run the simulations. The first step is running the script `INAF.m`, which we present below. This code allows the user to choose which simulation will be run and adjust certain properties of the model.

```
%Brian Hogle, April 2021

%INAF- Initialize parameters across firms

WP='CIR'; %Use 'Jacobi' for Jacobi process, 'CIR' for CIR process,
%'VminJac', 'VmaxJac', 'UMJac', 'kappaJac', or 'sigmavJac' for other ...
    options.

WhichFirms='NO'; %Use 'YES' to get only firms that meet convergence
                  %Criterion. Use 'No' to get only firms that do not.

doSeries='NO'; %Use 'Yes' if you want to eliminate firms based on
               %the convergence criterion derived in Hogle's PhD thesis

CbarEst='YesCbar'; %Use 'NoCbar to use set variable Cbar1 below.
                   %Use 'YesCbar' to estimate Cbar.
Cbar1=-3.7; %BGN value

%Use average monthly stock market returns, or
%Change ROATYPE to avoid using monthly stock market returns.

MKTret=.0083; %Monthly market return.

ROATYPE='Market'; %Either 'Market' or 'RetOnAssets'

muType='noDrift'; %If muType is set to 'Agg',
                    %mean(mu) will be used across
```

```
                        %all firms.
                        %'noDrift' will use mu=0 for
                        %all firms. Change to anything else to use firm
                        %specific mu.

%END OF OPTIONS/PREFERENCES

simlen=1750; %Time-frame of simulation.
N=950; %Terminate sum over n=s-t=1 to \infty at N=s-t=950.
K=450; %Index over second sum in paper.
nPaths=1000; %Number of paths used for monte carlo simulation.

pi1=.99; %Probability Bernoulli r.v. is equal to 1.
         %Same for all firms. Determines lifetime of projects.

%The parameters below are related to how processes are correlated.
%It's important to note that rhorcj for example is the correlation
%between dWr and dWCj, not the correlation of the processes r and Cj
%themselves, as there is sometimes a negative sign in front of the
%diffusion term.

rhorcj=.2; %Correlation between B.M.'s driving the interest
           %rate and cash flows.
rhomr=-.175; %Correlation between B.M.'s driving SDF and interest rate.

rhomcjmax=1;%Upper bound on r.v. rhomcj.
rhomcjmin=0;%Lower bound on r.v. rhomcj.

rhomcj=[.0001 .01 .03 .07 .11 .2]; %Can change the length of this
                                   %vector with no other adjustments.
            %Also, consider changing distribution of rhomcj. Current
            %set up is discrete uniform distribution. Changing ...
                distriubtion
            %will require changes to other segments of the code.


```

```
rhon=length(rhomcj);

lambda=.4; %Market price of risk.

%Interest rate.
sigmar=.002;
a=.05;
b2=.006236;
rparams=[a b2 sigmar];

boundtol=10^(-14);%Adjustment when Jacobi process goes out of bounds.

%Below are parameters for the process I(t). Note that the value I(t)
    %significantly affects the value of the growth options.
    %If I(t) decreases(increases) the growths option values will
    %decrease(increase). We will assume I(t)=1 for all t.
muI=0;  %Growth rate of investment process I(t).
sigmaI=0; %Volatility of investment process I(t).

% r and SDF are same across all firms.
buff=20;%We create a buffer. This is useful for example when using
    %mulcorFun to generate dWCj correlated to dWr and dWm.
[r,M,Wm,dWr,dWm]=SimMr(simlen+buff,rhomr,rparams,lambda);

%Recall the constant C1 is the same across all firms.
C1=lambda*sigmar*rhomr/a-b2+sigmar^2/(2*a^2);
%C2 & C3 are same across firms. They depend on r(t).
C2=C2r(r,b2,a,lambda,sigmar,rhomr); C2=C2(1:simlen);
C3=sigmar^2/(4*a^3)-C2; C3=C3(1:simlen);

%We will make Jacobi process parameters firm specific.
vn=10; %vn is number of grid points for [v_min,v_max].
           %Partition this to approximate g.

sigma=1;  %Coefficient in volatility of cash flow process.

```

```
%Load Jacobi or CIR
if strcmp(WP,'Jacobi')
V=readmatrix('Jacobi_RFS_withCSHOQ.xlsx');
theta=V(:,5);
kappa=V(:,4);
sigmav=V(:,1);
vmin=V(:,3);
vmax=V(:,2);
mu=V(:,6);
ROA=V(:,7);
vdiff=V(:,8);
vparams=[theta kappa sigmav vmin vmax];
CSHOQ=V(:,9);
elseif strcmp(WP,'CIR')
V=readmatrix('CIR_RFS_ACTQ.xlsx');
theta=V(:,3);
kappa=V(:,2);
sigmav=V(:,1);
mu=V(:,4);
vparams=[theta kappa sigmav];
elseif strcmp(WP,'VminJac') %For Jacobi
load('Vmin_vars','vparams')
elseif strcmp(WP,'VmaxJac') %For Jacobi
load('Vmax_vars','vparams')
elseif strcmp(WP,'UMJac') %For Jacobi
load('um_vars','vparams')
elseif strcmp(WP,'sigmavJac') %For Jacobi
load('sigmav_vars','vparams')
elseif strcmp(WP,'kappaJac') %For Jacobi
load('kappa_vars','vparams')
elseif strcmp(WP,'kappaCIR') %For Jacobi
load('kappa_vars_CIR','vparams')
%Want Left \leq Right
end

```

```
if strcmp(WP,'VminJac') || strcmp(WP,'VmaxJac') || strcmp(WP,'UMJac') ... ||...
        strcmp(WP,'sigmavJac') || strcmp(WP,'kappaJac')
theta=vparams(:,1);
kappa=vparams(:,2);
sigmav=vparams(:,3);
vmin=vparams(:,4);
vmax=vparams(:,5);
Left=sigmav.^2.*(vmax-vmin)./(sqrt(vmax)-sqrt(vmin)).^2;
Right=2*kappa.'.*min(vmax-theta,theta-vmin);
end

if strcmp(doSeries,'Yes') && strcmp(WP,'Jacobi')
 %Series convergence criterion. Must have SerConv<0.
   SerConv=C1+mu-lambda*sigma*vmin.*rhomcj+log(pi1);
   if strcmp(WhichFirms,'YES')
   B=SerConv<0; %1 if true, 0 if not.
   B2=sum(B,2);
   B3=(B2==length(rhomcj));
   vparams=vparams(B3,:); ROA=ROA(B3); mu=mu(B3);  theta=theta(B3);
   kappa=kappa(B3); sigmav=sigmav(B3); vmin=vmin(B3); CSHOQ=CSHOQ(B3);
   vmax=vmax(B3);
   elseif strcmp(WhichFirms,'NO')
   B=SerConv≥0; %1 if true, 0 if not.
   B2=sum(B,2);
   B3=(B2≥1);
   vparams=vparams(B3,:); ROA=ROA(B3); mu=mu(B3);  theta=theta(B3);
   kappa=kappa(B3); sigmav=sigmav(B3); vmin=vmin(B3);
   vmax=vmax(B3); CSHOQ=CSHOQ(B3);
   end

end


   if strcmp(muType,'Agg')
       mu=.0124*ones(size(vparams,1),1);
```

```
    end

    if strcmp(muType,'noDrift')
        mu=zeros(size(vparams,1),1);
    end


    if strcmp(ROATYPE,'Market')
        ROA=MKTret*ones(size(vparams,1),1);
    elseif strcmp(ROATYPE,'RetOnAssets')
        ROA=.054*ones(size(vparams,1),1);

    end

   if strcmp(CbarEst,'YesCbar')
    L=100; %Number of months. This is for uncoditional expectation.
    Cbar=-log(1./(ROA*L).*sum(pi1.^(1:L).*exp(mu.*(1:L)),2));
    SS(Cbar(:))
   elseif strcmp(CbarEst,'NoCbar')
       Cbar=repmat(Cbar1,size(vparams,1),1);
   end

    %Gridpoints for Jacobi process
    if contains(WP,'Jac')
     vt=zeros(size(vparams,1),vn);
     for i=1:size(vparams,1)
        vt(i,:)=linspace(vmin(i),vmax(i),vn);
     end
     vt(:,1)=vt(:,1)+10^(-14);
     vt(:,end)=vt(:,end)-10^(-14);
    elseif contains(WP,'CIR')
     vt=linspace(.001,.6,vn);
     vt=repmat(vt,size(vparams,1),1);
    end

    save(strcat('initialize',WP));
```

The next step is to run the function `Getgsurf.m` for all appropriate indices. Each index corresponds to five firms. The total number of firms was broken into groups due to memory issues. The code is vectorized. While this speeds up the code, it requires more memory than for loops without vectorization.

```
function xx = Getgsurf(index,str)

%BRIAN HOGLE 2021

%Getgsurf calulate g(v,t,T,j)
%Use the appropriate string str to specify the run. For example, '
%use str='UMJac to run the specific version analyzing changes in UM
%for the Jacobi process.

%Note for UM and sigmav, only need index=1,2. For vmax and vmin, need
%index=1,...,6.

  str2=strcat('initialize',str);
  load(str2,'vt','rhomcj','vparams','nPaths','sigma','sigmar',...
        'rhorcj','a','lambda','N','boundtol');

  str3=strcat('gsurface',str);

  xx=(1:5)+5*(index-1);

 if xx(end)>size(vparams,1) && (mod(size(vparams,1),10)≤5)
       xx=xx(1:mod(size(vparams,1),10));
 elseif xx(end)>size(vparams,1) && (mod(size(vparams,1),10)>5)
       xx=xx(1:(mod(size(vparams,1),10)-5));
 end
     if contains(str,'Jac')

     [gval,Q]=gsurf(vt(xx,:),rhomcj,vparams(xx,:),nPaths,sigma,...
```

```
                    sigmar,rhorcj,a,lambda,N,boundtol);

      save(strcat(str3,num2str(index),'.mat'),'gval','Q');

      elseif contains(str,'CIR')

      [gval,Q]=gsurfCIR(vt(xx,:),rhomcj,vparams(xx,:),nPaths,sigma,...
                sigmar,rhorcj,a,lambda,N);

      save(strcat(str3,num2str(index),'.mat'),'gval','Q');
      end

end
```

Below, we present the function **gsurf.m** used in **Getgsurf.m** to generate values of $g(v,t,T,j)$ when the Jacobi process is used to model volatility.

```
function [gval,Q] = gsurf(vt,rhomcj,vparams,nPaths,sigma,sigmar,...
                          rhorcj,a,lambda,N,boundtol)

%BRIAN HOGLE 2021

%gsurf: generate function g(v,t,T,rho^{M,C_j})
    %This is done according to our partition of
    %[vmin,vmax]x[rhomcjmin,rhomcjmax]
%INPUTS
    %vt=partition of [vmin,vmax] for each firm. size(vt,1)=
        %number of firms. size(vt,2)=number of partition points
        %vt=linspace(vmin+10^(-10),vmax-10^(-10),vn); gives
        %starting points V(t)=v
    %N=place to terminate sum over s-t
    %Seems g is close to zero after around 200 time points.
%Each partition point of (vmin,vmax) will
%be a starting point of V(t) at time t. i.e. represents |V(t)=v.
%OUTPUTS
```

```
%gval=g(v,t,T,rhomcj) for different values V(t)=v and rhomcj
%Q=conditional expectation used in cash flows. See paper

rhon=length(rhomcj);
gg=sigma*sigmar/a*rhorcj/2.*(exp(-a.*(2:(N+1)))-exp(-a));

[v,outbounds] = vsim(vt,vparams,N,nPaths,boundtol);

C6=C6calc(sigma,sigmar,rhorcj,a);
C7=zeros(length(rhomcj),1);

for i=1:length(rhomcj)
   C7(i)= C7calc(sigma,sigmar,rhorcj,a,lambda,rhomcj(i));
end

EF=C6*exp(-a*((1:N)-1));
G=bsxfun(@plus,EF,C7);
v2=permute(repmat(v,1,1,1,1,length(rhomcj)),[1 2 3 5 4]);
G2=permute(repmat(G,1,1,size(v,1),size(v,2),size(v,3)),[3 4 5 1 2]);
vG=v2.*G2;

gval=zeros(size(v,1),size(v,2),nPaths,length(rhomcj),N);
%size(gval)=(# sets of different Jacobi process parameters)x(size of
%partition of [v_min,v_max])xnPathsxlength(rhomcj)xN
for i=1:N
  gval(:,:,:,:,i)=exp(trapz(vG(:,:,:,:,(1:i)),5));
end

[v,outbounds]=vsim(vt,vparams,2,nPaths,boundtol);
[¬,idx]=min(abs(permute(vt,[2 1])-permute(v(:,:,:,2),[2 1 3])));
    idx=squeeze(idx);

v3=v(:,:,:,1)+v(:,:,:,2)*exp(a);
v4=repmat(v3,1,1,1,N);
gg2=permute(repmat(gg(1:N)',1,size(v4,1),...
             size(v4,2),size(v4,3)),[2 3 4 1]);
```

```
gv4=exp(gg2.*v4);
gv5=permute(repmat(gv4,1,1,1,1,rhon),[1 2 3 5 4]);

gval=squeeze(mean(gval,3));%Average over nPaths

Q=zeros(size(gval,1),nPaths,length(rhomcj),size(gval,4));
for i=1:size(gval,1)
    for j=1:nPaths
Q(i,j,:,:)=squeeze(gval(i,idx(i,j),:,:));
    end
end

Q2=permute(repmat(Q,[1 1 1 1 size(vt,2)]),[1 5 2 3 4]).*gv5;

Q=squeeze(mean(Q2,3));%Average over nPaths

end
```

Similarly, we have the function **gsurfCIR.m** for calculating $g(v, t, T, j)$ when the CIR process is used to model volatility.

```
function [gval,Q] = gsurfCIR(vt,rhomcj,vparams,nPaths,sigma,sigmar,...
                                rhorcj,a,lambda,N)

%BRIAN HOGLE 2021

%gsurfCIR: generate function g(v,t,T,j) when CIR is used to model vol.
    %This is done according to our partition of
    %[vmin,vmax]x[rhomcjmin,rhomcjmax]
%INPUTS
    %vt=partition of [vmin,vmax] for each firm. size(vt,1)=
        %number of firms. size(vt,2)=number of partition points
        %vt=linspace(vmin+10^(-10),vmax-10^(-10),vn); gives
        %starting points V(t)=v
    %N=place to terminate sum over s-t
```

```
    %Seems g is close to zero after around 200 time points.
%Each partition point of (vmin,vmax) will
%be a starting point of V(t) at time t. i.e. represents |V(t)=v.
%OUTPUTS
%gval=g(v,t,T,rhomcj) for different values V(t)=v and rhomcj
%Q=conditional expectation used in cash flows. See paper

theta=vparams(:,1);
kappa=vparams(:,2);
sigmav=vparams(:,3);

rhon=length(rhomcj);
gg=sigma*sigmar/a*rhorcj/2.*(exp(-a.*(2:(N+1)))-exp(-a));

    nPeriods=N-1;
    nSteps=1;
    v=zeros(size(vparams,1),size(vt,2),N,nPaths);
    for jj=1:size(vt,2)
    for kk=1:size(vparams,1)
    obj=cir(theta(kk),kappa(kk),sigmav(kk),'Startstate',vt(kk,jj));
    v(kk,jj,:,:)=squeeze(simByTransition(obj,nPeriods,...
        'nTrials',nPaths,'nSteps',nSteps));
    end
    end
    v=permute(v,[1 2 4 3]);


C6=C6calc(sigma,sigmar,rhorcj,a);
C7=zeros(length(rhomcj),1);

for i=1:length(rhomcj)
   C7(i)= C7calc(sigma,sigmar,rhorcj,a,lambda,rhomcj(i));
end

EF=C6*exp(-a*((1:N)-1));
G=bsxfun(@plus,EF,C7);
```

```
v2=permute(repmat(v,1,1,1,1,length(rhomcj)),[1 2 3 5 4]);
G2=permute(repmat(G,1,1,size(v,1),size(v,2),size(v,3)),[3 4 5 1 2]);
vG=v2.*G2;

gval=zeros(size(v,1),size(v,2),nPaths,length(rhomcj),N);
%size(gval)=(# sets of different Jacobi process parameters)x(size of
%partition of [v_min,v_max])xnPathsxlength(rhomcj)xN
for i=1:N
  gval(:,:,:,:,i)=exp(trapz(vG(:,:,:,:,(1:i)),5));
end

    nPeriods=1;
    nSteps=1;
    v=zeros(size(vparams,1),size(vt,2),2,nPaths);
    for jj=1:size(vt,2)
    for kk=1:size(vparams,1)
    obj=cir(theta(kk),kappa(kk),sigmav(kk),'Startstate',vt(kk,jj));
    v(kk,jj,:,:)=squeeze(simByTransition(obj,nPeriods,...
        'nTrials',nPaths,'nSteps',nSteps));
    end
    end
    v=permute(v,[1 2 4 3]);

[¬,idx]=min(abs(permute(vt,[2 1])-permute(v(:,:,:,2),[2 1 3])));
             idx=squeeze(idx);

v3=v(:,:,:,1)+v(:,:,:,2)*exp(a);
v4=repmat(v3,1,1,1,N);
gg2=permute(repmat(gg(1:N)',1,size(v4,1),...
           size(v4,2),size(v4,3)),[2 3 4 1]);
gv4=exp(gg2.*v4);
gv5=permute(repmat(gv4,1,1,1,1,rhon),[1 2 3 5 4]);

gval=squeeze(mean(gval,3));%Average over nPaths

Q=zeros(size(gval,1),nPaths,length(rhomcj),size(gval,4));
```

```
for i=1:size(gval,1)
    for j=1:nPaths
Q(i,j,:,:)=squeeze(gval(i,idx(i,j),:,:));
    end
end

Q2=permute(repmat(Q,[1 1 1 1 size(vt,2)]),[1 5 2 3 4]).*gv5;

Q=squeeze(mean(Q2,3));%Average over nPaths

end
```

We now present the function **vsim.m**, which is used to simulate paths of the Jacobi process. We do not present a corresponding function for the CIR process since Matlab has a built in function that does this.

```
function [v,outbounds] = vsim(vt,vparams,simlen,nPaths,boundtol)

%BRIAN HOGLE 2021

%vsim Simulate the Jacobi process
%boundtol= how much to adjust above below vmin vmax if Jacobi goes out of
            %bounds
outbounds=0;
 v=zeros(size(vt,1),size(vt,2),nPaths,simlen);
    v(:,:,:,1)=repmat(vt,[1 1 nPaths]);
    vmin1=repmat(vparams(:,4),[1 size(vt,2) nPaths]);
    vmax1=repmat(vparams(:,5),[1 size(vt,2) nPaths]);
    theta1=repmat(vparams(:,1),[1 size(vt,2) nPaths]);
    kappa1=repmat(vparams(:,2),[1 size(vt,2) nPaths]);
    sigmav1=repmat(vparams(:,3),[1 size(vt,2) nPaths]);

    for i=2:simlen
      v(:,:,:,i)=v(:,:,:,i-1)+kappa1(:,:,:).*(theta1(:,:,:)...
          -v(:,:,:,i-1))+sigmav1(:,:,:).*sqrt((v(:,:,:,i-1)...
```

```
            -vmin1(:,:,:)).*(vmax1(:,:,:)-v(:,:,:,i-1))...
            ./(sqrt(vmax1(:,:,:))-sqrt(vmin1(:,:,:))).^2)...
            .*randn(size(vt,1),size(vt,2),nPaths);

        A=v(:,:,:,i);
        IA=find(A≥vmax1);
        outbounds=outbounds+numel(IA);
        A(IA)=vmax1(IA)-boundtol;

        IB=find(A≤vmin1);
        outbounds=outbounds+numel(IB);
        A(IB)=vmin1(IB)+boundtol;
        v(:,:,:,i)=A;

    end
end
```

After running **gsurf.m** for the Jacobi process or **gsurfCIR.m** for the CIR process for the appropriate indices, we merge the resulting variables from these runs by using **CombineGsurf.m**. We present the code below.

```
str='CIR'; %If str='Special, combine for specific cases.
     %Otherwise, combine the general version for Jacobi or CIR

if strcmp(str,'CIR')
    Groupend=18;
elseif strcmp(str,'Jacobi')
    Groupend=31;
elseif strcmp(str,'VmaxJac') || strcmp(str,'VminJac')
    Groupend=6;
elseif strcmp(str,'sigmavJac') || strcmp(str,'UMJac') ||...
       strcmp(str,'kappaJac') || strcmp(str,'kappaCIR')
    Groupend=2;
end

```

```
if contains(str,'Jac')
load(strcat('gsurface',str,num2str(1)))
gval1=gval;
Q1=Q;
for i=2:Groupend
    load(strcat('gsurface',str,num2str(i)))
    Q1=[Q1;Q];
    gval1=[gval1;gval];
end
gval=gval1;
Q=Q1;
clearvars -except gval Q str
save(strcat('gvalQcombined',str))

elseif strcmp(str,'CIR')
load(strcat('gsurfaceCIR',num2str(1)))
gval1=gval;
Q1=Q;
for i=2:18
    load(strcat('gsurfaceCIR',num2str(i)))
    Q1=[Q1;Q];
    gval1=[gval1;gval];
end
gval=gval1;
Q=Q1;
clearvars -except gval Q
save gvalQcombinedCIR

elseif strcmp(str,'Special')
 strlist=["sigmavJac";"UMJac";"VmaxJac";"VminJac"];
 for i=1:length(strlist)
     if strcmp(strlist(i),"sigmavJac") || strcmp(strlist(i),"UMJac")
     load(strcat('gsurface',strlist(i),num2str(1)));
     Q1=Q; gval1=gval;
     load(strcat('gsurface',strlist(i),num2str(2)));
     Q=[Q1;Q]; gval=[gval1;gval];
```

```
      clearvars -except i Q gval strlist
      save(strcat('gvalQcombined',strlist(i)));
      elseif strcmp(strlist(i),"VmaxJac") || strcmp(strlist(i),"VminJac")
        load(strcat('gsurface',strlist(i),num2str(1)));
        Q1=Q; gval1=gval;
        for j=2:6
            load(strcat('gsurface',strlist(i),num2str(j)))
            Q1=[Q1;Q];
            gval1=[gval1;gval];
        end
        gval=gval1;
        Q=Q1;
        clearvars -except gval Q i strlist
        save(strcat('gvalQcombined',strlist(i)));

      end
  end
end
```

We now desire to acquire the functions F_3 and r^*, which we do through the code `F3rstar.m`.

```
%BRIAN HOGLE, 2021

%F3rstar: Find F3 and rstar. Run after CombineGsurf.m

str='CIR'; %If str='Special, combine for specific cases.
     %Otherwise, combine the general version

load(strcat('initialize',str),'rparams','mu','lambda','rhomr','K',...
     'Cbar','C1','vt','rhomcj','pi1');
load(strcat('gvalQcombined',str));

[F3,F3star,C8]=F3calc(rparams,mu,lambda,rhomr,K,Cbar,C1);

```

```
rstar=findrstar(K,pi1,rparams,gval,F3);

save(strcat('gvalQF3rstar',str),'gval','Q','F3','rstar','C8')



if strcmp(str,'Jacobi')
load('initializeJacobi','rparams','mu','lambda','rhomr','K',...
     'Cbar','C1','vt','rhomcj','pi1');
load('gvalQcombinedJacobi');

[F3,F3star,C8]=F3calc(rparams,mu,lambda,rhomr,K,Cbar,C1);

rstar=findrstar(vt,rhomcj,K,pi1,rparams,gval,F3);

save('gvalQF3rstarJacobi','gval','Q','F3','rstar','C8')

elseif strcmp(str,'CIR')
load('initializeCIR','rparams','mu','lambda','rhomr','K',...
     'Cbar','C1','vt','rhomcj','pi1');
load('gvalQcombinedCIR');

[F3,F3star,C8]=F3calc(rparams,mu,lambda,rhomr,K,Cbar,C1);

rstar=findrstar(vt,rhomcj,K,pi1,rparams,gval,F3);

save('gvalQF3rstarCIR','gval','Q','F3','rstar','C8')

elseif strcmp(str,'Special')
    strlist=["sigmavJac";"UMJac";"VmaxJac";"VminJac"];
 for i=1:length(strlist)
     load(strcat('gvalQcombined',strlist(i)))
     load(strcat('initialize',strlist(i)),'rparams','mu','lambda',...
         'rhomr','K','Cbar','C1','vt','rhomcj','pi1');
     [F3,F3star,C8]=F3calc(rparams,mu,lambda,rhomr,K,Cbar,C1);

```

```
    rstar=findrstar(vt,rhomcj,K,pi1,rparams,gval,F3);

    save(strcat('gvalQF3rstar',strlist(i)),'gval','Q','F3','rstar','C8')
 end
end
```

Here we list the code `F3calc.m`, which is used to calculate F_3 and C_8.

```
function [F3,F3star,C8] = F3calc(rparams,mu,lambda,rhomr,K,Cbar,C1)

%BRIAN HOGLE, APRIL 2021

%F3calc calculate F_3
%INPUTS
%K=upper limit on summation over k
%OUTPUTS (All defined in thesis/paper)
%F3
%F3star
%C_8

a=rparams(1);
b2=rparams(2);
sigmar=rparams(3);

C8=Cbar+b2-3*sigmar^2/(4*a^3)-lambda*sigmar*rhomr/a^2;

F3star=(C1+mu).*(1:K)+(sigmar^2/a^3+lambda*sigmar*rhomr/a^2-b2)....
        *exp(-a.*(1:K))-sigmar^2.*exp(-2*a.*(1:K))./(4*a^3);

F3=F3star+C8;

end
```

Now, we present the code `findrstar.m`, which is used to calculate $r*$.

```
function rstar = findrstar(K,pi1,rparams,gval,F3)
%findrstar calculate r*(v(s),rhomcs)
%For inputs, use vt for vvals and rhomcj for rhomcjvals
%INPUTS
%vvals= simulated values of v(s)\in[v_min,v_max]. is a vector
%rhomcjvals= simulated values of rhomcj(s)\in[rho_min,rho_max].
            %is a vector
%K= upper limit on sum over k=1 to \infty
%pi1=.99 determines lifetime of projects
%gval= calculated from gsurf
%OUTPUTS
%rstar= 2-D array rstar(i,j) of size vnxrhon
a=rparams(1);
rstar=zeros(size(gval,1),size(gval,2),size(gval,3));
for i=1:size(gval,1)
    for j=1:size(gval,2)
        for l=1:size(gval,3)
        xx=squeeze(gval(i,j,l,1:K));
        f=@(rs)-1+sum(pi1.^(1:K).*exp(F3(i,1:K)+rs....
        *(exp(-a.*(1:K))-1)./a).*xx');
        rstar(i,j,l)=fzero(f,0);
        clear f xx rs;
        end
    end
end

end
```

The function `GOFun.m` calculates the value of growth options. Again, "index" is used due to a lack of memory. Five firms are run at a time.

```
function Lstar1 = GOFun(index,str,tstart)

%BRIAN HOGLE, 2021
```

```
%GOFun Evaluate growth options
%INPUTS
%index= vparams is separated into groups due to memory constraints
%str= specialized routine. Leave this out for general routine
%tstart= where to start for loop over time t=tstar:simlen

%Must always include index. case 2 is for index and tstart. case 3
%include str.

      str2=strcat('initialize',str);
      str3=strcat('gvalQF3rstar',str);
      load(str2,'N','K','rparams','simlen','r','lambda',...
                'rhomr','pi1','muI','vparams');
      load(str3,'gval','F3','rstar');

xx=(1:5)+5*(index-1);

if xx(end)>size(vparams,1) && (mod(size(vparams,1),10)<=5)
    xx=xx(1:mod(size(vparams,1),10));
elseif xx(end)>size(vparams,1) && (mod(size(vparams,1),10)>5)
    xx=xx(1:(mod(size(vparams,1),10)-5));
end

rstar=rstar(xx,:,:);
gval=gval(xx,:,:,:);
F3=F3(xx,:);

Lstar=zeros(length(xx),simlen-tstart+1);
Lqq=zeros(length(xx),simlen-tstart+1);
I=ones(1,simlen-tstart+1);

r=r(tstart:simlen);

for t=1:(simlen-tstart+1)
[Lstar1,Lqqs] = GOcal(N,K,rparams,r,I,rstar,lambda,...
```

```
    rhomr,gval,F3,pi1,t,muI);
fprintf('Value of GO')
t
Lstar1
Lqqs
Lstar(1:length(xx),t)=Lstar1;
Lqq(1:length(xx),t)=Lqqs;

end

save(strcat('GO',str,num2str(index),'.mat'),'Lstar','Lqq');

end
```

We now present the function `GOcal.m` from `GOFun.m`. This function is used to calculate the growth option values at each time t.

```
function [Lstar,Lqq] = GOcal(N,K,rparams,r,I,rstar,...
                                        lambda,rhomr,gval,F3,pi1,t,muI)

%BRIAN HOGLE 2021
%GOcalc calculate the time t and time t+1 value of growth options given
%information at time t.
%INPUTS
%N=upper limit on sum over s-t=1 to s-t=N
%K=upper limit on sum over k=1 to k=K
%rstar= solution from fzero for corresponding (v(s),rhomcj(s)).
%F3= function of k alone.
%OUTPUTS
%Lqq=L^**(t)
%Lstar=L^*(t)

rt=r(t);
gval1=gval(:,:,:,1:K);

```

```
%parameters for interest rate process
a=rparams(1);
b2=rparams(2);
sigmar=rparams(3);

Kstar=repmat(rstar,1,1,1,K).*permute(repmat(((exp(-a.*(1:K))...
    -1)./a)',1,size(rstar,1),size(rstar,2),size(rstar,3)),[2 3 4 1]);

d2=((b2-rt+repmat(rstar(:,:,:)-b2,1,1,1,N)...
    .*permute(repmat(exp(a.*(1:N))',1,size(rstar,1),size(rstar,2),...
    size(rstar,3)),[2 3 4 1]))./sigmar...
    +permute(repmat((lambda*rhomr/a*(exp(a.*(1:N))-1)...
    +sigmar/(2*a^2)*(exp(a.*(1:N)./2)-exp(-a.*(1:N)./2)).^2)',...
    1,size(rstar,1),size(rstar,2),size(rstar,3)),[2 3 4 1]))...
    .*permute(repmat(sqrt(2*a./(exp(2*a.*(1:N))-1))',1,size(rstar,1),...
    size(rstar,2),size(rstar,3)),[2 3 4 1]);
%fqq will denote f^{**} (from thesis)
%fqq is a function of rt and k
fqq=exp(((rt-b2).*exp(-a)+b2)./a.*(exp(-a.*(1:K))-1)...
    +sigmar^2*(1-exp(-2*a)).*(1-exp(-a.*(1:K))).^2/(4*a^3));

B4=(b2-rt)*exp(-a)/a.*(1-exp(-a.*(1:N)))-b2.*(1:N);

B3=(b2-rt)./a.*(1-exp(-a.*(1:N)))-b2.*(1:N);%size of B3star is 1xN.
%Note rt is not a vector
%VYs=Var(Y*(t,s))

%note n=s-t in all of this, which is why s-t-1 is represented by (1:N)-1
VYs=(lambda^2+sigmar^2/a^2+2*lambda*sigmar*rhomr/a).*((1:N)-1)+...
    sigmar^2/a^2*(exp(-a)-exp(-a.*(1:N))).^2.*(exp(2*a)-1)/(2*a)+...
    sigmar^2.*(1-exp(-2*a.*(1:N)+2*a))/(2*a^3)-...
    2*(lambda*sigmar*rhomr/a^2+sigmar^2/a^3).*(1-exp(-a.*(1:N)+a));

%VY=.5*Var(Y(t,s)). Note the 1/2 is already included.
VY=.5*(lambda^2+sigmar^2/a^2+2*lambda*sigmar*rhomr/a).*(1:N)...
    +sigmar^2.*(1-exp(-2*a.*(1:N)))/(4*a^3)-...
```

```
    (lambda*sigmar*rhomr/a^2-sigmar^2.*exp(-a.*(1:N)-a*t)/a^3)...
    .*(1-exp(-a.*(1:N)));

d3=repmat((rt*exp(-a.*(1:N))/a+(b2/a-lambda*rhomr*sigmar/a^2-...
    sigmar^2/a^3).*(1-exp(-a.*(1:N))))',[1,K])...
    .*repmat(exp(-a.*(1:K))-1,[N,1])...
    +repmat((sigmar^2*(exp(-a*(1:K))-1).^2/(4*a^3)+...
    sigmar^2*(exp(-a*(1:K))-1)/(2*a^3)),[N,1])...
    .*repmat((1-exp(-2*a*(1:N)))',[1,K]);

gvl1=size(gval,1); gvl2=size(gval,3);

d1=repmat(d2,1,1,1,1,K)...
    +sigmar/a*permute(repmat(bsxfun(@times,sqrt((1-...
    exp(-2*a.*(1:N)))./(2*a))'...
    ,(1-exp(-a*(1:K)))),1,1,gvl1,size(gval,2),gvl2),[3 4 5 1 2]);

fp=(permute(repmat(exp((muI-.5*lambda^2).*(1:N)+B3(1:N)+VY(1:N))',...
    1,size(gval,1),size(gval,2),size(gval,3),K),[2 3 4 1 5])...
    .*permute(repmat((pi1.^(1:K))',1, size(gval,1),size(gval,2),...
    size(gval,3),N), [2 3 4 5 1]) ...
    .*permute(repmat(exp(F3(:,1:K)),1,1,size(gval,2),size(gval,3),N),...
    [1 3 4 5 2])).*permute(repmat(gval1,1,1,1,1,N),[1 2 3 5 4])...
    .*(exp(permute(repmat(d3,1,1,size(gval,1),size(gval,2),...
    size(gval,3)),[3 4 5 1 2])).*normcdf(d1)...
    -exp(permute(repmat(Kstar,1,1,1,1,N),[1 2 3 5 4]))...
    .*normcdf(repmat(d2,1,1,1,1,K)));

fp=squeeze(mean(fp,2)); fp=squeeze(mean(fp,2));
fp=squeeze(sum(fp,2)); fp=squeeze(sum(fp,2));

Lstar=I(t)*fp;

clearvars fp d1 d2 d3

d2star=((b2-rt+repmat(rstar(:,:,:)-b2,1,1,1,N)...
```

```
    .*permute(repmat(exp(a.*(1:N))',1,size(rstar,1),...
    size(rstar,2),size(rstar,3)),[2 3 4 1])./sigmar...
    +permute(repmat((lambda*rhomr/a*(exp(a.*(1:N))-exp(a))...
    +sigmar/(2*a^2)*(exp(a.*(1:N))-exp(a)-exp(-a)...
    +exp(-a.*(1:N))))',1,size(rstar,1),size(rstar,2),...
    size(rstar,3)),[2 3 4 1])).*permute(repmat(sqrt(2*a./...
    (exp(2*a.*(1:N))-1))',1,size(rstar,1),size(rstar,2),...
    size(rstar,3)),[2 3 4 1]);
d5star=(-rt*exp(-a)+b2*(exp(-a)-1)+rstar)*sqrt(2*a/(1-exp(-2*a)))/sigmar;

%VY stands for 1/2Var(Y(t,s))
%Directly below, Lqq1 is for the first term in L**
d6star=repmat(d5star,1,1,1,K)...
    +permute(repmat((sigmar*(1-exp(-a*(1:K)))*sqrt((1-...
    exp(-2*a))/(2*a^3)))',...
    [1,size(d5star,1),size(d5star,2),size(d5star,3)]),[2 3 4 1]);

d1star=repmat(d2star,1,1,1,1,K)...
    +sigmar/a*permute(repmat(bsxfun(@times,sqrt((1-...
    exp(-2*a.*(1:N)))./(2*a))',...
    (1-exp(-a*(1:K)))),1,1,gvl1,size(gval,2),gvl2),[3 4 5 1 2]);

d4=bsxfun(@times,((rt-b2)*exp(-a*(1:N))+b2)',(exp(-a*(1:K))-1)/a)...
    +bsxfun(@times,((1-exp(-2*a*(1:N)))/(4*a^3))',sigmar^2*...
    (1-exp(-a*(1:K))).^2)...
    +bsxfun(@times,((-(lambda*rhomr/a+sigmar/a^2)*(exp(a*(1:N))-exp(a))...
    +sigmar/(2*a^2)*((exp(-a)-exp(-a*(1:N)))*(1-exp(2*a))+...
    exp(a*(1:N))-exp(2*a-a*(1:N))))...
    .*sigmar/a.*exp(-a*(1:N)))',(exp(-a*(1:K))-1));

fn=permute(repmat((pi1.^(1:K).*exp(F3(:,1:K)))',...
    [1 1 size(gval1,2) size(gval1,3)]),[2 3 4 1]).*gval1(:,:,:,:)...
    .*(permute(repmat((fqq)',...
    [1 size(gval1,1) size(gval1,2) size(gval1,3)]),[2 3 4 1])...
    .*normcdf(d6star(:,:,:,:))-...
    repmat(normcdf(d5star(:,:,:)),1,1,1,K).*exp(Kstar(:,:,:,:)));
```

```
 fm=zeros(size(gval,1),size(gval,2),size(gval,3),size(gval,4),K);

 B41=B4(1:(end-1));

fm(:,:,:,2:N,:)=permute(repmat(exp((muI-.5*lambda^2)*(2:N)+B41...
    +.5*VYs(2:N))',1,size(gval,1),size(gval,2),size(gval,3),K),...
    [2 3 4 1 5]).*permute(repmat((pi1.^(1:K))',1,size(gval,1),...
    size(gval,2),size(gval,3),N-1),[2 3 4 5 1])...
    .*permute(repmat(exp(F3(:,1:K)),1,1,size(gval,2),...
    size(gval,3),N-1),[1 3 4 5 2])...
    .*permute(repmat(gval1(:,:,:,:),1,1,1,1,N-1),[1 2 3 5 4])...
    .*(exp(permute(repmat(d4(2:N,:),1,1,size(gval,1),size(gval,2),...
    size(gval,3)),[3 4 5 1 2]))...
    .*normcdf(d1star(:,:,:,2:N,:))...
    -exp(permute(repmat(Kstar(:,:,:,:),1,1,1,1,N-1),[1 2 3 5 4]))...
    .*normcdf(repmat(d2star(:,:,:,2:N),1,1,1,1,K)));

fn=squeeze(mean(fn,2)); fn=squeeze(mean(fn,2));

Lqq1=I(t)*exp(muI-.5*lambda^2)*sum(fn,2);

%We now find L** for all rest terms

fm=squeeze(mean(fm,2)); fm=squeeze(mean(fm,2));
fm=squeeze(sum(fm,2)); fm=squeeze(sum(fm,2));

Lqq2=I(t)*fm;
Lqq=Lqq1+Lqq2;

end
```

Finally, we present the code GetTS.m, which calculates the time series generated for the cash flows.

```
function countproj = GetTS(index,str,Nfirms)

%BRIAN HOGLE, APRIL 2021

%GetTS Generate time series
%INPUTS
%index=used to separate into groups due to memory issues
%str= identifies specialized run, if included
%Nfirms= number of realizations generated.

str2=strcat('initialize',str);
str3=strcat('gvalQF3rstar',str);
load(str2,'N','rparams','simlen','r','lambda',...
    'rhomr','pi1','muI','vparams','dWr','dWm','muI','C1','C2',...
    'C3','mu','sigmaI','Cbar','vt','rhorcj','sigma','rhomcj') ;
load(str3,'gval','Q');

xx=(1:5)+5*(index-1);

if xx(end)>size(vparams,1) && (mod(size(vparams,1),10)≤5)
    xx=xx(1:mod(size(vparams,1),10));
elseif xx(end)>size(vparams,1) && (mod(size(vparams,1),10)>5)
    xx=xx(1:(mod(size(vparams,1),10)-5));
end

if contains(str,'CIR')

gval=gval(xx,:,:,:);
Q=Q(xx,:,:,:);
mu=mu(xx);
Cbar=Cbar(xx);
vparams=vparams(xx,:);
vt=vt(xx,:);

b=zeros(Nfirms,size(vparams,1),simlen);
```

```
CF=zeros(Nfirms,size(vparams,1),simlen);
Vstar=zeros(Nfirms,size(vparams,1),simlen);
countproj=zeros(Nfirms,size(vparams,1));

parfor i=1:Nfirms

[b1,countproj1,CF1,Vstar1]=FirmValCIR(N,rparams,r,dWr,dWm,lambda,rhomr...
    ,gval,pi1,muI,C1,C2,C3,mu,simlen,rhomcj,vparams,Q,sigmaI,Cbar,vt,...
    rhorcj,sigma);

b(i,:,:)=b1;
CF(i,:,:)=CF1;
Vstar(i,:,:)=Vstar1;
countproj(i,:)=countproj1; %number projects rejected for i-th firm.

end %end parfor loop
elseif contains(str,'Jac')

gval=gval(xx,:,:,:);
Q=Q(xx,:,:,:);
mu=mu(xx);
Cbar=Cbar(xx);
vparams=vparams(xx,:);
vt=vt(xx,:);

b=zeros(Nfirms,size(vparams,1),simlen);
CF=zeros(Nfirms,size(vparams,1),simlen);
Vstar=zeros(Nfirms,size(vparams,1),simlen);
countproj=zeros(Nfirms,size(vparams,1));

parfor i=1:Nfirms

[b1,countproj1,CF1,Vstar1]=FirmVal(N,rparams,r,dWr,dWm,lambda,rhomr...
    ,gval,pi1,muI,C1,C2,C3,mu,simlen,rhomcj,vparams,Q,sigmaI,Cbar,vt,...
    rhorcj,sigma);

```

```
b(i,:,:)=b1;
CF(i,:,:)=CF1;
Vstar(i,:,:)=Vstar1;
countproj(i,:)=countproj1; %number projects rejected for i-th firm.

end %end parfor loop
end
save(strcat('TS',str,num2str(index),'.mat'),'b','CF',...
                'Vstar','countproj');

end
```

Below, we present the SAS code which was used for parameter estimation.

```
/*
BRIAN HOGLE 2021
*/


/* This code uses quarterly OIBDPQ for the jacobi process
   with 3 different ways of scaling.*/

proc datasets library=work kill nolist;
quit;

%let x=%sysfunc(pathname(sasautos));
%put &x ;
filename nwords "C:\Users\18594\Documents\";
options append=sasautos=(nwords) mrecall mautosource ;
filename winsorize "C:\Users\18594\Documents";
options append=sasautos=(winsorize) mrecall mautosource ;

%include "C:\Users\18594\Documents\nwords.sas";
%include "C:\Users\18594\Documents\winsorize.sas";

```

```
/*
data first(drop=UCEQQ);
set 'C:\Users\18594\Downloads\JacobiCF11Quar.sas7bdat';
run;
*/

data first(drop=UCEQQ);
set 'C:\Users\18594\Downloads\JacobiCF11QuarwCSHOQ.sas7bdat';
run;


data second2;
set first;
if ACTQ=. then delete;
run;

*Here we get rid of mergers;
data second2;
set second2;
if REVTQ_FN1='AB' then delete;
run;

*delete if common equity is ≤ 0;
data second2;
set second2;
if CEQQ le 0 then
delete;
run;

data second2;
set second2;
if SIC le 4999 and SIC ge 4900 then
delete;
run;

*If total assets less than 0 then delete;
```

```
data third;
set second2;
if actq lt 0 then delete;
if revtq lt 0 then delete;
run;

data third2;
set third;
if actq=. then delete;
if revtq=. then delete;
if lctq=. then delete;
if OIBDPQ=. then delete;
*if CSHOQ=. then delete;
run;

*Here we get rid of firms with too many negative
    cash flow values;
data fifth;
set third2;
by gvkey;
retain Negvals;
if first.gvkey then
   NegVals=0;
    if OIBDPQ<0 then
        NegVals + 1;
    if last.gvkey;
run;
data fifth;
set fifth;
if NegVals>0 then delete;
run;

data NoNeg;
     merge third2(in=a) fifth(in=b);
     by gvkey;
     if a and b;
```

```
run;

data NoNeg;
set NoNeg;
if revtq lt 0 then delete;
run;

*sort by gvkey;
proc sql;
create table want as
  select *
   from NoNeg
    group by gvkey
     having count(*) ge 90 ;
quit;

*Below we sort based on Ticker. Within ticker we sort by ascending date;
 PROC SORT DATA = want OUT = want4;
     BY gvkey datadate;
    run;

data want4;
set want4;
netasset=actq-lctq;
run;
data want6(DROP=OIBDPQ CSHOQ);
set want4;
scaled2=log(OIBDPQ/actq);
run;


PROC EXPAND DATA=want6 OUT=MOVINGSTD;
CONVERT scaled2=STD2 / TRANSFORMOUT=(MOVSTD 20);
RUN;

data Movingstd;
```

```
set movingstd;
std2=std2/sqrt(3);
run;
*change 20 below if changing size of moving window;

data d4(drop=count);
  set movingstd(drop=time);
  by gvkey;
  if first.gvkey then count=0;
  count+1;
  if count ge 20 then output;
run;

proc sort data=d4 out=one2;
by gvkey std2;
run;
data two2(keep=gvkey smax2);
set one2;
by gvkey;
smax2=std2;
if last.gvkey then output;
run;

data three2(keep=gvkey smin2);
set one2;
by gvkey;
smin2=std2;
if first.gvkey then output;
run;


proc means data=d4 noprint MEAN;
var std2;
by gvkey;
OUTPUT out=four;
run;
```

```
data five(keep= gvkey _FREQ_ thetamean1 thetamean2 thetamean3);
set four;
if _STAT_='MEAN' then output;
RENAME STD2=thetaMean2;
run;

*The goal is to find weight based of of CSHOQ;
proc contents data=first;
run;
proc means data=first noprint MEAN;
var CSHOQ;
by gvkey;
OUTPUT out=fourCSHOQ;
run;

data meanCSHOQ(keep= gvkey CSHOQ);
set fourCSHOQ;
if _STAT_='MEAN' then output;
*RENAME CSHOQweight=thetaMean2;
run;
*End getting weights based off of CSHOQ;

data want8(DROP=_TYPE_ _FREQ_ _STAT_ indfml scaled1 scaled2 scaled3
SIC datadate bookval negvals hetasset revtq popsrc prccq revtq_fn1
datafmt datafqtr costat consol actq LCTQ indfmt fyr fyearq fqtr fic ...
    datacqtr ceqq curcdq cshoq_fn netasset);
merge d4 two2 three2 five;
by gvkey;
run;

*We add the Q here;
data withQ;
set want8;
Qanybound2=sqrt((std2-smin2)*(smax2-std2))/(sqrt(smax2)-sqrt(smin2));
run;
```

```
data withQ;
set withQ;
if Qanybound2=0 then Qanybound2=.1;
run;

data withQ;
set withQ;
vdiff2=smax2-smin2;
run;

*We add a lag;
data Lagged;
set withQ;
Qanyboundlag2=lag1(Qanybound2);
vlag2=lag1(std2);
v2=std2;
run;

*Eliminate first element in each group;
data Lagged1(drop=count);
  set Lagged;
  by gvkey;
  if first.gvkey then count=0;
  count+1;
  if count ge 2 then output;
run;

data SetRet2;
set Lagged1;
DVany2=v2/Qanyboundlag2;
IVany2=vlag2/Qanyboundlag2;
IVany22=1/Qanyboundlag2;
run;

proc reg data = SetRet2 noprint outest=estimates22;
```

```
      model DVany2=IVany2 IVany22 / noint;
      by gvkey;
run;
proc reg data = SetRet2;
      model DVany2=IVany2 IVany22 / noint;
 ods output parameterestimates=parms2;
     by gvkey;
run;
data estimates22(drop=_RMSE_ DVany2 _DEPVAR_ _MODEL_ _TYPE_);
set estimates22;
sigmav2=_RMSE_;
run;

data parms2;
set parms2;
if Probt ge .01 then delete;
run;

*Only keep firms with no deletions due to p-values;

proc sql;
create table parms22 as
  select *
   from parms2
    group by gvkey
     having count(*) ge 2 ;
quit;

PROC FREQ data=parms22;
  tables gvkey/out=gvkey_counts2 noprint;
run;

*Merge the data sets. Need 3 separate sets as p-values are different ...
   in each set
    which leads to certain firms being deleted while others not;

```

```
data Aest2(drop=count percent);
     merge estimates22(in=a) gvkey_counts2(in=b);
     by gvkey;
     if a and b;
run;


data withq22(keep=gvkey smax2 smin2 vdiff2);
set withq;
if first.gvkey then output;
by gvkey;
run;

data bound2;
     merge Aest2(in=a) withq22(in=b);
     by gvkey;
     if a and b;
run;
*convert Ivany and IVany2 to kappa and theta;

data KT2(drop=ivany2 ivany22);
set bound2;
kappa2=1-Ivany2;
theta2=IVany22/(1-Ivany2);
run;

data KT2;
set KT2;
rename smax2=vmax2 smin2=vmin2;
run;
data KT2;
set KT2;
if vmax2 le theta2 or vmin2 ge theta2 then delete;
run;
data KT2;
set KT2;
```

```
myo=1;
run;


data KT3;
set KT2;
if sigmav2**2*(vmax2-vmin2)/(sqrt(vmax2)-sqrt(vmin2))**2 le ...
    2*kappa2*min(vmax2-theta2,theta2-vmin2) then JC=1;
run;

data KT3(drop=myo JC);
set KT3;
if JC=. then delete;
run;

data KT4(drop=count percent);
     merge KT3(in=a) Meancshoq(in=b);
     by gvkey;
     if a and b;
run;

PROC EXPORT DATA= WORK.KT3
            OUTFILE= ...
                "C:\Users\18594\OneDrive\Documents\Jacobi_RFS_wCSHOQ.XLS"
            DBMS=EXCEL REPLACE;
     SHEET="Jacobiparams";
RUN;
```

5.1 How to run the simulation

In this section, we describe how to run the simulation in an itemized list.

1. Run `INAF.m` to initialize the variables across all of the firms. `INAF.m` allows the user to decide if the cash flows do not grow ($\mu = 0$), if the cash flow growth is firm specific, or if the cash flow growth is given the same positive value across all of the firms. Options are

available to run the code for the Jacobi process or CIR process at the beginning, and there are also certain specific scenarios available to examine one parameter at a time.

2. We compute the function $g(v, t, T, j)$ at specified grid points by running `Getgsurf.m`. This needs to be broken into pieces due to memory issues. Later, we combine the variables g and Q from these runs.

3. Combine the saved variables g and Q by running `CombineGsurf.m`. The initial setting "Special" is for the specific cases in which isolated parameters are examined. "Jacobi" or "CIR" is for the general version with the corresponding volatility process.

4. Get F_3 and r^* by running `F3rstar.m`.

5. Run the function `GOFun.m`, which contains `GOcalc.m`, for all of the appropriate indices to calculate growth option values. Note the special cases of σ_V and u_M require only two indices, while $v_{\max}$ and $v_{\min}$ require six indices.

6. Run the function `GetTS.m` for all of the appropriate indices. Note this can be run at the same time as `GOFun.m`.

7. Combine all of the indexed `TS.mat` and `GO.mat` files to get `GOandTS_All.mat` by running `TScombine.m`.

REFERENCES

[1] M. Schulmerich, *Real Options Valuation The Importance of Interest Rate Modelling in Theory and Practice*, 2nd ed. Berlin Heidelberg: Springer-Verlag, 2010.

[2] A. K. Dixit and R. S. Pindyck, *Investment under Uncertainty*. Princeton, N.J.: Princeton University Press, 1993. DOI: 10.1515/9781400830176.

[3] M. Musiela and M. Rutkowski, *Martingale Methods in Financial Modelling*, 2nd ed. Berlin Heidelberg: Springer-Verlag, 2002. DOI: 10.1007/978-0-387-78169-3.

[4] M. Avellaneda, A. Levy, and A. ParÁs, "Pricing and hedging derivative securities in markets with uncertain volatilities," *Applied Mathematical Finance*, vol. 2, no. 2, pp. 73–88, 1995. DOI: 10.1080/13504869500000005.

[5] J. Fouque and N. Ning, *Uncertain volatility models with stochastic bounds*, 2017. [Online]. Available: arXiv:1702.05036.

[6] R. Buff, *Uncertain Volatility Models- Theory and Application*. Berlin Heidelberg: Springer-Verlag, 2002. DOI: 10.1007/978-3-642-56323-2.

[7] L. E. Brandão, "Volatility estimation for stochastic project value models," *European Journal of Operational Research*, vol. 220, no. 3, pp. 642–648, 2012. DOI: 10.1016/j.ejor.2012.01.059.

[8] R. Durrett, *Probability Models for DNA Sequence Evolution*. Berlin Heidelberg: Springer-Verlag, 2008. DOI: 10.1007/978-0-387-78169-3.

[9] W. H. Fleming and M. Viot, "Some measure-valued markov processes in population genetics theory," *Indiana University Mathematics Journal*, vol. 28, no. 5, pp. 817–843, 1979.

[10] P. A. Jenkins and D. Spano, "Exact simulation of the wright-fisher diffusion," *Annals of Applied Probability*, vol. 27, no. 3, pp. 1478–1509, 2017. DOI: 10.1214/16-AAP1236.

[11] F. Delbaen and H. Shirakawa, "An interest rate model with upper and lower bounds," *Asia-Pacific Financial Markets*, vol. 9, no. 3, pp. 191–209, 2002. DOI: 10.1023/A:1024125430287.

[12] D. Ackerer, D. Filipovic, and S. Pulido, "The jacobi stochastic volatility model," *Finance and Stochastics*, vol. 22, no. 3, pp. 667–700, 2018. DOI: 10.1007/s00780-018-0364-8.

[13] C. Gourieroux and J. Jasiak, "Multivariate jacobi process with applications to smooth transitions," *Journal of Econometrics*, vol. 131, no. 1-2, pp. 475–505, 2006. DOI: 10.1016/j.jeconom.2005.01.014.

[14] C. Gourieroux and P. Valery, *Estimation of a jacobi process*, 2004. [Online]. Available: .

[15] J. B. Berk, R. C. Green, and V. Naik, "Optimal investment, growth options and security returns," *Journal of Finance*, vol. 54, no. 5, pp. 1153–1607, 1999. DOI: 10.1111/0022-1082.00161.

[16] R. McDonald and D. Siegel, "The value of waiting to invest," *The Quarterly Journal of Economics*, vol. 101, no. 4, pp. 707–728, 1986. DOI: 10.2307/1884175.

[17] W. A. Brock, M. Rothschild, and J. E. Stiglitz, "Stochastic capital theory i. comparative statics," *NBER Working Paper*, no. t0023, pp. 642–648, 1982. DOI: https://ssrn.com/abstract=579731.

[18] G. Grullon, E. Lyandres, and A. Zhdanov, "Real options, volatility, and stock returns," *Journal of Finance*, vol. 67, no. 4, pp. 1499–1537, 2012. DOI: 10.1111/j.1540-6261.2012.01754.x.

[19] K. G. Nishimura and H. Ozaki, "Irreversible investment and knightian uncertainty," *The Quarterly Journal of Economics*, vol. 136, no. 1, pp. 668–694, 2007. DOI: 10.1016/j.jet.2006.10.011.

[20] J. Gomes, L. Kogan, and L. Zhang, "Equilibrium cross section of returns," *Journal of Political Economy*, vol. 111, no. 4, pp. 693–732, 2003. DOI: 10.2139/ssrn.264883.

[21] L. Kogan and D. Papanikolaou, "Growth opportunities, technology shocks, and asset prices," *Journal of Finance*, vol. 69, no. 2, pp. 675–718, 2013. DOI: 10.1111/jofi.12136.

[22] L. Zhang, "The value premium," *Journal of Finance*, vol. 60, no. 1, pp. 67–103, 2005. DOI: 10.1111/j.1540-6261.2005.00725.x.

[23] H. Ai and D. Kiku, "Volatility risks and growth options," *Management Science*, vol. 62, no. 3, pp. 741–763, 2016. DOI: 10.1287/mnsc.2014.2129.

[24] P. E. Protter, *Stochastic Integration and Differential Equations*, 2nd ed. Berlin Heidelberg: Springer-Verlag, 2005.

[25] N. Privault, *Notes on stochastic finance*, 2020. [Online]. Available: https://www.ntu.edu.sg/home/nprivault/indext.html.

[26] R. L. Schilling and L. Partzsch, *Brownian Motion an Introduction to Stochastic Processes*, 2nd ed. De Gruyter, 2014.

[27] F. C. Klebaner, *Introduction to Stochastic Calculus with Applications*, 3rd ed. Imperial College Press, 2012. DOI: 10.1007/978-0-387-78169-3.

[28] M. O. Keefe and M. Yaghoubi, "The influence of cash flow volatility on capital structure and the use of debt of different maturities," *Journal of Corporate Finance*, vol. 38, pp. 18–26, 2016. DOI: 10.1016/j.jcorpfin.2016.03.001.

[29] B. Rountree, J. P. Weston, and G. Allayannis, "Do investors value smooth performance?" *Journal of Financial Economics*, vol. 90, no. 3, pp. 237–251, 2008. DOI: 10.1016/j.jfineco.2008.02.002.

VITA

Brian Hogle

Education

Master of Science in Mathematics with Computational Finance Specialization at Purdue University, West Lafayette, IN, May 2019.

Bachelor of Science with majors in Mathematics and Physics at the University of Louisville, Louisville, KY, May 2014.

Employment

Graduate Teaching Assistant, Department of Mathematics, Purdue University, August 2014-present. Responsibilities include: being a teaching assistant, a grader, a lecturer for Applied Calculus Math 16010, proctoring exams, and working in the Math Resource Room.